X-RAY DIFFRACTION STUDIES ON LIQUID CRYSTALS

THESIS SUBMITTED FOR THE DEGREE OF
DOCTOR OF PHILOSOPHY (SCIENCE)
OF THE
UNIVERSITY OF NORTH BENGAL
DECEMBER—1988

BIMAL MAJUMDER, M. Sc.
LIQUID CRYSTAL LAB
DEPARTMENT OF PHYSICS
UNIVERSITY OF NORTH BENGAL
INDIA : 734430

A C K N O W L E D G E M E N T

I express my heartiest gratitude to Dr.(Mrs.) Sukla Paul, Reader, Department of Physics, University of North Bengal for her untiring help, encouragement and guidance throughout the period of my research work. I also express my gratefulness to Professor Ranjit Paul, University of North Bengal for his valuable suggestions and discussions.

I also extend my gratefulness to Prof. Siddhartha Roy, IACS, Calcutta for his many valuable suggestions. I am also indebted to Prof. H.Schenk and Goubitz, University of Amsterdam for help in solving the crystal structure.

I am greateful to Late Prof. M. Wada of Tohoku University for supplying us the samples BBBA and PBBA. I acknowledge to M/s. Hoffmann-La-Roche, Basel, Switzerland for supplying other samples.

I convey my thanks to University of North Bengal for allowing me to do Part-time research work.

I convey my thanks to Mr. T.K.Bose of State Bank of India for his inspirations. Thanks to all my collegues at N.B.U.Campus Branch for their good wishes and inspirations. Thanks are also due for my collegues at Siliguri and Danguajhar Branches.

I wish to express my sincerest thanks to Dr.A.Majumdar, Dr.G.S.S.Murty, Dr.Rabindra Nath Mukherjee, Dr. Asis Nanda, Dept. of Chemistry,NBU for their help and suggestions in purifying x samples and forming single crystals. I am also thankful to Mr. Subhas Biswas, Glass Blower,Chemistry Dept.,NBU for his help. Thanks are also due to Dr. R.K.Samanta, Mr.C.R.Nayak,Mr.A.K.Roy, Mr. B.N.Paul of Computer Centre,NBU for their help during computational work.

Contd.....2

I am grateful to Dr.Pradip K.Mandal,Lecturer in Physics, North Eastern Hill University, Dr.Mukul K.Mitra, Mrs.K.Bhattacharjee for their help during some experimental works and Dr.B.Jha, Dr.(Mrs.) B.Bhattacharjee, Dr.(Miss) I.Choudhury, Mr.M.Santait, Miss Sakuntala Gupta, Dept. of Physics for their help and suggestions.

I also like to thank Mr.Sajal K.Sarkar,Sr.Tech.Asstt. Dept. of Physics,NBU for his constant help in the maintenance and repairing of the instrument and Mr.B.K.Nagm and all other USIC/Workshop (Physics Dept.) staffs for their help in repairing and fabrication of instruments. Thanks to Mr. S.Choudhury,Senior Assistant,NBU for timely typing the thesis.

I am also like to convey my thanks to all my good wishers whose names are not mentioned here and many of my friends for their inspirations.

Finally, I wish to express my gratefulness to my beloved son whose sweet laugh inspired me and my wife, whose constant inspiration lend me to the completion of the thesis.

I also express my gratefulness to my father, brother, sister and other members of my family where ever-living memory encouraged me during this work.

Lastly, I pay my homage of my mother whose memory hunch me every time in every work.

Bimal Majumder

Dated the 10th.November,1988, (BIMAL K. MAJUMDER)
University of North Bengal.

CHAPTER I

GENERAL INTRODUCTION

Introduction

Certain long organic molecules can exist in phases intermediate between liquid and solid. These phases have some of the properties of a liquid, such as fluidity and inability to support a shear. They have also some properties of a crystal. Lehmann[1] named this phase as 'Liquid Crystals'. Friedel[2,3] suggested the term 'Mesomorphic State'.

Liquid crystals exhibit anisotropic properties as do solid crystals. The mesophase can be identified visually by its characteristic turbidity or by a polarising microscope by its optical birefringence.

Liquid crystals in general can be formed by two processes, by "solvent" effect (lyotropic mesomorphism) and by thermal processes (thermotropic mesomorphism). In this study we are only concerned with the latter, where compounds exhibit liquid crystal phases on heating from the solid.

The macroscopic anisotropy of liquid crystal is attributed to long range molecular orientational order with possible additional one or two dimensional positional order. In general, liquid crystal molecules are highly elongated with a fairly rigid long axis and thus have an energetic advantage in cooperative alignment, the position of benzene rings and polar groups on the molecule determines the range and type of the phase, by influencing the form of the intermolecular potential. The measure-

ment of suitably defined order parameters related to orientational and positional molecular order, provides valuable information on the nature of the intermolecular forces responsible for phase transitions and other thermodynamic properties of liquid crystal.

Classification and Nomenclature

There are three basic type of thermotropic liquid crystals. Following the classification of Friedel[3] they are named as Smectic, Nematic and Cholesteric.

1. Nematic:

i) Nematic liquid crystals have no translational order (Fig. 1.A).

ii) The molecules have free rotational motions about their long axis, but they have orientational order,

iii) The molecules tend to align parallel to some direction, $\vec{n}$.

iv) The molecules are assumed either to lack, or the dipoles are equally distributed in opposite directions. Statistically speaking, this means that the states of $+\vec{n}$ and $-\vec{n}$ are indistinguishable.

v) The nematic liquid crystals are optically uniaxial.

vi) The lattice space groups is $C_{\infty v}$

vii) The molecules are either optically inactive or, if they are optically active, there is a (1:1) mixture of right and left handed species in the nematic crystal.

de Vries[4] found another type of nematic phase called cybotactic nematic in which molecules group themselves into isolated planar arrays.

2. Smectic Liquid Crystals

i) All smectic liquid crystals have a layered structure (Fig. 1.2). The centre of gravity of the elongated molecules are arranged in equidistant planes.

ii) The long axes of the molecules are parallel to a preferred direction $\vec{n}$ which may be normal to the planes or tilted by a certain angle.

iii) The arrangement of the centre of gravity within the planes may be at random or regular.

iv) The inter layer attractions are small in comparison to the lateral forces and the layers are able to slide over one another. There are several types of smectic phases. Smectic A is the one in which the director is perpendicular to the plane of the layers, while in smectic C phase the director is tilted with respect to normal to the plane of the layers. The classification and characterisation of smectic phases are mainly done by Hermann[5], Sackmann[6] and Demus, Arnold[7].

The classifications were done by different workers by different methods, such as miscibility criterion, texture studies, X-ray datas. The smectic phases can be

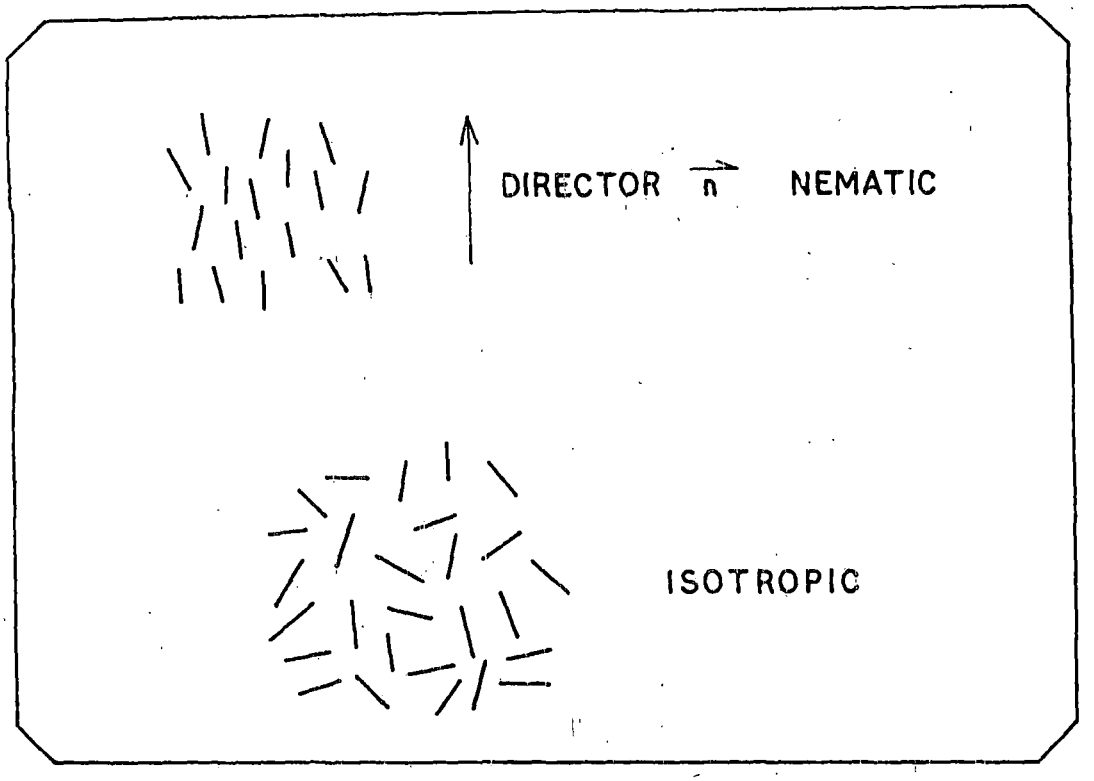

FIG. I.1. SCHEMATIC REPRESENTATION OF MOLECULES IN NEMATIC AND ISOTROPIC STATES.

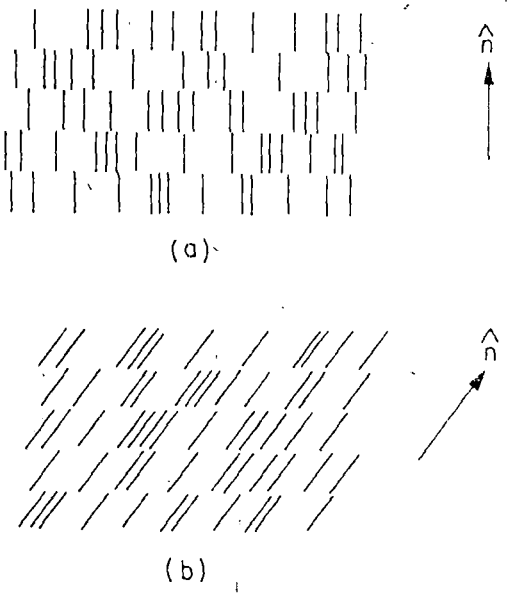

Fig I.2. Schematic representation of two types of smectic order: (a) smectic A order; (b) smectic C order.

arranged sequentially as smect, A, D, C, D, E, F, G, H....., where lower temperature phases stand further to the right.

3. Cholesteric Structure

i) The structure is a two dimensional nematic (Fig. 1.3).

ii) There is no long range order in the centres of gravity.

iii) The molecules are aligned along a perferred axis $\vec{n}$.

iv) $\vec{n}$ is not a constant in space and has a helical symmetry.

v) The pitch of the helix is temperature and concentration dependent.

Another type of liquid crystals was discovered by S.Chandrasekhar and Co-workers[8] a few years ago, called columner phase or canonic phase, where the flat disc like molecules are stacked in columns and so the plane of the molecules are perpendicular to the direction contrary to the former types where the molecules are parallel to the directors[9], (Fig. 1.4).

If a substance has both the phases, smectic and nematic, then on heating the crystalline solid phase melts into a smectic phase which subsequently transforms to the nematic isotropic phases.

$$C \rightleftharpoons S \rightleftharpoons N \rightleftharpoons I$$

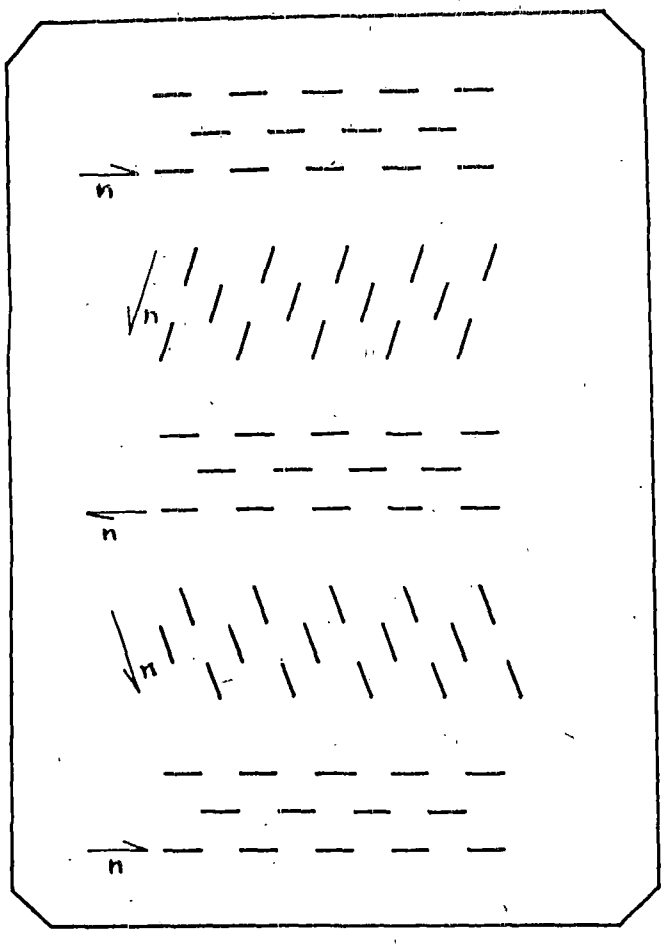

FIG. 1.3. SCHEMATIC REPRESENTATION OF CHOLESTERIC STRUCTURE.

(a)

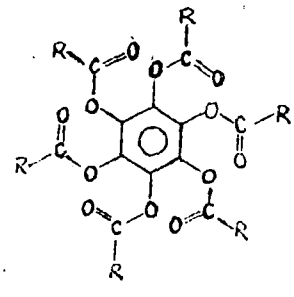

Disk Molecules

(b)

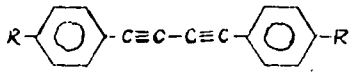

Diacetylenes

(c)

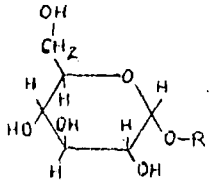

Glucopyranosides

Fig. 1.4. New Liquid Crystals

For example, terepthal-bis-(-p-butyl aniline) TBBA which has the chemical structure[10]

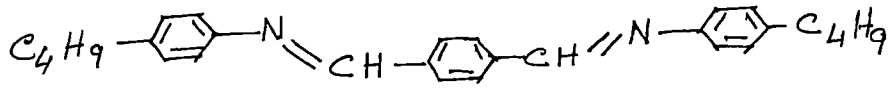

has the phases and transition temperature (°C) as given below:

$$C \underset{113^{\circ}C}{\rightleftharpoons} S_B \underset{144^{\circ}C}{\rightleftharpoons} S_C \underset{172^{\circ}C}{\rightleftharpoons} S_A \underset{200^{\circ}C}{\rightleftharpoons} N \underset{236^{\circ}C}{\rightleftharpoons} I$$

For a material having only smectic phase with the increase of temperature, the sequence of phase will be

$$C \rightleftharpoons S_n \rightleftharpoons I$$

With cholesterics and smectics, it has been observed experimentally that

(i) S ⟶ Ch ⟶ I

(ii) S ⟶ Smectic A ⟶ Ch ⟶ I

No substances has been found to exhibit both nematic and cholesteric phases, though cholesteric can undergo to nematic under the action of external electric and magnetic fields.

Gladis[11] found in binary mixtures of some mesogenic cyano compounds, that they followed on cooling the

scheme:- isotropic ⟶ nematic ⟶ smectic A nematic. The low temperature nematic, below the smectic phase, is called the re-entrant nematic phase. This phenomenon has also been observed by Cladis et al at elevated pressure[12,13] and by others at atmospheric pressure[14-16] in pure compounds.

Molecular Structure:-

Molecules showing mesomorphism possesses the following structure -

(i) The molecules are geometrically anisotropic, they are either rod-shaped, flat or lath shaped.

(ii) The molecules have some rigidity along the long axes so that parallel orientation may not be broken. The molecules should possess strong dipolar (Permanent or induced) and easily polarisable groups. The forces responsible for the mesophases are primarily dipole-dipole interactions and dispersive forces.

The melting point must not be too high, lest only supercooled metastable mesophases be formed monotropically. However, polarity of the terminal part frequently gives rise to very strong intermolecular attractions resulting in the rise of melting point.

Most of the thermotropic mesogens can be represented by

Terminal group 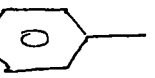 Central group  Terminal group

The terminal groups may be same or different. The central core is usually attached to the para positions of the benzene ring. These are easily polarisable and planar. The aromatic rings may also be connected directly[17] as in p-cyano-p'-pentyl biphenyl.

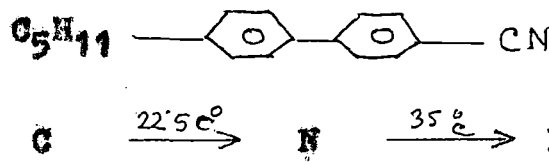

The mesomorphic behaviour is greatly influenced if the length of the rigid π core is increased by introducing additional aromatic rings, as in p-cyano-p'-n-pentyl terphenyl[17]

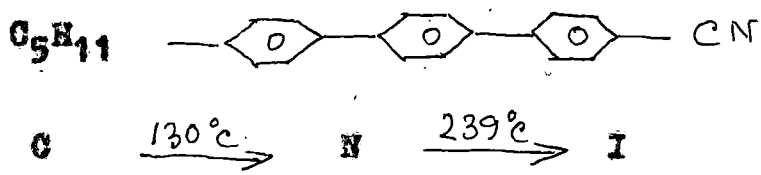

Often the central group certain multiple bonds to maintain rigidity and linearity as in P-azoxyanisole (PAA)

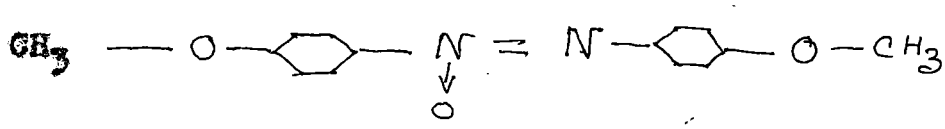

By studying the homologous series Gray[18,19] observed that certain general types of curves relating the transition temperatures to the number of carbon atoms in the series might be obtained and this could be used to correlate all the members of the series. He found - (i) The different phase transition temperatures (N — I, S — I, S — N) give smooth curve though the melting point do not show any uniformity. (ii) The clearing points of nematic phase decreases with increasing chain length. (iii) The N-I temperatures fit in two curves one for even and other for odd number of carbon atoms in n-alkyl chain, giving rise to the so-called 'Odd-even' effect. The N - I temperature decreases with a distinct alternation and the amplitude of the alternation also reduces with increasing chain length.

(iv) The plot of clearing points of smectics and the S - N transition temperatures usually reaches a maximum of a moderate chain-length and decreases gradually with further elongation of the chain. This plot normally shows no distinct odd-even effect[21].

(v) In a homologous series, shorter chains exhibit purely or predominantly nematic phases, while smectic phases dominate in longer chain molecules, at the expense of nematic thermal stability[18-21].

The effect of broadening of a molecule by introducing one or more substituents in place of hydrogens along the side of the core structure is given in detail by Gray[18].

The broadening reduces the anisotropic polarisability and consequently the intermolecular attractions. Young and his co-worker[22] studied the following compounds -

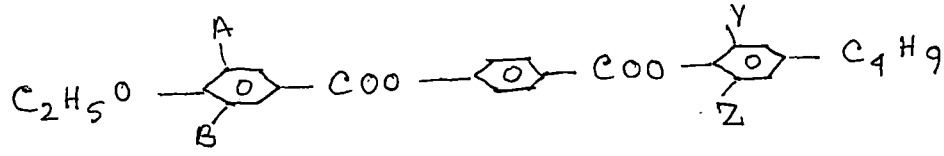

and found a systematic decrease in N —— I temperatures as the number of CH_3 group inserted at positions A, B or Y, Z was increased.

Theories of Nematic Liquid Crystals

In a macroscopic volume of a nematic liquid crystal, the preferential direction n is in general not uniform, but changes from place to place under the action of disturbing forces such as convection, flow, wall x effects, etc. However, even large samples can be aligned by both magnetic and electric fields.

In a homogeneously ordered liquid crystal sample the long axes of the molecules are parallel to the preferred direction. This holds only in a time or space average. In reality, due to their thermal energy, the individual molecules or small groups of molecules tumble about the preferred direction. The efficiency of the molecular orientation along $\vec{n}$ can be described by a single order parameter $\langle P_2 \rangle$

$$\langle P_2 \rangle = \tfrac{1}{2} \langle 3\cos^2\theta - 1 \rangle$$

where the brackets mean the time or space average and θ is the angle between the long molecular axis and the preferred direction. This ideal nematic order will be possible near the absolute zero point of the temperature only if material would not freeze. For an isotropic liquids $\langle P_2 \rangle = 0$.

The order parameter $\langle P_2 \rangle$ can be determined by measuring the principal refractive indices or the diamagnetic susceptibilities or X-ray diffraction. Other methods use the ultraviolet or infrared dichroism or nuclear magnetic resonance spectra.

Molecular Statistical Theory.

Maier and Saupe[23-25] developed a statistical theory to describe the liquid crystalline state and the molecular ordering for the nematic phase. In analogy to the treatment of ordering phenomenon in ferromagnetics or ferroelectrics this theory describes the intermolecular orientation forces by a mean field method. Each individual molecule feels a nematic potential which is given

$$U = - \frac{A}{V^2} \langle P_2 \cos\theta \rangle P_2 (\cos\theta)$$

where V is the molar volume, and A is a constant characteristic of the molecule, related to its polarizability.

The derivation is based on the model that the molecule alignment is caused by dispersion forces.

Only the induced dipole-dipole contribution is considered. The anisotropy of the molecular polarizability causes an angular dependence of the intermolecular dispersion forces and therefore is responsible for mesomorphic phase.

Humphries[26] have, however, shown that the assumption of the anisotropic dispersion forces for the formation of nematic phase was not essential. Thus a single molecule potential (mean field) can be set up to give particular orientation dependence (i) U should be minimum when the molecule is parallel to the director and maximum when the molecule is perpendicular to the director, thus U may be chosen to be proportional to

$$- P_2(\text{Cos } \theta) = - (3 \text{ Cos}^2 \theta - 1)/2 \qquad \ldots(2)$$

(ii) U must be proportional to $\langle P_2 \rangle$ the average degree of orientation. This potential which is responsible for nematic phase formation should vanish when $\langle P_2 \rangle = 0$ and be minimum when the molecules are highly ordered. Thus

$$U(\cos \theta) = - \upsilon \langle P_2 \rangle \text{Cos}\,\theta \rangle \theta \, P_2(\cos\theta) \qquad \ldots(3)$$

Orientational distribution function.

Orientational distribution function $f(\text{Cos } \theta)$ gives the probability of finding a molecule whose axis makes an angle θ with the director $\vec{n}$.

Orientational distribution function corresponding to the single molecule potential has the form

$$f(\cos\theta) = Z^{-1} \exp[-\beta U \cos\theta]$$

$$Z = \int_0^1 \exp[-\beta U(\cos\theta)] \, d(\cos\theta) \qquad \ldots(4)$$

where Z is the single molecule partition function $\beta = \frac{1}{KT}$, K is the Boltzmann's constant. T is the temperature in absolute unit. The limit of integration has been restricted within 0 and 1 because $\vec{n}$ and $-\vec{n}$ are indistinguishable. The dependence of the order parameter $\langle P_2 \rangle$ on the temperature T can be found by solving the self-consistency equation

$$\langle P_2 \rangle = \int_0^1 P_2(\cos\theta) f(\cos\theta) \, d(\cos\theta) \qquad \ldots(5)$$

using equation (4) in equation (5)

$$\langle P_2 \rangle = \frac{\int_0^1 P_2(\cos\theta) \exp[\beta v P_2(\cos\theta) \langle P_2 \rangle] \, d(\cos\theta)}{\int_0^1 \exp[\beta v P_2(\cos\theta) \langle P_2 \rangle] \, d(\cos\theta)} \qquad \ldots(6)$$

A computer programs has been used to obtain the value or values of $\langle P_2 \rangle$ (for any particular T (or β) that satisfies equation (6). $\langle P_2 \rangle = 0$ is a solution at all T, below certain temperature determined by $KT/v = 0.22284$, two other solutions appear. Of the three solutions below the critical temperature the one which satisfies the thermodynamic condition of minimum free energy will give the stable phase.

Extension of the Maier-Saupe Theory.

Humphries, James and Luckhurst[26] developed a more comprehensive concept by including higher order terms in the mean field potential for cylindrically symmetric molecules.

Their result is

$$U_1(\cos\theta) = \sum_L v_L \langle P_L \rangle (\cos\theta) \qquad \ldots(7)$$

U_1, is the single-molecule potential in the mean field approximation.

$$\langle P_L \rangle = \int_0^1 P_L(\cos\theta) f_1(\cos\theta)\, d(\cos\theta) \qquad \ldots(8)$$

where $f_1(\cos\theta)$ is the orientational distribution function and P_L's are the Lth. order terms of the Legendre Polynomial (L takes only even values). It has been the terms with L = 0 in (7) may be dropped since it is merely an additive constant. Then

$$U_1(\cos\theta) = v_2 \langle P_2 \rangle P_2(\cos\theta) + v_4 \langle P_4 \rangle P_4(\cos\theta) \qquad \ldots(9)$$

retention of only first term of equation (9) gives the Maier-Saupe theory.

Crystal Structure of Thermotropic liquid Crystals.

It is now well established that for proper understanding and interpretation of several physical properties of liquid crystalline phases a knowledge of the molecular structure in the crystalline phase is very useful. The molecular conformation in the crystalline state predetermines the molecular organisation in the mesomorphic state.

The first attempt to correlate the molecular arrangement in the mesophases with the crystal structure of the mesogenic material was undertaken by Bernal and Crowfoot[27] in the nearly 1930's. Upto 1974 only seven crystal structures had been determined[28]. This situation changed drastically with the advent of computer program in the late 1970s'. Now a large number of structures have been determined, most of them being nematic.

Preliminary survey of the present knowledge regarding solid mesophase relationships was given by Bryan[29]. On the basis of the evidence at hand it can be stated -

i) The molecules of the organic crystals when heated to the liquid crystalline state adopt an arrangement somewhat similar to that in the crystals[27].

ii) In nematic crystals the long narrow molecules are found to be more of less parallel and interleave one another to form an 'imbricated packing' (described by Bernal and Crowfoot). The transformation from the solid to the nematic phase is characterised by the breakdown of the positional order of the molecules but not of the orientational order[30].

iii) For smectic compounds the molecules are found to be packed in parallel array, as predicted[31].

This is true at least the majority of cases, so far known but at this stage we must be cautious to

generalise it[31]. Brown[32] found an imbricated packing for a nematogenic compound with the non-planner molecules arranged in herringbone fashion in planes perpendicular to the long axis. Brown and his co-workers[33] also found a herringbonic compound with a tilt relative to the layers. Bryan, Focier and Miller[34-36] also discussed the role of hydrogen bond in the formation of mesogenic compounds.

Applications:

Considerable basic research on the optical and electrical characteristics of liquid crystal was carried out during the later half of the this century to develop the applications of liquid crystals. It has been found that liquid crystals have got a wide range of scientific application.

The sharp changes in the color of x cholesteric liquid crystals with small changes in temperature have resulted in a number of unique temperature sensing applications[37]. As a result, applications to medical diagnostics, electronic component testing and aerodynamic structure analysis became feasible.

Nematic and cholesteric liquid crystals have already found wide application in display devices as many of their physical properties such as birefringence, optical activity etc. are sensitive to weak external perturbations. The remarkable electro-optic effects have

rendered it possible to prepare liquid crystal displays whose main advantage over the other types is that they do not require emissions of light, and so consume very low power. Liquid crystals are used in displays for watches, clocks, calculators, panel meters and other digital displays.

The x extremely low power requirements of the display coupled with further improvements in complimentary symmetry metal oxide semiconductor integrated circuits has made possible the development of pocket computer.

Liquid crystal displays are gaining acceptance in the digital instrument field, replacing light-emitting displays in applications where portability is of prime interest.

Liquid crystals are used in the flat pannel television displays. The progress of electronics, especially semiconductor electronics directs microtechnology which requires low voltage and low current devices. In this point of view LCD is most promising among various devices.

Recently, ferroelectric liquid crystals (S_c^*) have been used for a new generation of fast versatile liquid crystal devices.

Scope and Aim of the Work

Liquid crystals have enormous remarkable applications. For this purpose, identification of different phases, their electro-optic properties and molecular and crystal structure analysis are important. In the f present work six liquid crystalline substances namely PCCPP, PCTP, PBBA, EBBA, BPCPP and 5OCB have been chosen.

From X-ray diffraction photographs of magnetically aligned samples PCCPP, PCTP, PBBA and EBBA, orientational distribution function f(β), order parameters $\langle P_2 \rangle$ and $\langle P_4 \rangle$, have been calculated. X-ray diffraction studies in liquid crystalline phases of the samples BPCPP and 5OCB were done earlier in our laboratory. In the present work, optical birefringence studies of the samples PCCPP, PCTP, PBBA, BPCPP and 5OCB are done. The crystal and molecular structure of the sample PCCPP have been determined from X-ray diffraction. All the experimental works are reported in Chapter III and IV.

References

1. O.Lehmann: Z. Physik.Chem. 4 462 (1889)
2. G.Friedel: In Colloid Chemistry, Ed. J.Alexander Vol. I, P. 102 f f, The chemical catalogue company, Inc., N.Y. (1926).
3. G.Friedel and E.Friedel: Z.Krist. 79, 1, (1931).
4. A. de Vries: Crystallography in North America, Ed. D. McLachlan and T.P. Glusker, Am.Crystallographic Assoc., p. 333 (1983).
5. E.Alexander and K.A.Herrmann: Kristallogr. Kristallogeom. Abt. A69 285 (1928).
6. H.Sackmann and D.Demus: Fortschr. Chem. Forsch 12 349, (1969) Molecular Crystals, 2 81 (1966).
7. H.Arnold: Dissertaion, Halle 1959, East Germany.
8. S.Chandrasekhar, B.K.Sadashiva and K.A.Suresh: Pramana, 9 471 (1977).
9. C.Destrade, M.C.Bernand, H.Gasparoux, A.M.Levelut and N.H.Tinh: Liquid Crystals. Proceedings of Int. Conf. Bangalore, India, Dec. 3-8, 1979; Ed.S.Chandrasekhar, Heyden, p.29 (1980).
10. P.G.deGennes: The Physics of Liquid Crystals Clarendon Press, Chpter - 1 (1974).
11. P.E.Cladies, Phys. Rev.Letts. 35 48 (1975).
12. P.E.Cladies, R.K.Bogardus, W.Daniels and G.M.Taylor: Phys. Rev.Lett. 39 720 (1977).
13. P.E.Cladies, R.K.Bogardus and D.Adsen: Phys.Rev. A 18 2292 (1978).

14. N.V.Madhusudana, B.K.Sadashiva and K.P.L.Moodithaya: Curr.Sci. 48 613 (1979).

15. N.H.Tinh and H.Gasparovk: Mol.Cryst.Liq.Cryst.Lett. 49 287 (1979).

16. P.E.Cladis: Proc. Int.Liq.Cryst.Conf.Bangalore, Dec. 3-8, 1979, Ed.S.Chandrasekhar, P. 105,Heyden (1980).

17. G.H.Gray: The Molecular Physics ∗ of Liquid Crystals, Academic Press, Ed. G.R.Luckhurst and G.W.Gray, p.6 (1979).

18. G.H.Gray: Mol.Structure and Properties of Liquid Crystals, Academic Press, N.Y. (1962).

19. G.W.Gray; Advance in Liquid Crystals, Ed.G.H.Brown Academic Press, N.Y. (1976).

20. H.Kelker and R.Hats: Hand Book of Liquid Crystals, Verlag Chemie, Ch.2 (1980).

21. G.W.Gray: Liquid Crystals and Plastic Crystals,vol.1, Chapt.4, Ed.G.W.Gray, P.A.Winsor and Ellis Horwood (1974).

22. W.R.Young, I.Heller and D.C.Green: J.Organ.Chem. 37 3707 (1972), W.R.Young and D.C.Green: Mol.Cryst.Liq. Cryst. 26, 7 (1974).

23. W.Maier and A.Saupe: Z.Naturforsch. 13a 564(1958).

24. W.Maier and A .Saupe: Z.Naturforsch, 14a 882 (1959).

25. W.Maier and A.Saupe: Z.Naturforsch 15a 287 (1960).

26. R.L.Humphries, P.G.James and G.R.Luckhurst: J.Chem. Soc.Faraday Trans. II, 68 1031 (1972).

27. J.D.Bernal and D.Crowfoot: Trans.Faraday Soc. 29 1032 (1933).

28. D.B.Chung: Ph.D.Dissertation, Kent State University, p. 38 (1974). Pub.University Microfilms International, Ann Arbor, Michigan, USA, 75-11, 987.

29. R.F.Bryan: Proc.of the Pre-Congress Symp. on Orgn. Crystals Chem.Poznan, Poland, p-105 (1979).

30. S.Chandrasekhar: Liquid Crystals, Cambridge Univ. Press, P-14 (1977).

31. A.J.Leadbetter and M.A.Mazid: Mol.Cryst.Liq.Cryst. 51, 85 (1979), 65 265 (1981).

32. G.H.Brown: Advances in Liquid Crystals, Academic Press, NY (1976); J.Colloid Interface Sci. 58 534 (1977).

33. D.B.Chung, R.B.Carpenter, A deVries, J.W.Reed and G.H. Brown: J.Cryst. Mol.Struct. 8(2), 81 (1978).

34. R.F.Bryan, P.Hartley, R.W.Miller and M.Shen: Mol. Cryst.Liq.Cryst; 62 281 (1980).

35. R.F.Bryan, P. Hartley and R.W.Miller: Mol.Cryst. Liq. Cryst. 62 311 (1980).

36. R.F.Bryan and P.Hartley: Mol.Cryst.Liq.Cryst. 69 47 (1981).

37. J.Pergason: Mol.Cryst. 1 309 (1966).

CHAPTER II

THEORETICAL BACKGROUND FOR X-RAY WORK.

2.1. Introduction

In the references[1-4] the X-ray diffraction studies of liquid crystals have been reviewed and the detailed theoretical considerations are given in references[5-6]. From X-ray diffraction study we can get idea about molecular interactions in liquid crystals. First attempt was made by Lingen[7] and Friedel[8]. Generally nematic liquid crystals samples consist of a large number of domains, the molecules are ordered within x each domain x in a preferred direction (director $\vec{n}$) but there is no preferred direction for the specimen as a whole. So the X-ray diffraction pattern has a symmetry of revolution around the direction of the X-ray beams. It is evident from the uniform halo just like that of an isotropic liquid. Diffraction photograph of the sample oriented by some means are therefore, needed to specify the state of ordering. With the help of intensity distribution in the equatorial plane of the diffraction pattern (oriented) one can obtain the cylindrical distribution function, giving the probability of finding two atoms at a particular distance, the atoms however, may belongs to same or different molecules. Moreover, according to Chistyakov[3], the method involves an integration over the scattering vector from zero to infinity which can never be fulfilled by photographic methods with a flat plate camera, the plate being normal to the X-ray beam. Calculation of cylindrical distribution

function and order parameters from X-ray diffraction works has been done by de Vries[9], while orientational distribution function and order parameters have been calculated by various workers[10-14].

2.2. Average Intermolecular Distance, Apparentlength of the Molecules and Layer Thickness (in case of smectic)

In general it is possible to calculate a spacing X, from the position of a diffraction maxima by a formula of the type

$$2X \sin\alpha = K_1 n\lambda \qquad \ldots(1)$$

Here 2α is the diffraction angle measured between the incident and diffracted beams, $\vec{n}$ is the order of reflection, K_1 is a constant depending on the shape and arrangement of the molecule.

De Vries has discussed the equations and, their applications and their limit in details[15,16], We used K = 1 in equation (1) for determining the apparent molecular length.

For both the oriented and un-oriented samples we have used K = 1.117 to calculate the intermolecular distance (D). This is because of the fact that, considering the x scattering from a pair of molecules of a distance D apart, if the chains are allowed to rotate freely around each other, the positions of the maxima along the equator are determined by the function[15],

$$J_0(x) = \int_0^{2\pi} \cos(x\cos\alpha)\, d\alpha$$

where $X = 4\pi/\lambda \cdot D \sin\alpha$ and this gives for first maxima $K_1 = 1.117$.

Wendorff et al[17] calculated K values from the photograph of some cholesteral esters by taking K values in eqn. (1) from completely extended form of the molecules and found that K lies between 1 for perfectly order molecule and 1.229 for random orientation of the molecules.

2.3. Orientational distribution functions and order parameters.

For a system of cylindrically symmetric molecules one can define an orientational distribution function $f(\beta)$ depending on the angle between the molecular symmetry axis and the directors[14], which gives an average states of orientation of the long axis of the molecules. The X-ray diffraction photographs record intensities averaged over a sufficiently long time and over a sufficiently large volume, so the molecules may be assumed to have an average cylindrical symmetry, even if they are not rotating about their long axes[4]. For a system of rigid rods the order parameters $\langle P_2 \rangle$ and $\langle P_4 \rangle$ may be defined by

$$\langle P_L \rangle = \frac{\int_0^{\pi/2} P_L(\cos\beta) f(\beta) \sin\beta d\beta}{\int_0^{\pi/2} f(\beta) \sin\beta \, d\beta} \qquad \ldots(2)$$

where $L = 2$ and 4; $P_L(\cos\beta)$ is a well known Legender polynomial of order L. Leadbetter et al[11,12] reported the measurements of $f(\beta)$, by X-ray method.

In relating the X-ray intensities $I(\Psi)$ around the diffuse equatorial arc (Fig. 2.1) with the orientational distribution function, Leadbetter and Norris[11] assumed the molecules as rigid rods perfectly aligned in a cluster of a small number of molecules and obtained

$$I(\Psi) = c \int_{\beta=\Psi}^{\pi/2} f_d(\beta) \sec^2\Psi \left[\tan^2\beta - \tan^2\Psi\right]^{-\frac{1}{2}} \sin\beta \, d\beta \qquad \ldots(3)$$

where $f_d(\beta)$ describes the distribution function of the clusters in which the molecules are perfectly aligned. They also assumed that for a perfect aligned sample $[f_d(\beta) = \delta(\beta)]$, the scattering is zero except for the directions of the scattering vector perpendicular to cluster axis. They have however, calculated the effects and shown that the deviations are negligible except for highly ordered, phases ($\langle P_2 \rangle \geq 0.8$). Further comparing the values $f_d(\beta)$ with $f(\beta)$ of the same samples obtained by other methods they have shown that the values of $f_d(\beta)$ is same as that of the true singlet orientational distribution function.

Because of the molecular distribution in the nematic phase centro-symmetric, the distribution function and intensity distribution function can be expanded in the form[11,18]

$$I(\Psi) = \sum_{n=0}^{\infty} a_{2n} \cos^{2n}\Psi \qquad \ldots(4)$$

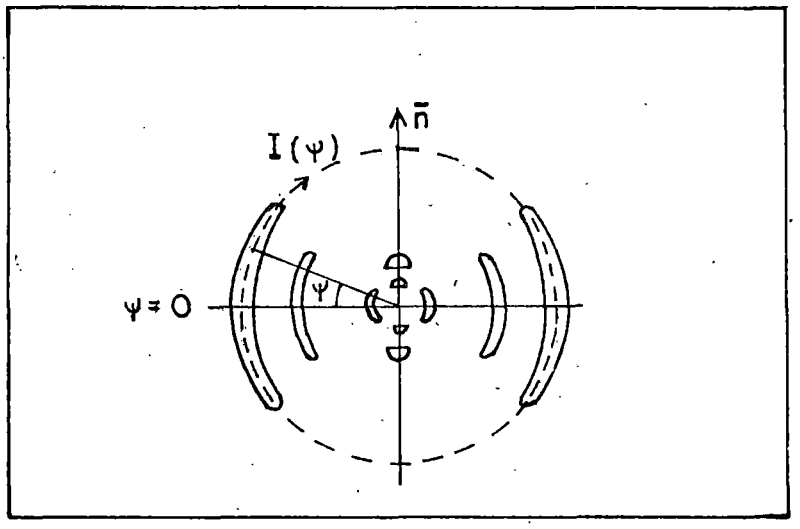

Fig. 2.1. Schematic representation of the X-ray diffraction photograph of an oriented liquid crystal.

$$f(\beta) = \sum_{n=0}^{r} b_{2n} \cos^{2n}\beta \qquad \ldots(5)$$

In eqn. (2) by substituting $\sin\alpha = \cos\beta \sec\psi$ we get,

$$I(\psi) = c\int_0^{\pi/2} f_1(\alpha) \sin\alpha \, d\alpha \qquad \ldots(6)$$

From eqn. (3), (4) and (5) we get,

$$\sum_{n=0}^{r} a_{2n}\cos^{2n}\psi = \int_0^{\pi/2} \sum_{n=0}^{r} b_{2n}\cos^{2n}\psi \sin^{2n+1}\alpha \, d\alpha$$
$$= \sum_{n=0}^{r} b_{2n}\cos^{2n}\psi \int_0^{\pi/2} \sin^{2n+1}\alpha \, d\alpha$$

$\ldots(7)$

As ψ is arbitrary, the coefficients of $\cos^2\psi$ must be equal. Now

$$\int_0^{\pi/2} \sin^{2n+1}\alpha \, d\alpha = \frac{2^n (n!)^2}{(2n+1)!}$$

so

$$b_{2n} = a_{2n} \frac{(2n+1)!}{2^{2n}(n!)^2} \qquad \ldots(8)$$

The series in eqn. (4) and (5) converges rapidly. Keeping eight terms in the truncated series, a least square fitting is made to obtain the coefficients from

eqn. (4) with the corrected experimental intensity values. We find the calculated intensity values agreed with the observed values in all cases. These values of a_{2n} are then used to calculate the coefficients b_{2n} in the truncated series for $f(\beta)$ in eqn. (5) with the help of eqn. (8) $f(\beta)$ is then calculated using eqn.(5).

By calculating the ingegral

$$\int_0^{\pi/2} f(\beta) \sin\beta \, d\beta = K \quad \text{say}$$

and then dividing all the b_{2n} values by K we obtain the normalised values of the orientational distribution function so that now

$$\int_0^{\pi/2} f(\beta) \sin\beta \, d\beta = 1 \qquad \ldots(9)$$

Substituting eqn.(4) in eqn.(1)

$$\langle P_2 \rangle = \frac{1}{2} \frac{\int_0^1 (3\cos^2\beta - 1) \sum_{n=0}^{\infty} b_{2n} \cos^{2n}\beta \, d(\cos\beta)}{\int_0^1 \sum_{n=0}^{\infty} b_{2n} \cos^{2n}\beta \, d(\cos\beta)} \qquad \ldots(10)$$

This can be written in terms of standard integrals and $\langle P_2 \rangle$ can be calculated. Similarly $\langle P_4 \rangle$ also can be calculated.

Vainshtein[19] obtained a fairly good approximation for the order parameters by replacing $f(\beta)$ values with $I(\Psi)$ values keeping the Bragg angle constant in eqn(1).

We calculated the order parameter value using Vainshtein's approximation and designated them as $\langle P_2 \rangle_V$ and $\langle P_4 \rangle_V$

2.4. Experimental Technique and Data Analysis.

All the X-ray diffraction photograph were taken in flat plate camera, (Fig. 2.2) fabricated in our laboratory with M/s. Radon House (India) X-ray Unit fitted with copper target. The details of experimental set up has been described by B.Jha et al[20]. The set up has the high temperature attachment, has the provisions for interchanging collimeter, changeable spacer to vary the sample to filament distance and changable gap between pole pieces of the electromagnet, all the material used are non-magnetic.

The temperatures of the sample was regulated within $\pm$ 0.5°C by a Indotherm 101, Temperature Controller. The S sample holder was calibrated upto 250°C with know m.p. samples. Strength of the magnetic field between the pole-pieces was measured with a sensitive gaussmeter (ECIL model GH 867). Ni filter of thickness 0.009 was used for all photographs to obtain nearly monochromatic CuK_α radiation of wavelength 1.542 Å. The Collimater used was of 1 mm. aparture. The exact distance between the film and the sample was determined by taking Aluminium Powder X-ray diffraction pattern. For Al, the unit cell dimension is known, the Bragg angle for hkl reflecting

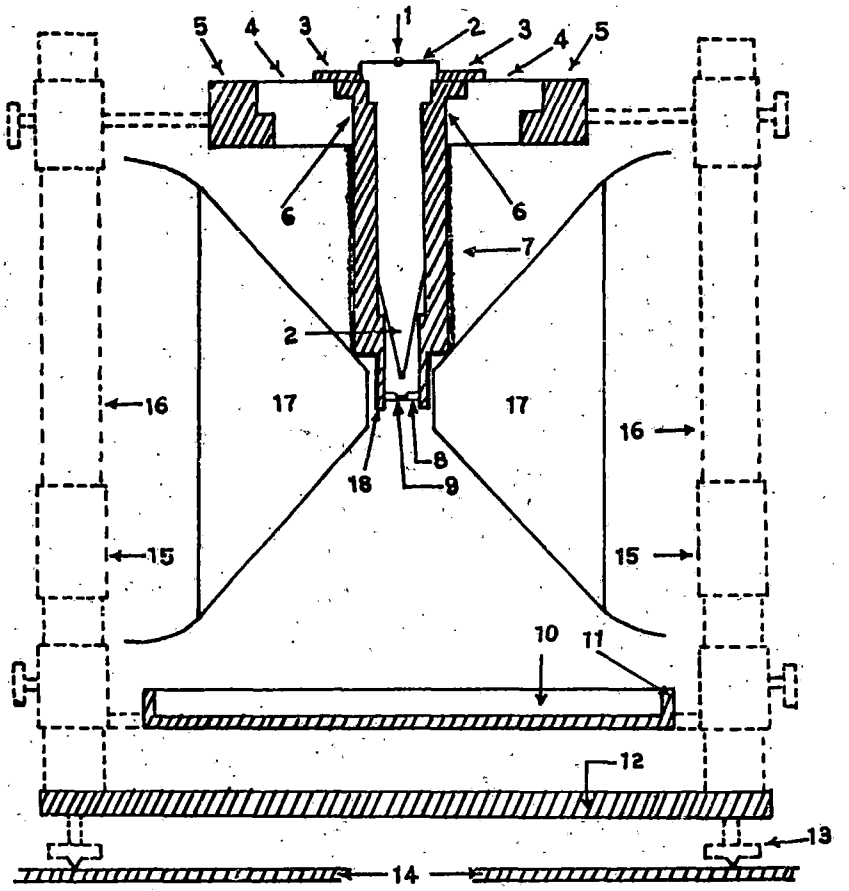

Fig.2.2 Sectional diagram of the camera:
(1) X-Ray; (2) Collimator; (3) Brass Ring; (4) Ring of Syndanio Board; (5) Brass Ring; (6) Cylindrical Brass Chamber; (7) Asbestos insulation and Heater Winding; (8) Specimen Holder and Thermocouple; (9) Specimen; (10) Film Cassette; (11) Film Cassette Holder; (12) Base Plate; (13) Levelling Screw; (14) Brass Plates over the Coils of Electromagnet; (15) Removable Spacer; (16) Supporting Brass Stands; (17) Polepieces; (18) Asbestos insulation.

plane can be determined from

$$\sin\theta' = \frac{\lambda}{2a}\sqrt{h^2+k^2+l^2} \qquad \ldots(11)$$

Measuring the diameter of the diffraction ring corresponding to (111) and (200) reflections[21] the exact distance between the sample and the film can be obtained from the relation

$$\tan 2\theta' = \frac{\text{Radius of the ring}}{\text{Sample to film distance}} \qquad \ldots(12)$$

Then the correction term was calculated and applied to the spacer separation to obtain the exact distance.

2.5. Conversion of Optical Density to X-ray Intensity.

The X-ray diffraction photographs were scanned with a Carl Zeiss Microdensitometer (MD 100) both linearly and circularly. The Microdensitometer has potentiometries recording (K200) facility for linear scanning and the circularly scanning was done mannuallky with a rotation stage modified to enable 360° scan by us. The optical density values thus obtained were converted to relative intensity values by a method explained by Klug and Alexander[21](Fig. 2.3).

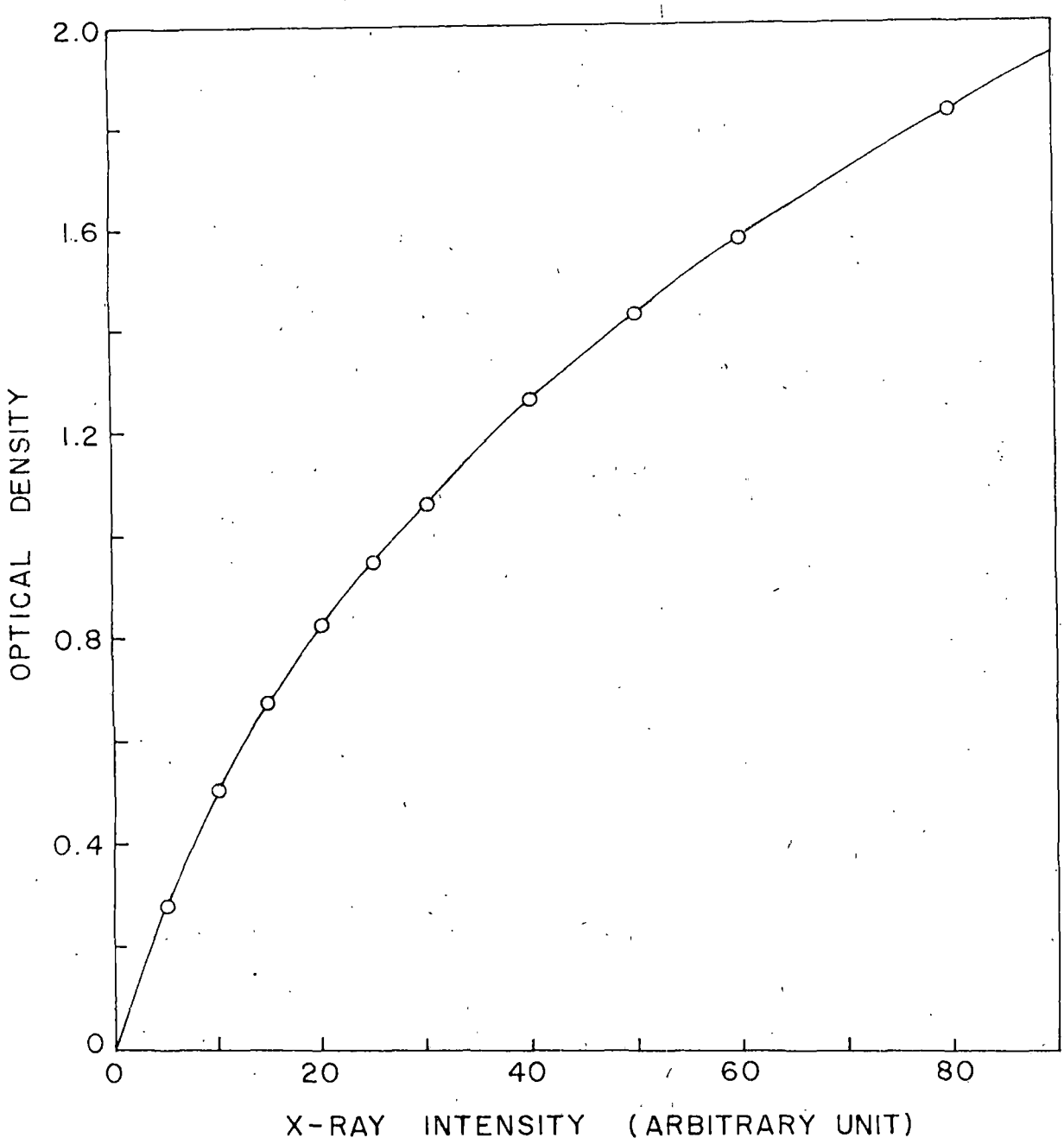
2.0
1.6
1.2
0.8
0.4
0
OPTICAL DENSITY
0
20
40
60
80
X-RAY INTENSITY (ARBITRARY UNIT)

Fig. 2.3

2.6. Linear Scanning and Location of Peak Positions.

A graph relating optical density VS. linear distance is obtained from the linear scan of the outer maxima (Fig. 2.4) through the central spot using the potentiometer recorder. The difference between the peak points of the outer maxima gives its diameter. Peak points can be located by different well known methods (Fig. 2.5), when the peak is well defined we simply take the Po position in some cases we used other positions also ($P_{1/2}$, $P_{3/2}$) . After knowing the diameter, the Bragg angle corresponding to this diffraction is determined by using eqn. (12) and then average intermolecular distance (D) is calculated using eqn. (1). The same procedure is applied to determine diameter of the inner ring.

Actually in order to get the diameter of the outer crescents accurately, several linear scans were made with different azimuthal angular positions. Considering $I(\Psi) \neq 0$ at the maximum intensity x position, the linear scan were done for $\Psi = 0, \pm 30^{\circ}$. The mean of the diameters obtained was taken as the actual diameter.

2.7. Circular Scanning and $I(\Psi)$ Versus Ψ Curves Plotting.

To determine the orientational distribution function $f(\beta)$ and order parameters $\langle P_2 \rangle$ and $\langle P_4 \rangle$ circular scanning is necessary. The values of the optical density obtained from microdensitometric circular scan were converted to X-ray intensities with the help of the calibration

curve. This values were plotted against azimuthal angular position. The correction was done for the background intensity values arising due to the air scattering. The peak intensity position which corresponds to $\Psi = 0$ was determined (Fig. 2.6). However, in some cases some unwanted spots for even a slight non-uniformity in film coating create some problems. In such cases a smooth curve was drawn through the large number of points. Symmetric curve around $\Psi = 0$ was drawn very carefully. Mean I (Ψ) values of the four quadrants were used to obtain $Ff(\beta)$. $\langle P_2 \rangle$ and $\langle P_4 \rangle$ values.

Considering nineteen I (Ψ) values from $\Psi = 0^0$ to $\Psi = 90^0$ at 5^0 intervals from the smooth I (Ψ) VS Ψ curve, f (β) $\langle P_2 \rangle$ and $\langle P_4 \rangle$ values were calculated by using Leadbetter's approximation. f(β) VS β curve was drawn. To perform this calculations a computer program has been developed and used in Hipro Series 8600 Computer.

2.8. Refractive Index

Theoretical considerations -

The birefringence of liquid crystals is the visible manifestation of their long-range order and it is defined only for a uniformly ordered domain. Its value is determined by the degree of order S and by the principal polarizabilities, α_o and α_e for unixial systems. These are interrelated by the following equation

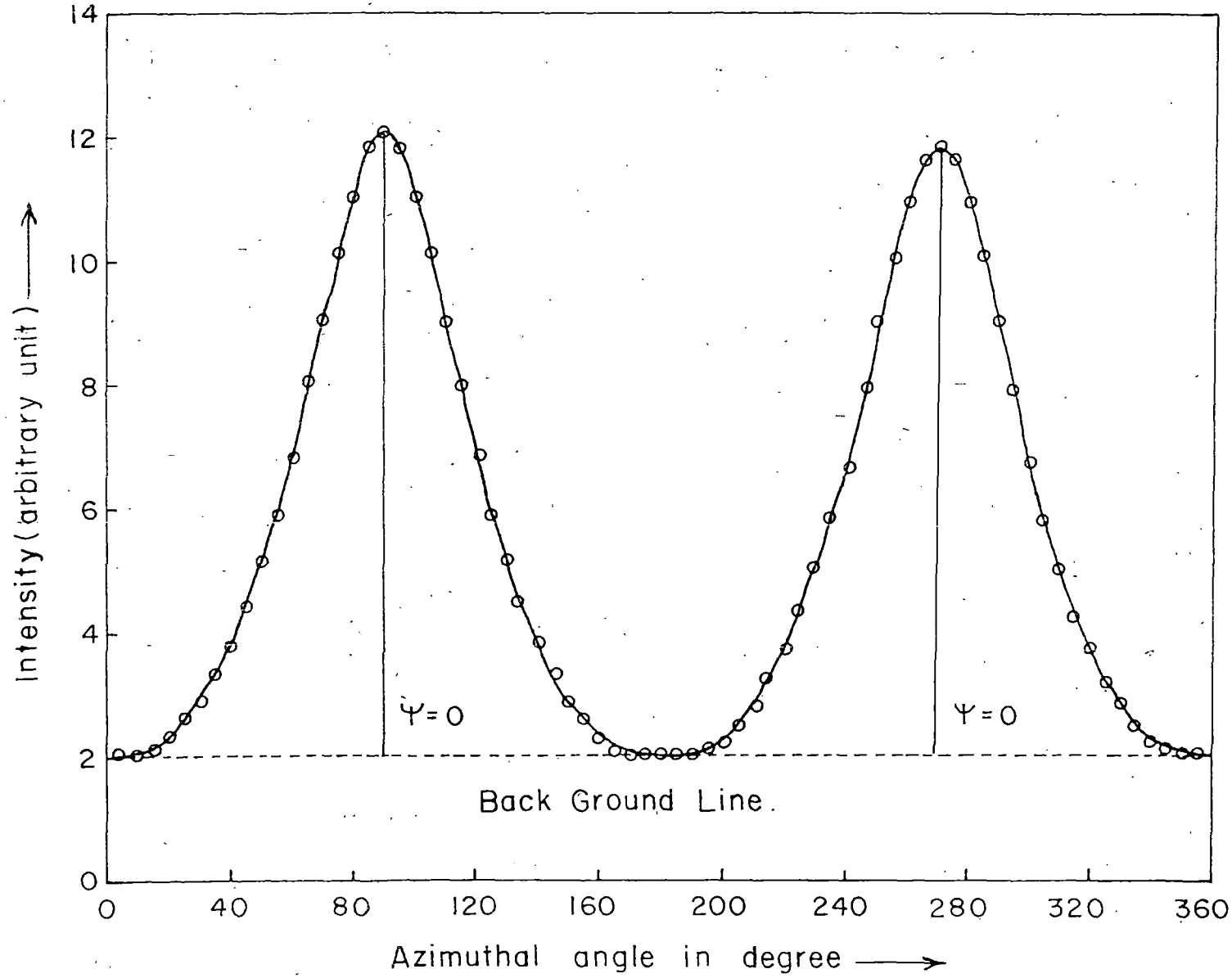
14
12
10
8
6
4
2
0
Intensity (arbitrary unit)
Ψ = 0
Ψ = 0
Back Ground Line.
0
40
80
120
160
200
240
280
320
360
Azimuthal angle in degree

Fig. 2.6

$$S = \frac{(\alpha_e - \alpha_o)_{nematic}}{(\alpha_e - \alpha_o)_{S=1}} \qquad \ldots(13)$$

By studying the birefringence we can estimate the orientational ordering in the liquid crystals at different temperatures. Because of the anisotropy of the molecular arrangements in the liquid crystalline phase the well-known Lorentz-Lorentz formula for liquid phase is generally replaced by Vuks'[22] formula, Neugebauers' relations[23] or Saupe and Maier anisotropic model[24]. Chandrasekhar suggested the most comprehensive theory started with the total interaction energy U. We have used both Vuks' and Neugebauer's equations to calculate the polarisabilities

2.9. Vuk's relation

$$(n_o^2 - 1)/(n^2 + 2) = 4\pi N\alpha_o/3 \qquad \ldots(14)$$

and

$$(n_e^2 - 1)/(n^2 + 2) = 4\pi N\alpha_e/3 \qquad \ldots(15)$$

Neugebauer's equations for calculating the polarisabilities are as follows

$$\frac{1}{\alpha_e} + \frac{2}{\alpha_o} = \frac{4\pi N}{3}\left[\frac{n_e^2 + 2}{n_e^2 + 1} + \frac{2(n_o^2 + 2)}{n_o^2 - 1}\right] \qquad \ldots(16)$$

and

$$\alpha_e + 2\alpha_o = \frac{9}{4\pi N}\left[\frac{n^2 - 1}{n^2 + 2}\right] \qquad \ldots(17)$$

Here $n^2 = (2n_o^2 + n_e^2)/3$, n is the mean refractive index and N is the number of molecules per c.c.

The relation between the order parameters and polarizabilities (α_o, α_e) is given by[25]

$$\alpha_e = \alpha + \frac{2}{3}\alpha_a . S$$
$$\alpha_o = \alpha - \frac{1}{3}\alpha_a . S$$

where $\alpha = (2\alpha_o + \alpha_e)/3$ is the mean polarizability $\alpha_a = (\alpha_{11} - \alpha_\perp)$ is the molecular polarizability anisotropy.

Therefore $$S = \frac{\alpha_e - \alpha_o}{\alpha_{11} - \alpha_\perp} \qquad \ldots(18)$$

To get the value of ($\alpha_{11} - \alpha_\perp$) we followed the most widely used Haller's extrapolation procedure[26].

2.10. Experimental Procedures.

Refractive indices were measured with the help of hollow glass prisms with a refracting angle of about 1^0. The prisms are made up of optically flat glass plates. The plates were rubbed parallel to one of their edges they were then treated with 1 percent polyvinyl alcohol solution and then dried. Again they were rubbed along the same direction as before. The prisms were formed keeping the treated surface inside and rubbing directions parallel to the edge of the prism. The prisms were precalibrated by measuring the refractive indices of distilled water and glycerine at different temperatures. They were compared with those measured with Abbe's refractometer.

The liquid crystal samples were allowed to flow in the prism by melting a few crystals at the top. The samples were then cooled very slowly in the presence of magnetic field (0.6 Tesla) applied in the direction of rubbing. The combination of rubbing and flow together with the x magnetic field produced a homogeneous nematic specimen with the optic axis parallel to the edge of the prism. The experimental details of this procedure were given by Zeminder et al[27]. The prismswere put inside a brass thermostat heated electrically and controlled by a temperature controller to $\pm$ 0.5°C. A precision spectrometer and a nicol prism were used to measure the refractive indices (n_o , n_e), for different wave lengths. The densities were determined (within $\pm$ 0.1 %) by putting weighed samples inside a glass capillary tube which was placed in a water both heated using a temperature controller. Sufficient time was allowed for attaining the desired temperature. The length of the column was measured by a travelling. The densities were calculated after correcting for the expansion of the glass capillary.

References

1. J.Flagueirettes and P.Delord: Liquid Crystals and Plastic Crystals. Ed. G.W.Gray and P.A.Dinsor, Vol.2 Ch. 3, Ellis Horwood (1974).
2. H.Kelker and R.Hatz, Hand Book of Liquid Crystals Ch. 5, Verlag Chemie (1980).
3. I.G.Chistyakov; Sov. Phys. Usp. 9, 551 (1967).
4. L.V.Azaroff; Mol.Cryst. Liq.Cryst. 60, 73 (1980).
5. B.K.Vainshtein; Diffraction of X-rays by Chain Molecules; Elsevier Publishing Co., (1966).
6. A.J.Leadbetter; In the Molecular Physics X of Liquid Crystals, Ed. G.R.Luckhurst and G.W.Gray, Ch. 13, Academic Press (1979).
7. J.S.V.D.Lingen; Ber.Dt.Chem.Ges. 15, 913 (1913).
8. G.Friedel; Annls.Phys. 18, 273 (1922).
9. A.deVries; J.Chem.Phys. 56, 4489 (1972).
10. P.Delord and J.Palgueirettes, C.r.hebd; Seanc. S.Acad. Sci. Paris 260 2468 (1965).
11. A.J.Leadbetter and E.K.Norris; Mol.Phys. 38, No.3, 669 (1979).
12. A.J.Leadbetter and P.G.Wrighton; J.De Physique Collogue, 40 c, 3-234 (1979).
13. B.Bhattacharjee, S.Paul and R.Paul, Mol.Phys. 44,No.6, 1391 (1981).
14. C.Zannoni; The Mol.Phys. of Liquid Crystals, Ed. G.R.Luckhurst and G.W.Gray,Academic Press, Ch.3(1979).

15. A. deVries; Mol.Cryst.Liq.Cryst. 10 31 & 219 (1970)

16. A. deVries; Mol.Cryst.Liq.Cryst., 11, 361 (1970), 20 119 (1973).

17. J.H.Wendorff and E.P.Price; Mol.Cryst.Liq.Cryst. 24, 129 (1973).

18. P.G.deGennes; The Physics of Liquid Crystals Ch.2, Oxford (1974).

19. B.K.Vainshtein; Diffraction of X-rays by Chain Molecules, Elsevier, Pub.Co. (1966).

20. B.Jha and R.Paul; Proc.Nucl.Phys.Solid State Physics Symp. India 19c, 491 (1976).

21. H.P.Klug and L.E.Alexander; X-ray Diffraction Procedures; John Wiley and Sons, Ch.3 (1974).

22. M.F.Vuks; Optics and Spectroscopy; 20, 361 (1966)

23. H.E.J. Neugebauer; Canad.J.Phys. 32, 1 (1954).

24. Ref. 23, 24 and 25 of Chapter 1.

25. P.G.de Gennes; Mol.Cryst.Liq.Cryst. 12, 193 (1971).

26. I.Haller,H.A.Huggins, H.R.Lilinthal and T.R.McGuire, J.Phys.Chem.77, 950 (1973).

27. A.K.Zeminder,S.Paul and R.Paul; Mol.Cryst.Liq.Cryst. 61, 191 (1980).

CHAPTER - III

EXPERIMENTAL RESULTS

3.1. X-ray Diffraction and Bi-refringence Studies on PCCPP, PCTP and PBBA.

3.1.1. Introduction:

We have determined order parameters from X-ray diffraction studies and also from bi-refringence measurements for some compounds having nematic phase. The names, structural formulae and transition temperatures are given below

I. 5-(4''- n-Pentyl Cyclohexyl)-2-(4'-Cyanophenyl)-Pyrimidine (PCCPP in short).

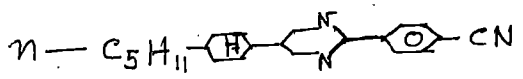

Solid $\underset{68^{\circ}C}{\overset{100.6^{\circ}C}{\rightleftharpoons}}$ Nematic $\overset{234.9^{\circ}C}{\rightleftharpoons}$ Isotropic

II. 4''-n-Pentyl-4-Cyano-p-terphenyl (PCTP in short)

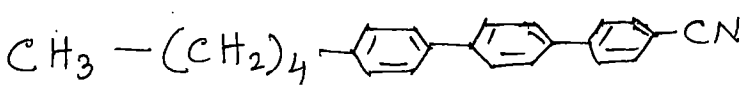

Solid $\overset{129.8^{\circ}C}{\rightleftharpoons}$ Nematic $\overset{238.5^{\circ}C}{\rightleftharpoons}$ Isotropic

III. p-n-Propoxy benzylidene-p-n-butylaniline (PBBA in short)

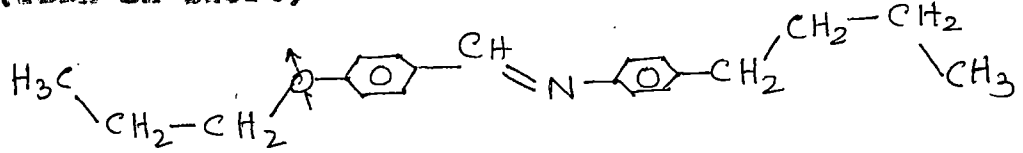

Solid $\underset{<0^{\circ}C}{\overset{40.5^{\circ}C}{\rightleftharpoons}}$ Nematic $\overset{58.5^{\circ}C}{\rightleftharpoons}$ Isotropic

The samples I and II was supplied by M/s. F.Hoffmann La-Roche & Co. in the purified form and sample III by Prof. M. Wada of Tohoku University, Japan. The sample III (PBBA) has a supercobling well-bellow the room temperature.

3.1.2. Texture Study

A polarizing microscope with magnification 150X equipped with a hot stage has been used to examine the melting behaviour of the liquid cryetals. The transition temperature and supercooling regions found thereof are as stated earlier. Under cross polarising microscope different phases were tried to identify. Nematic thread like textures are obtained in case of sample II and III and thread like textures with inversion line was obtained for the sample I.

3.1.3. X-ray Study:

X-ray diffraction photographs of the samples were taken at different temperature in presence of magnetic field using nickel filtered CuKa radiation of $\lambda = 1.5418$Å. The temperatures were measured and regulated with an accuracy of $\pm$ 0.5°C with the help of a temperature controller (Indotherm 401). The experimental set up, techniques and procedure for analysing X-ray diffraction photographs have already been discussed in the previous chapter. The samples were heated to isotropic state and a magnetic field of about 0.58 Tesla was applied to it. After the magnetic field is stabilised, the sample was allowed to cool slowly to the

desired temperature in the nematic state, and the X-ray photographs were then taken. All the photographs of aligned samples were scanned circularly and linearly with the help of a densitometer (VEB Carl-Zeiss Jena, Microdensitometer Modal - 100). The optical densities were converted to X-ray intensities and orientational order parameters were calculated with the help of computer program developed by us. The photographs of the aligned samples at different temperature distinctly indicate the presence of nematic phase, Fig. 3.1 - 3.3.

Intermolecular distance (D) and Apparent Molecular Length(l):-

The average intermolecular distance (D) and the apparent molecular length (l) have been calculated by using the procedure already stated in Chapt. II. Variation of D and l with temperature is shown in Fig. 3.4 - 3.6. With the help of stereo model unit (Prentice Hall Inc, West Nyack, New York) the possible conformations for the samples were constructed and the molecular lengths (L) in their most extended form were found to be 21 Å, 20.4 Å, and 20.5Å respectively. The average apparent molecular length of the oriented samples as determined from the inner ring of the X-ray diffraction photographs are 26.24 Å, 26.2 Å and 22 Å respectively. Table 3.1 shows the comparison of l and L values. The ratio of l to L are 1.25 and 1.28 for samples PCCPP and PCTP. This may be due to the local strong bi-molecular associations due to high dipole moments. The association is assumed to be an overlapping head to tail

Table 3.1

Compounds	Molecular length from model Kit(L)	Apparent molecular length (average) (l)	l/L
PCCPP	21	26.24	1.25
PCTP	20.4	26.2	1.28
PBBA	20.5	22	1.07

nature having a tendency to local layer formation. Similar results have been found in other nematics[1-3].

Normalised Orientational Distribution Function and Order Parameter $\langle P_2 \rangle$ and $\langle P_4 \rangle$.

For the three samples the normalised orientational distribution function $f(\beta)$ were calculated using the procedure described earlier. The order parameter values $\langle P_2 \rangle$ and $\langle P_4 \rangle$ were also calculated. Table 3.2 - 3.10 show the detail values of the samples for intensity $I(\Psi)$, calculated intensity $I(\Psi)$ and normalised distribution $f(\beta)$ at different temperatures. The Fig. 3.7, 3.8 and 3.9 show the plot of $f(\beta)$ Vs β at different temperatures.

The procedure for calculating $\langle P_2 \rangle$ and $\langle P_4 \rangle$ values have already been described. The $\langle P_2 \rangle$ and $\langle P_4 \rangle$ values of the samples are calculated from the distribution

function with Vainstein approximations and with Leadbetters' approximations. Fig. 3.10 - 3.12 show the variation of $\langle P_2 \rangle$ and $\langle P_4 \rangle$ values with temperature determined by different techniques.

3.1.4. Optical birefringence study:

The procedure for measuring the refractive indices (n_o, n_e) and density have already been described. The refractive indices (n_o, n_e) of the three compounds at different temperature and for different wave lengths atxdifferent are given in Table 3.11 - 3.13 respectively. Fig. 3.13 - 3.15 shows the variation of (n_o, n_e) with temperatures for different wavelengths for the compounds and Fig. 3.16 - 3.18 shows the variation of Δn with the wavelength of the samples I, II and III respectively. The principal polarizabilities (α_o , α_e) fxr from refractive index data were calculated by using both Vuk's formula and Neugebauer's relations. The orientational order parameters $\langle P_2 \rangle$ was calculated by using the relation $\langle P_2 \rangle = \frac{\alpha_e - \alpha_o}{\alpha_{11} - \alpha_\perp}$ Haller's[4] extrapolation procedure is used to get $\alpha_{11} - \alpha_\perp$ Table 3.14 - 3.19 shows the detail results of the three samples.

From bond polarizability values the mean polarizability α and $\alpha_{11} - \alpha_\perp$ was calculated using the values given in the paper by Le Feveres'[5,6] and by Dunmur and Tomes[7]. The results are given in Table 3.20.

Table 3.20

α and ($\alpha_{\parallel} - \alpha_{\perp}$) comparisons of Sample I, II and III

Sample No.	$\alpha \times 10^{24}$ cm^3		($\alpha_{\parallel} - \alpha_{\perp}$) $\times 10^{24}$ cm^3		
	Calculated from bond polarisability	Vuk's/ Neugebauers approach	Calculated from bond polarizability.	Haller's process (Vuk's data)	Haller's process (Neugebauer data)
I	44.56		21.74	27.00	21.32
II	47.21		32.16	40.02	32.80
III	36.88	36.02	18.75	28.00	19.00

3.1.5. Discussion on $\langle P_L \rangle$ values obtained from Different Techniques:

The orientational order parameters of the compounds obtained from X-ray diffraction and bi-refringence methods have been compared with the Maier-Saupe (M$) theoretical values. The samples PCCPP and PCTP are breaking at higher temperatures so appr experimental results at higher temperature i.e. near the transition temperature are not available.

Sample - I (PCCPP)

Fig. 3.19 shows the $\langle P_2 \rangle$ values of the sample. The $\langle P_2 \rangle$ values obtained from X-ray and R.I. data are in well agreement, but both the values are slightly lower than M.S. theoretical values mainly in the higher temperature near the

transition point. This type of results have already been reported[8,9]. The $\langle P_4 \rangle$ values from X-ray data is lower than that of M.S. theoretical values which also obtained by many others also[10-13].

Sample II (PCTP

The comparison of $\langle P_2 \rangle$ values determined by X-ray and R.I. methods with M.S. theoretical values are shown in Fig. 3.10. All the values shows a good agreement. Curiously enough $\langle P_4 \rangle$ values from X-ray data also agreed well with the M.S. values for this sample. Repeatation of the experiments confirm this.

Sample III (PBBA)

The order parameter values of the compound PBBA are compared with that obtained by different workers of our laboratory[14-16] for other Schiff's base compounds namely EBBA, APAPA, BBBA and MBBA. The $\langle P_2 \rangle$ values of PBBA obtained from different methods viz. X-ray. R.I. are in good agreement with M.S. theoretical values like all other Schiff's base compounds as shown in Fig. 3.12. The $\langle P_4 \rangle$ values are significantly lower at all temperature than the theoretical values (Fig. 3.12). Similar discrepancy has already been observed by others[10-13].

For all the three compounds it has been found that the experimental determinations of order parameter both by X-ray and R.I. measurements agree well except near the transition temperatures. But agreement with (M.S.) theoretical values are not the same in all cases. This may be due to the fact that several types of intermolecular forces (such as dipole-dipole, interactions) are not considered in the M.S. theory. We see molecular associations in all the three cases. In PCOPP the ratio of l/b is larger than the other two compounds. It is a cyano compound and dipole-dipole interactions are responsible for molecular associations. But pairs of molecules are not parallel as is evident from Fig. 4.6. Rigid part of one pair has flexibles parts of the other molecular pair as its nearest neighbour The axes of the rigid part and the flexible parts are not parallel (Fig. 4.6). This may cause lowering of the order parameter value.

TABLE 3.2

Sample - I.

Experimental intensity values I(Ψ) at different temperature after background correction.

Degree	378.5	379.5	387.5	396	411.5	418.5	426	440	433	448
0	25.0	10.4	10.75	8.25	51.0	46.00	30.75	18.00	26	34.00
5	22.7	9.75	10.15	7.60	48.5	44.63	29.25	17.25	244.50	32.5
10	19.9	8.25	8.95	6.75	44.25	41.00	27.25	15.63	22.00	30.50
15	16.7	6.8	7.25	5.95	38.25	35.25	23.63	14.00	21.75	28.00
20	11.0	5.45	5.90	4.90	32	28.63	19.75	11.63	16.25	24.75
25	8.2	4.65	4.45	3.80	26.5	22.25	17.38	9.88	13.00	20.75
30	6.2	3.25	3.20	2.75	20.75	16.50	11.88	8.10	10.25	16.75
35	4.6	2.35	2.35	1.95	15.25	12.13	8.38	6.25	7.25	13.00
40	2.9	1.60	1.60	1.25	7.55	8.63	6.25	4.75	4.75	10.25
45	1.6	0.90	0.90	0.70	4.75	6.13	4.38	3.25	3.50	7.75
50	0.6	0.25	0.35	0.35	2.75	4.13	3.00	2.00	2.50	5.00
55	0.2	0.05	0	0.10	0.5	2.63	1.88	1.13	1.75	3.25
60	0	0	0	0	0	1.63	1.30	0.50	1.50	1.50
65	0	0	0	0	0	1.00	0.63	0.25	0.75	0.75
70	0	0	0	0	0	0.63	0.25	0.01	0.50	0.25
75	0	0	0	0	0	0.38	0	0	0.25	0
80	0	0	0	0	0	0.25	0	0	0	0
85	0	0	0	0	0	0.25	0	0	0	0
90	0	0	0	0	0	0	0	0	0	0

TABLE 3.2

Sample - I. Calculated intensity values I(Ψ) at different temperatures.

(Degree)	370.5	379.5	387.5	396	411.5	418.5	426	433	440	448
0	24.609	10.266	10.677	8.029	50.619	46.030	30.559	25.469	17.878	33.376
5	23.345	9.752	10.207	7.736	48.862	44.683	29,712	24.838	17.314	32.818
10	20.012	8.440	8.964	6.953	44.258	40.870	27.364	23.026	15.811	30.923
15	15.725	6.853	7.349	5.901	38.289	35.234	23.989	20.26	13.807	28.021
20	11.633	5.440	5.760	4.796	32.198	28.697	20.102	16.885	11.734	24.455
25	8.408	4.338	4.413	3.762	26.354	22.229	16.104	13.311	9.815	20.611
30	6.087	3.411	3.314	2.824	20.520	16.569	12.288	9.945	8.051	16.826
35	4.357	2.496	2.375	1.978	14.597	12.052	8.909	7.106	6.360	13.322
40	2.916	1.579	1.546	1.249	9.049	8.634	6.180	4.956	4.725	10.194
45	1.677	0.794	0.853	0.683	4.635	6.076	4.194	3.471	3.230	7.456
50	0.728	0.273	0.357	0.309	1.835	4.141	2.854	2.493	1.998	5.11
55	0.157	0.035	0.078	0.108	0.524	2.689	1.943	1.821	1.102	3.183
60	-0.058	-0.011	-0.024	0.026	0.150	1.656	1.258	1.302	0.530	1.714
65	-0.054	0.014	-0.028	0.003	0.135	0.979	0.709	0.866	0.213	0.722
70	0.014	0.035	-0.004	0	0.144	0.575	0.394	0.509	0.062	0.171
75	0.048	0.028	0.010	-0.001	0.086	0.348	0.066	0.243	0.004	-0.038
80	0.030	0.004	0.008	-0.002	-0.007	0.226	-0.028	0.071	-0.009	-0.043
85	-0.009	-0.019	0	-0.002	-0.085	0.165	-0.43	-0.021	-0.008	0.022
90	-0.027	-0.028	-0.005	-0.003	-0.115	0.147	-0.039	-0.050	-0.006	0.056

(58)

TABLE 3.4

Sample II.

Experimental intensity values I(ψ) at different temperatures after background correction.

(Degree)	407.5	415	422.25	429.5	433	440	448	453.5	460.5	467.5	474.5
0	16.60	45.00	20.50	17.0	25.9	30.50	25.08	19.4	16.10	8.6	13.5
5	15.50	43.00	19.40	16.0	24.6	28.35	24.35	18.3	15.20	8.1	12.9
10	13.50	37.50	16.65	14.3	21.8	26.45	22.25	15.7	13.60	7.3	12.1
15	10.8	33.5	13.00	12.2	18.5	22.20	19.08	13.2	12.00	6.3	11.0
20	7.9	25.0	10.20	9.6	15.1	17.65	15.35	10.6	9.60	5.5	9.7
25	5.60	19.0	7.45	7.2	11.5	12.55	11.66	8.2	8.10	4.4	8.2
30	3.80	13.5	5.35	5.3	8.7	9.55	8.53	6.4	6.60	3.5	6.9
35	2.30	9.5	3.85	3.8	6.0	7.00	6.23	4.8	5.30	2.6	5.6
40	1.30	6.25	3.00	2.8	4.0	5.20	4.72	3.8	4.10	2.0	4.5
45	0.80	4.5	2.05	1.9	2.9	3.90	3.75	3.0	3.10	1.5	3.6
50	0.50	2.5	1.40	1.4	2.2	2.90	3.07	2.10	2.10	1.2	2.6
55	0.30	1.75	1.05	1.0	1.5	2.15	2.49	1.4	1.50	0.8	1.8
60	0.20	1.0	0.65	0.7	0.8	1.40	1.95	1.0	0.90	0.6	1.1
65	0.10	1.0	0.35	0.4	1.1	0.90	1.42	0.7	0.50	0.4	0.5
70	0.10	0.5	0.25	0.3	0	0.60	0.96	0.55	0.20	0.2	0.3
75	0	0.25	0.15	0.2	0	0.30	0.55	0.20	0	0	0
80	0	0	0.10	0.1	0	0.10	0.25	0.10	0	0	0
85	0	0	0.05	0	0	0	0.06	0	0	0	0
90	0	0	0	0	0	0	0	0	0	0	0

Table 3.5

Sample II.

Calculated intensity values I(Ψ) at different temperatures

(Degree)	407.5	415	422.5	429.5	433	440	448	453.5	460.5	467.5	474.5
0	16.442	44.645	20.406	16.793	25.618	30.055	25.089	19.173	15.920	8.45	13.326
5	15.652	43.031	19.390	16.167	24.670	29.055	24.362	18.320	15.335	8.167	13.030
10	13.546	38.582	16.714	14.459	22.108	26.236	22.244	16.075	13.787	7.412	12.203
15	10.755	32.305	13.268	12.089	18.612	22.110	19.076	13.187	11.765	6.403	11.001
20	7.950	25.431	9.965	9.55	14.404	17.436	15.351	10.405	9.756	5.351	9.615
25	5.560	18.994	7.328	7.227	11.470	13.016	11.666	8.136	8.024	4.369	8.206
30	3.712	13.598	5.411	5.312	8.520	9.431	8.535	6.396	6.580	3.482	6.875
35	2.355	9.417	4.011	3.837	6.113	6.870	6.225	5.009	5.313	2.692	5.656
40	1.400	6.349	2.923	2.741	4.260	5.254	4.706	3.831	4.145	2.022	4.547
45	0.781	4.185	2.059	1.947	2.924	3.947	3.747	2.834	3.077	1.499	3.530
50	0.433	2.718	1.407	1.38	1.996	2.976	3.076	2.045	2.157	1.115	2.602
55	0.271	1.853	0.951	0.978	1.322	2.132	2.502	1.465	1.421	0.829	1.780
60	0.198	1.153	0.646	0.686	0.786	1.428	1.949	1.046	0.873	0.592	1.097
65	0.148	0.765	0.434	0.466	0.360	0.893	1.418	0.726	0.489	0.384	0.586
70	0.096	0.486	0.277	0.296	0.075	0.522	0.941	0.466	0.240	0.211	0.254
75	0.045	0.269	0.159	0.166	-0.053	0.278	0.545	0.256	0.090	0.086	0.079
80	0.004	0.102	0.074	0.076	-0.061	0.122	0.250	0.100	0.007	0.009	0.012
85	-1.020	-0.006	0.023	0.023	-0.023	0.034	0.069	0.006	-0.034	-0.03	0
90	-0.028	-0.044	0.005	0.006	-0.002	0.005	0.007	-0.026	-0.009	-0.042	0

TABLE 3.6

Mean Intensity Value

Experimental intensity at values I(Ψ) at different temperatures ~~from comperative chart.~~ SAMPLE-III

Degree	296	303	308	313	318	323	328
0	6.32	6.65	5.30	4.92	5.03	4.65	4.10
5	6.01	6.18	5.03	4.57	4.82	4.50	3.94
10	5.49	5.69	4.46	4.15	4.47	4.25	3.67
15	4.70	4.70	3.83	3.64	4.04	3.85	3.34
20	3.83	4.13	3.26	3.18	3.53	3.41	2.97
25	2.99	3.35	2.66	2.71	3.06	2.95	2.61
30	2.28	2.63	2.01	2.19	2.55	2.50	2.20
35	1.73	2.03	1.58	1.81	1.92	2.01	1.84
40	1.30	1.54	1.14	1.41	1.59	1.65	1.52
45	1.00	1.18	0.84	1.13	1.29	1.33	1.42
50	0.78	0.89	0.66	0.87	1.05	1.02	1.05
55	0.61	0.65	0.50	0.62	0.82	0.80	0.86
60	0.50	0.45	0.39	0.47	0.63	0.61	0.69
65	0.38	0.30	0.28	0.32	0.46	0.48	0.51
70	0.26	0.18	0.23	0.21	0.28	0.35	0.39
75	0.18	0.13	0.17	0.13	0.15	0.26	0.22
80	0.11	0.07	0.11	0.10	0.09	0.19	0.18
85	0.05	0.04	0.09	0.03	0.05	0.13	0.11
90	0	0	0.05	0	0.03	0.10	0.04

TABLE 3.7

Mean Intensity value

Calculated intensity I (Ψ) at different temperatures. ~~from compared chart.~~ SAMPLE III

Degree	298	303	308	313	318	323	328
0	6.269	6.529	5.236	4.809	4.972	4.626	4.052
5	6.063	6.292	5.043	4.645	4.849	4.526	3.961
10	5.495	5.665	4.534	4.217	4.515	4.250	3.710
15	4.696	4.845	3.870	3.668	4.051	3.857	3.355
20	3.821	4.022	3.202	3.129	3.536	3.406	2.959
25	22994	3.289	2.599	2.655	3.012	2.942	2.568
30	2.289	2.648	2.063	2.231	2.488	2.486	2.205
35	1.727	2.076	1.580	1.827	2.017	2.050	1.875
40	1.302	1.572	1.161	1.443	1.600	1.650	1.579
45	0.993	1.159	0.838	1.105	1.290	1.304	1.316
50	0.773	0.850	0.622	0.834	1.020	1.022	1.083
55	0.614	0.629	0.468	0.629	0.818	0.800	0.877
60	0.489	0.462	0.397	0.470	0.653	0.624	0.690
65	0.378	0.325	0.315	0.337	0.455	0.478	0.521
70	0.272	0.209	0.234	0.224	0.295	0.354	0.370
75	0.175	0.119	0.161	0.132	0.170	0.252	0.245
80	0.95	0.056	0.106	0.066	0.086	0.175	0.151
85	0.042	0.021	0.073	0.027	0.040	0.129	0.094
~~90x~~ 90	~~0.042~~ 0.023	~~0.021x~~ 0.010	0.063	0.014	0.026	0.113	0.074

(57)

TABLE-3.8

Normalised distribution function $f(\beta)$ at different temperatures. SAMPLE-1

Degree	$f(\beta)$ at temperature in °K									
	370.5	379.5	387.5	396	411.5	418.5	426	433	440	448
0	12.499	11.045	10.625	7.763	9.590	8.160	5.696	9.003	5.54	5.368
5	11.752	10.241	10.045	8.055	8.586	7.834	6.255	7.899	6.046	5.454
10	9.785	8.437	8.535	8.457	6.548	6.977	7.513	5.810	7.132	5.543
15	7.290	6.325	6.641	7.861	4.899	5.847	7.942	4.324	7.431	5.262
20	5.009	4.589	4.889	5.909	4.065	4.672	6.249	3.742	5.649	4.442
25	3.341	3.410	3.542	3.729	3.801	3.578	3.724	3.672	3.385	3.377
30	2.277	2.661	2.595	2.293	3.582	2.622	2.052	3.423	1.972	2.484
35	1.613	2.103	1.905	1.588	2.844	1.837	1.326	2.506	1.423	1.911
40	1.134	1.506	1.321	1.248	1.654	1.239	1.106	1.381	1.361	1.570
45	0.706	0.828	0.780	0.927	0.691	0.816	1.047	0.672	1.427	1.291
50	0.336	0.296	0.351	0.488	0.233	0.531	0.859	0.376	1.169	0.943
55	0.109	0.062	0.112	0.147	0.033	0.339	0.495	0.284	0.576	0.556
60	0	0	0	0.025	0.029	0.208	0.303	0.270	0.733	0.262
65	0	0	0	0.003	0.014	0.120	0.078	0.239	0.043	0.109
70	0	0	0	0	0.008	0.065	0.04	0.140	0.014	0.047
75	0	0	0	0	0.006	0.034	0.034	0.033	0.008	0.038
80	0	0	0	0	0.005	0.019	0	0.013	0	0
85	0	0	0	0	0	0.012	0	0	0	0
90	0	0	0	0	0	0.011	0	0	0	0

TABLE 3.9

ple II.

Normalised distribution function f(β) at different temperatures.

Degree	f (β) at temperature in °K									
	407.5	415	422.5	429.5	433	440	448	453.5	467.5	474.5
0	17.652	12.787	14.989	11.908	8.274	11-511	10.642	12.385	10.443	10.341
5	14.026	10.630	12.362	10.093	8.306	9.770	8.937	10.306	8.686	8.515
10	8.150	6.886	7.754	6.801	8.112	6.609	5.935	6.626	5.614	5.411
15	4.802	4.506	4.763	4.567	7.138	4.466	4.013	4.216	3.665	3.542
20	3.702	3.667	3.527	3.650	5.373	3.589	3.346	8.253	2.990	2.994
25	3.663	3.642	3.188	3.444	3.542	3.391	3.356	3.079	3.070	3.231
30	3.509	3.510	2.930	3.186	2.245	3.125	3.241	2.985	3.851	3.497
35	2.344	2.528	2.182	2.334	1.514	2.279	2.367	2.369	2.777	2.867
40	0.0982	1.258	1.213	1.272	1.126	1.252	1.246	1.418	1.734	1.626
45	0.324	0.522	0.580	0.605	0.866	0.616	0.587	0.733	0.907	0.770
50	0.128	0.253	0.313	0.332	0.610	0.360	0.349	0.425	0.516	0.428
55	0.083	0.180	0.231	0.253	0.358	0.295	0.323	0.332	0.382	0.349
60	0.084	0.175	0.218	0.248	0.177	0.305	0.412	0.326	0.337	0.379
65	0.088	0.162	0.196	0.230	0.083	0.279	0.478	0.298	0.257	0.366
70	0.057	0.094	0.118	0.141	0.043	0.154	0.317	0.180	0.118	0.202
75	0.019	0.029	0.042	0.050	0	0.046	0.101	0.064	0.030	0.054
80	0.004	0.006	0.011	0.013	0	0.010	0.021	0.016	0.005	0.010
85	0	0.002	0.003	0.004	0	0.003	0.005	0.005	0	0
90	0	0	0.002	0.003	0	0.002	0.003	-	0	0

TABLE 3.10

Sample III.

Normalised distribution function f (β) at different temperature

Degree	f (β) values at temp. (^{o}K)						
	298	303	308	313	318	323	326
0	9.327	9.637	8.766	8.318	6.621	5.506	5.504
5	8.272	8.294	7.937	7.212	5.971	5.196	5.113
10	6.177	5.790	6.196	5.126	4.664	4.489	4.260
15	4.523	4.023	4.675	3.630	3.632	3.6784	3.473
20	3.661	3.282	3.747	3.007	3.148	3.279	2.979
25	3.263	3.155	3.215	2.938	3.017	2.928	2.704
30	2.836	3.053	2.725	2.928	2.848	2.573	2.448
35	2.096	2.456	2.065	2.481	2.320	2.103	2.054
40	1.277	1.532	1.350	1.662	1.573	1.568	1.560
45	0.722	0.835	0.816	0.974	0.981	1.108	1.229
50	0.461	0.498	0.519	0.611	0.667	0.795	0.850
55	0.375	0.382	0.383	0.479	0.550	0.609	0.703
60	.369	0.358	0.325	0.444	0.519	0.492	0.616
65	0.350	0.319	0.281	0.393	0.456	0.390	0.509
70	0.250	0.204	0.213	0.259	0.298	0.279	0.332
75	0.122	0.083	0.132	0.114	0.135	0.178	0.198
80	0.048	0.027	0.074	0.040	0.050	0.108	0.102
85	0.021	0.010	0.045	0.016	0.022	0.073	0.059
90	0.015	0.007	0.037	0.011	0.016	0.063	0.048

TABLE 3.11

Refractive indices (n_o, n_e) at different temperatureof sample I

Temp.	6907 Å		5780 Å		5461 Å		4758 Å		Mean
(^oC)	n_o	n_e	n_o	n_e	n_o	n_e	n_o	n_e^b	P_2
90	1.545	1.781	1.551	1.784	1.551	1.796	1.557	1.835	.746
98	1.548	1.780	1.551	1.784	1.554	1.793	1.557	1.832	.743
107	1.550	1.780	1.551	1.784	1.554	1.790	1.557	1.832	.741
115	1.553	1.778	1.554	1.778	1.557	1.790	1.562	1.825	.726
123	1.557	1.775	1.557	1.775	1.562	1.787	1.569	1.825	.71
131	1.560	1.775	1.557	1.775	1.562	1.784	1.569	1.814	.693
139	1.560	1.770	1.559	1.773	1.566	1.780	1.575	1.814	.681
146	1.563	1.770	1.562	1.773	1.569	1.778	1.580	1.808	.663
153	1.565	1.768	1.566	1.769	1.573	1.775	1.580	1.796	.65
160	1.563	1.763	1.569	1.767	1.573	1.774	1.587	1.793	.622
167	1.567	1.763	1.573	1.764	1.578	1.774	1.589	1.793	.614
175	1.569	1.760	1.578	1.762	1.580	1.764	1.599	1.784	.582
181	1.575	1.760	1.578	1.760	1.593	1.760	1.599	1.772	.55
188	1.580	1.750	1.593	1.750	1.605	1.754	1.580	1.758	.501
195	1.580	1.748	1.580	1.748	1.605	1.748	1.605	1.748	.471

TABLE 3.12

Refractive indices (n_o, n_e) at different temperatures of sample II

Temp. in °C	6907 Å		5780 Å		5461 Å		4758 Å	
	n_o	n_e	n_o	n_e	n_o	n_e	n_o	n_e
123	1.461	1.758	1.477	1.776	1.477	1.782	1.495	1.865
135	1.461	1.753	1.477	1.764	1.477	1.776	1.495	1.865
142	1.461	1.747	1.477	1.758	1.477	1.764	1.495	1.859
149	1.465	1.747	1.478	1.759	1.477	1.764	1.495	1.859
153	1.465	1.734	1.480	1.747	1.477	1.758	1.495	1.847
153	1.465	1.728	1.486	1.747	1.477	1.758	1.495	1.847
160	1.465	1.722	1.486	1.74	1.477	1.753	1.495	1.845
167	1.465	1.722	1.486	1.727	1.486	1.743	1.504	1.845
175	1.465	1.722	1.486	1.727	1.489	1.743	1.510	1.842
181	1.474	1.713	1.486	1.725	1.495	1.737	1.516	1.829
188	1.486	1.710	1.492	1.722	1.495	1.731	1.519	1.824
195	1.492	1.701	1.495	1.719	1.498	1.722	1.522	1.820
202	1.495	1.695	1.501	1.713	1.504	1.722	1.528	1.812
216	1.498	1.69	1.504	1.710	1.507	1.719	1.54	1.803
222	1.501	1.683	1.51	1.707	1.513	1.713	1.546	1.797
232	1.54		1.551		1.555		1.599	

Table 3.13

Refractive indices (n_o, n_e) at different temperatures of PBMA

Temp. (°C)	λ = 6907 Å		λ = 5790 Å		λ = 5461 Å		λ = 4358 Å	
	n_o	n_e	n_o	n_e	n_o	n_e	n_o	n_e
27.7	1.538	1.768	1.550	1.779	1.560	1.792	1.588	1.878
32	1.538	1.764	1.550	1.775	1.560	1.788	1.588	1.872
36	1.540	1.758	1.552	1.770	1.562	1.783	1.590	1.866
40	1.542	1.750	1.554	1.765	1.562	1.776	1.592	1.860
44	1.544	1.744	1.558	1.759	1.566	1.769	1.594	1.850
48	1.550	1.736	1.562	1.750	1.570	1.761	1.597	1.839
52	1.555	1.727	1.567	1.740	1.574	1.750	1.602	1.826
56	1.561	1.713	1.573	1.726	1.580	1.735	1.607	1.805
57	1.564	1.707	1.576	1.720	1.582	1.728	1.611	1.795
57.5(Iso)	1.590		1.602		1.612		1.660	
60	1.588		1.600		1.610		1.658	
62	1.586		1.598		1.608		1.656	

Table - 3.14: Density (ρ) Polarizability (α) and Orientational order Parameters P_2 of sample I (Vuks' approach)

Temp °C	Density (ρ) in gm/cm^3	6907 Å			5780 Å			5461 Å			4358 Å			Mean
		α_o	α_e	$\langle P_2 \rangle$	α_o	α_e	$\langle P_2 \rangle$	α_o	α_e	$\langle P_2 \rangle$	α_o	α_e	$\langle P_2 \rangle$	$\langle P_2 \rangle_{AV}$
90	1.098	35.92	56.25	.750	36.28	56.34	.743	36.17	57.27	.754	36.19	60.15	.753	.748
98	1.090	36.39	56.51	.742	36.55	56.75	.748	36.66	57.38	.740	36.48	60.35	.750	.745
107	1.083	36.75	56.83	.740	36.78	57.12	.750	36.92	57.51	.735	36.72	60.74	.750	.743
115	1.073	37.32	57.12	.731	37.42	56.78	.717	37.46	57.97	.732	37.45	60.62	.729	.727
123	1.067	37.82	57.10	.711	37.82	57.10	.714	38.03	57.93	.711	38.12	60.77	.712	.712
131	1.061	37.23	57.38	.705	38.14	56.46	.678	38.27	58.02	.705	38.44	60.24	.655	.693
139	1.053	38.57	57.63	.694	38.57	56.84	.676	38.87	58.03	.684	39.13	60.53	.673	.681
146	1.047	38.99	58.03	.688	38.99	57.09	.670	39.39	57.48	.646	39.74	60.26	.645	.662
153	1.036	39.56	58.12	.681	39.71	67.35	.653	40.03	58.39	.655	40.29	59.92	.617	.651
160	1.028	39.78	58.47	.676	40.25	57.47	.638	40.55	57.12	.592	41.11	59.95	.593	.625
167	1.020	40.37	58.47	.668	40.87	57.57	.618	41.22	57.44	.579	41.56	60.37	.591	.614
175	1.012	40.86	58.63	.656	41.67	56.89	.564	41.68	57.84	.577	42.68	59.83	.539	.584
181	1.022	41.68	59.05	.641	42.21	56.45	.527	43.05	57.74	.524	43.23	59.42	.509	.550
188	0.995	42.27	58.71	.606	42.90	54.77	.440	43.35	58.15	.501	44.15	58.17	.465	.503
195	0.989	42.71	58.67	.589	43.22	54.59	.421	44.55	57.51	.463	44.55	57.51	.407	.470

and are in 10^{-24} cm^3

TABLE 3.15

Density (ρ), Polarizability (α) and Orientational Order Parameters ($\langle P_2 \rangle$) of Sample II

Temp. in °C	Density in gm/cm	6907 Å		5780 Å		5461 Å		4758 Å		Mean
		α_o	α_e	α_o	α_e	α_o	α_e	α_o	α_e	$\langle P_2 \rangle$
123	0.980	36.43	67.12	37.49	68.36	37.43	68.93	37.98	76.21	.755
135	0.976	36.62	66.92	37.77	67.50	37.65	68.64	38.14	76.52	.737
142	0.975	36.72	66.41	37.86	66.99	37.80	67.57	38.24	76.05	.722
149	0.972	37.15	66.50	38.10	66.79	37.92	67.78	38.35	76.27	.712
153	0.971	37.31	65.32	38.36	66.13	38.02	67.27	38.52	75.20	.685
157	0.971	37.37	64.75	38.84	65.96	38.02	67.27	38.52	75.20	.665
160	0.969	37.51	64.31	38.99	65.43	38.15	66.93	38.62	75.17	.653
167	0.966	37.62	64.51	39.29	64.39	39.08	65.92	39.43	75.11	.638
175	0.963	37.74	64.71	39.35	64.68	39.44	66.04	40.05	74.86	.641
181	0.961	38.63	63.72	39.46	64.53	40.05	65.42	40.73	73.58	.615
188	0.958	39.74	63.29	40.09	64.27	40.24	65.05	41.15	73.24	.586
195	0.955	40.44	62.45	40.49	64.10	40.70	64.30	41.55	73.00	.559
202	0.951	40.91	62.05	41.21	63.62	41.35	64.40	42.29	72.34	.539
216	0.944	41.51	61.94	41.79	63.71	41.94	64.50	43.65	71.62	.522
222	0.939	42.05	61.50	42.53	63.59	42.71	64.09	44.42	71.23	.497

α_o, α_e are in 10^{-24} cm^3 and calculated from Vuk's formula.

TABLE 3.16

Density (ρ), Polarisability (α) and Orientational Order Parameter ($\langle P_2 \rangle$) of Sample III (Vuk's approach)

Temp. (°C)	Density (ρ) (gm/cm^3)	λ = 6907 Å			λ = 5780 Å			λ = 5461 Å			λ = 4358 Å		
		α_o	α_e	$\langle P_2 \rangle$	α_o	α_e	$\langle P_2 \rangle$	α_o	α_e	$\langle P_2 \rangle$	α_e	α_o	$\langle P_2 \rangle$
27.7	1.165	29.71	46.26	.6191	30.27	46.73	.6157	30.71	47.36	.6163	31.49	52.30	.6161
32	1.163	29.80	46.08	.6096	30.36	46.55	.6062	30.79	47.19	.6069	31.50	52.00	.6046
36	1.158	30.08	45.85	.5891	30.63	46.38	.5891	31.07	47.02	.5900	31.89	51.79	.5893
40	1.155	30.30	45.36	.5668	30.83	46.10	.5716	31.18	46.65	.5674	32.10	51.45	.5757
44	1.151	30.59	45.12	.5437	31.23	45.82	.5458	31.58	46.31	.5447	32.42	51.00	.5494
48	1.149	31.03	44.55	.5067	31.57	45.23	.5119	31.92	45.79	.5140	32.73	50.29	.5209
52	1.140	31.62	44.21	.4710	32.17	44.82	.4733	32.48	45.34	.4759	33.37	49.72	.4844
56	1.120	32.64	43.94	.4230	33.20	44.57	.4253	33.58	45.03	.4259	34.41	49.10	.4329
57	1.100	33.45	44.27	.4012	34.03	44.91	.4036	34.30	45.33	.4047	35.35	49.24	.4076
58	1.068(Iso)												

α_e and α_o are in units 10^{-24} cm^3

TABLE 3.17

Polarisabilities (α_o , α_e) of sample – I Using Neugebauer's relations

Temp. in ^oC	6907 Å		5780 Å		5461 Å		4758 Å		Mean
	α_o	α_e	α_o	α_e	α_o	α_e	α_o	α_e	P_2
90	37.29	53.52	37.64	53.62	37.61	54.40	37.86	56.81	.746
98	37.75	53.80	37.91	54.01	38.07	54.55	38.14	57.03	.743
107	38.11	54.12	38.16	54.36	38.32	54.71	38.39	57.40	.741
115	38.65	54.44	38.72	54.16	38.86	55.17	39.07	57.39	.726
123	39.12	54.49	39.12	54.48	39.39	53.20	39.71	57.59	.71
131	39.53	54.75	39.38	53.99	39.62	55.32	39.96	57.19	.693
139	39.84	54.83	39.80	54.37	40.18	55.41	40.63	57.53	.681
146	40.26	55.10	40.22	54.64	40.63	55.09	41.19	57.38	.663
153	40.81	55.51	40.90	54.95	41.29	55.07	41.66	57.18	.65
160	41.02	55.63	41.42	55.13	41.68	54.87	42.43	57.31	.622
167	41.60	56.01	42.01	55.29	42.32	55.22	42.89	57.72	.614
175	42.06	56.21	42.70	54.82	42.79	55.63	43.89	57.41	.582
181	42.67	56.68	43.17	54.53	44.06	55.71	44.37	57.15	.55
188	43.39	56.47	43.69	53.19	44.37	56.10	45.13	56.21	.501
195	43.80	56.50	43.98	53.08	45.45	55.71	45.45	55.71	.471

α_o, α_e are in $10^{-24} cm^{-3}$ unit

TABLE 3.18

Polarizability at different temperature of the sample II using Neuguebauer method.

Temp. in °C	6907 Å		5780 Å		5461 Å		4758 Å		Mean
	α_o	α_e	α_o	α_e	α_o	α_e	α_o	α_e	P_2
123	38.29	63.39	39.42	64.51	39.41	64.99	40.51	71.15	.758
135	38.46	63.25	39.61	63.81	39.58	64.77	40.67	71.45	.736
142	38.51	62.83	39.67	63.39	39.65	63.87	40.73	71.05	.720
149	38.93	62.94	39.87	63.24	39.77	64.07	40.86	71.26	.710
153	39.00	61.94	40.08	62.70	39.83	63.65	40.93	70.38	.682
157	39.02	61.46	40.52	62.58	39.83	63.65	40.93	70.39	.663
160	39.11	61.09	40.63	62.15	39.93	63.38	41.01	70.37	.653
167	39.24	61.28	40.79	61.29	40.74	62.58	41.79	70.38	.637
175	39.36	61.47	40.91	61.56	41.09	62.72	42.37	70.22	.641
181	40.14	60.69	41.01	61.45	41.64	62.25	42.92	69.20	.615
188	41.18	60.41	41.59	61.28	41.79	61.96	43.29	68.95	.586
195	41.78	59.76	41.96	61.17	42.17	61.36	43.66	68.78	.557
202	42.21	59.46	42.60	60.83	42.80	61.51	44.30	68.31	.541
216	42.76	59.44	43.15	60.38	43.35	61.67	45.54	67.84	.520
222	43.24	59.13	43.85	60.96	44.05	61.39	46.24	67.60	.495

α_o and α_e are in 10^{-24} cm^{-3} unit.

TABLE 3.19

Polarisability (α) and order parameter ($\langle P_2 \rangle$) for Sample III (PBBA)
(Using Neugebauer's relation)

Temp. (^oC)	λ = 6907 Å			λ = 5780 Å			λ = 5461 Å			λ = 4358 Å		
	α_o	α_e	$\langle P_2 \rangle$	α_o	α_e	$\langle P_2 \rangle$	α_o	α_e	$\langle P_2 \rangle$	α_o	α_e	$\langle P_2 \rangle$
27.7	30.81	44.07	.6143	31.38	44.51	.6146	31.85	45.09	.6181	33.01	49.26	.6128
32.0	30.87	43.87	.6054	31.44	44.37	.6067	31.91	44.94	.6102	33.08	49.03	.6034
36.0	31.12	43.76	.5893	31.69	44.28	.5919	32.16	44.84	.5960	33.34	48.89	.5904
40.0	31.29	43.37	.5657	31.86	44.04	.5761	32.23	44.54	.5803	33.50	48.63	.5766
44.0	31.55	43.21	.5479	32.21	43.86	.5530	32.59	44.30	.5546	33.77	48.29	.5559
48	31.92	42.77	.5135	32.49	43.39	.5208	32.87	43.90	.5252	34.00	47.74	.5288
52.0	32.45	42.55	.4811	33.03	43.13	.4861	33.35	43.59	.4910	34.55	47.36	.4960
56.0	33.38	42.45	.4367	33.96	43.05	.4481	34.30	43.47	.4448	35.47	46.99	.4520
57.0	34.16	42.85	.4200	34.76	43.46	.4250	35.05	43.84	.4280	36.35	47.25	.4300

α_o and α_e are in 10^{-24} cm^{-3} unit.

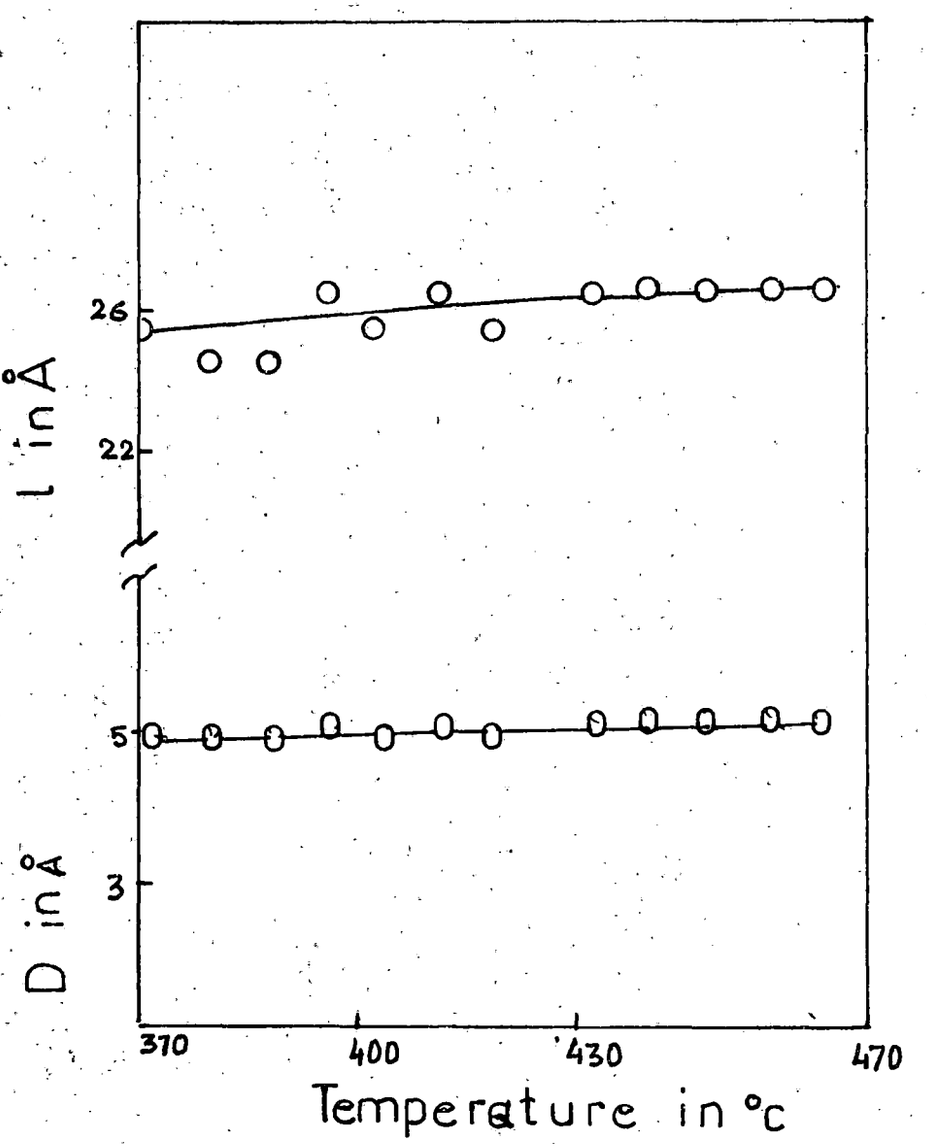

Fig. 3.4

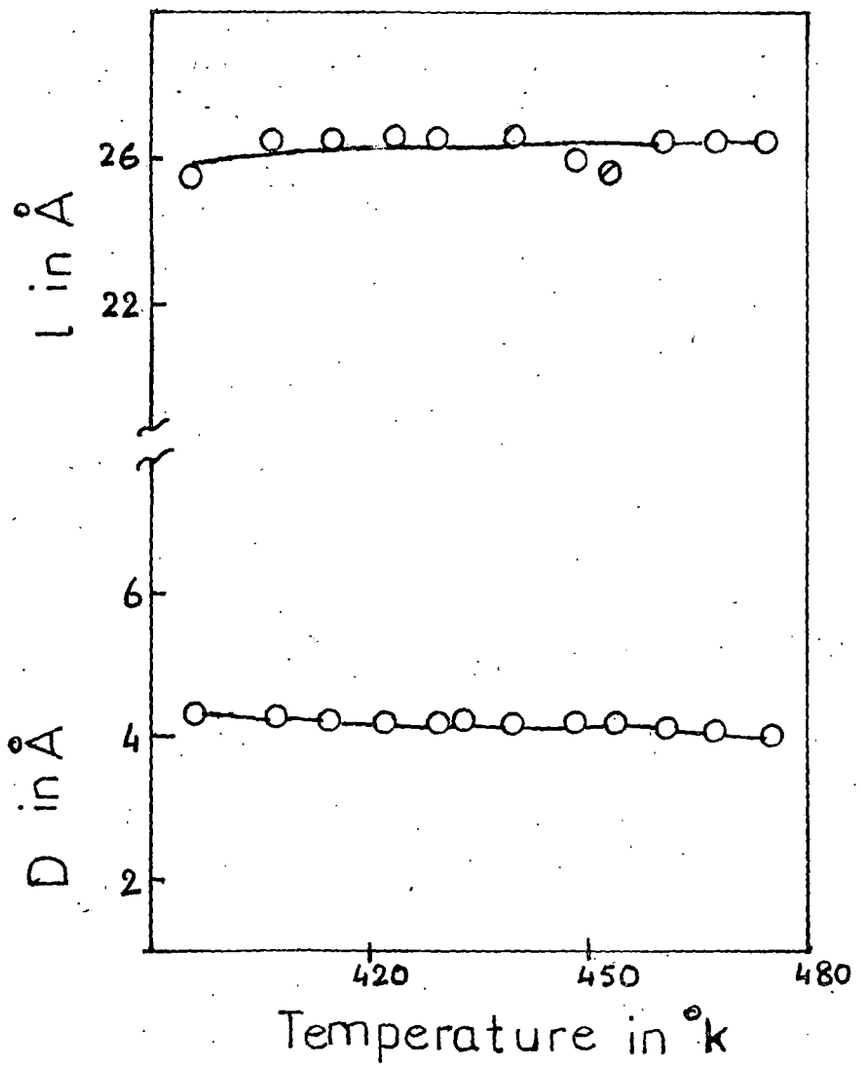

Fig. 3.5

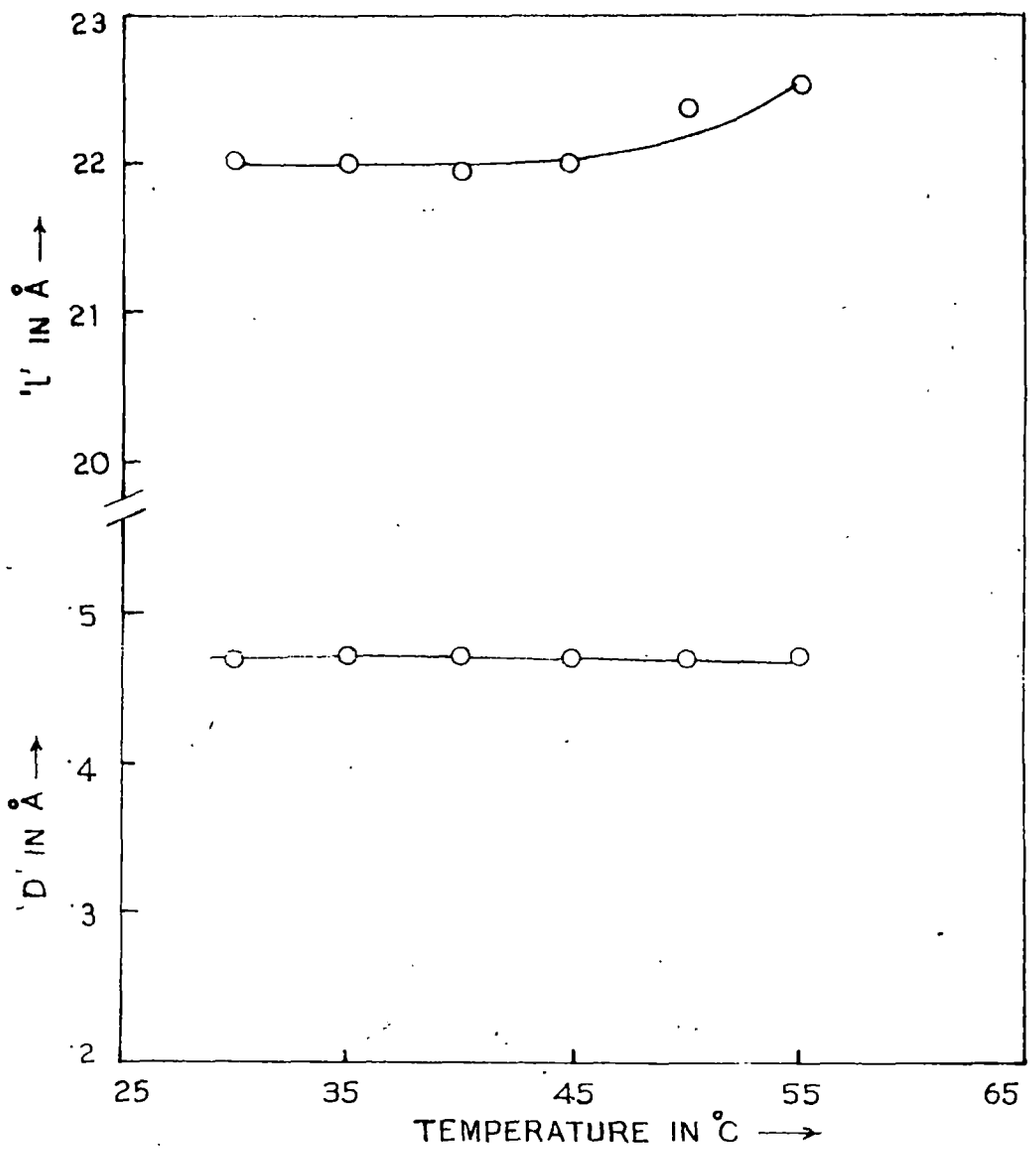

Fig. 3.6

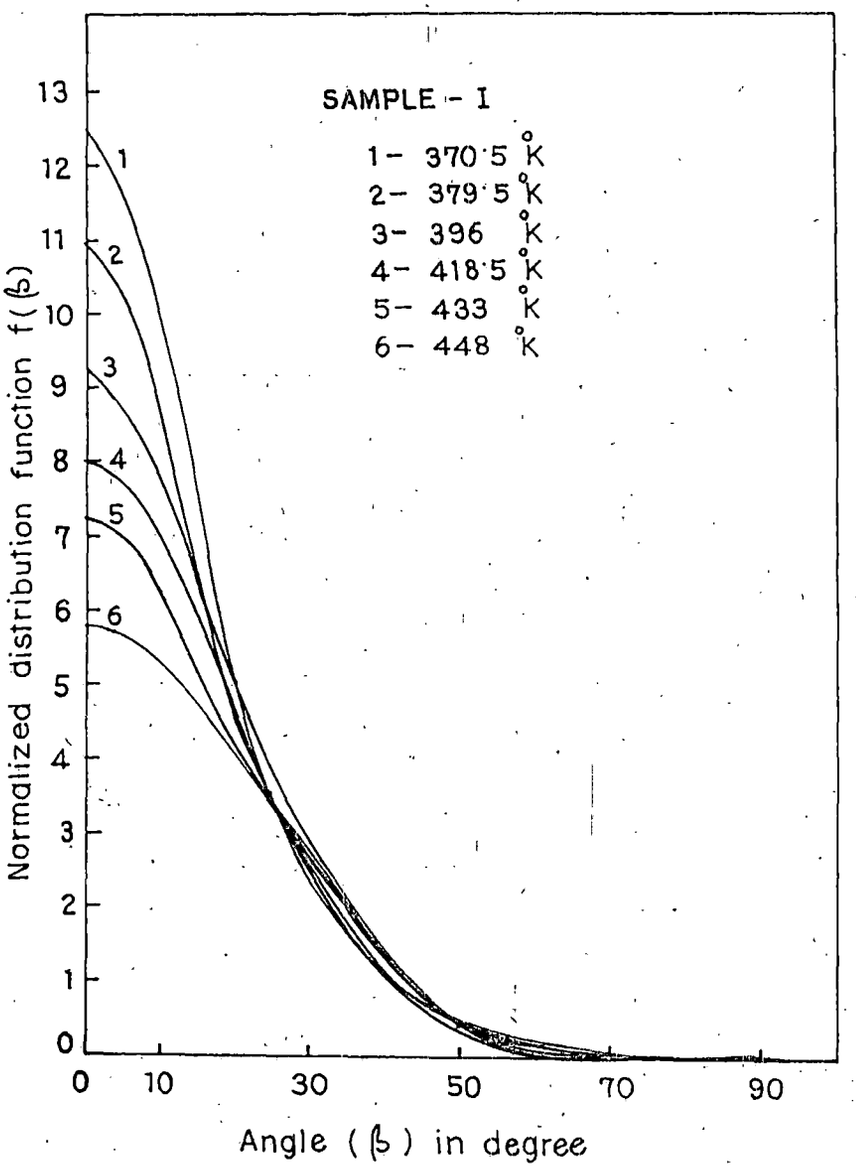
SAMPLE - I
1- 370·5 °K
2- 379·5 °K
3- 396 °K
4- 418·5 °K
5- 433 °K
6- 448 °K
Normalized distribution function f(β)
Angle (β) in degree
0
1
2
3
4
5
6
7
8
9
10
11
12
13
0
10
30
50
70
90

Fig. 3.7

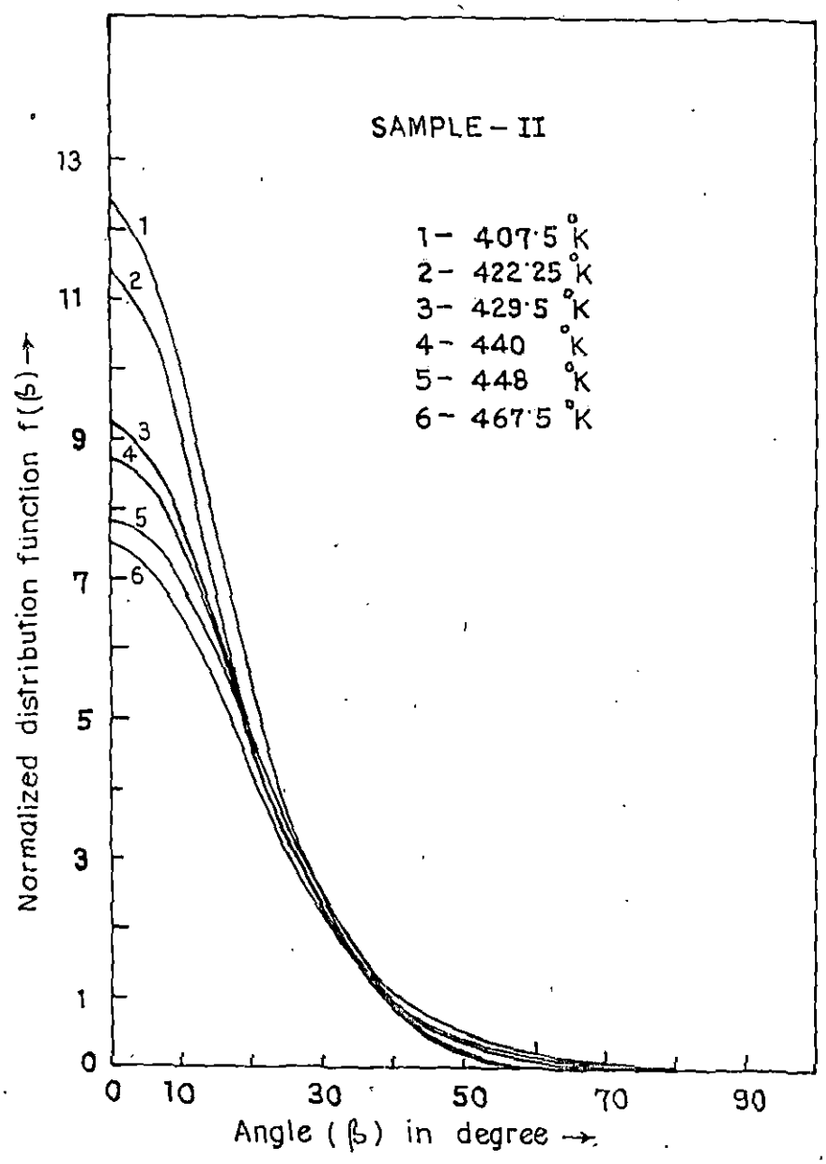
SAMPLE – II
1– 407·5 °K
2– 422·25 °K
3– 429·5 °K
4– 440 °K
5– 448 °K
6– 467·5 °K
Normalized distribution function f(β)→
Angle (β) in degree →
0
1
3
5
7
9
11
13
10
30
50
70
90

Fig. 3.8

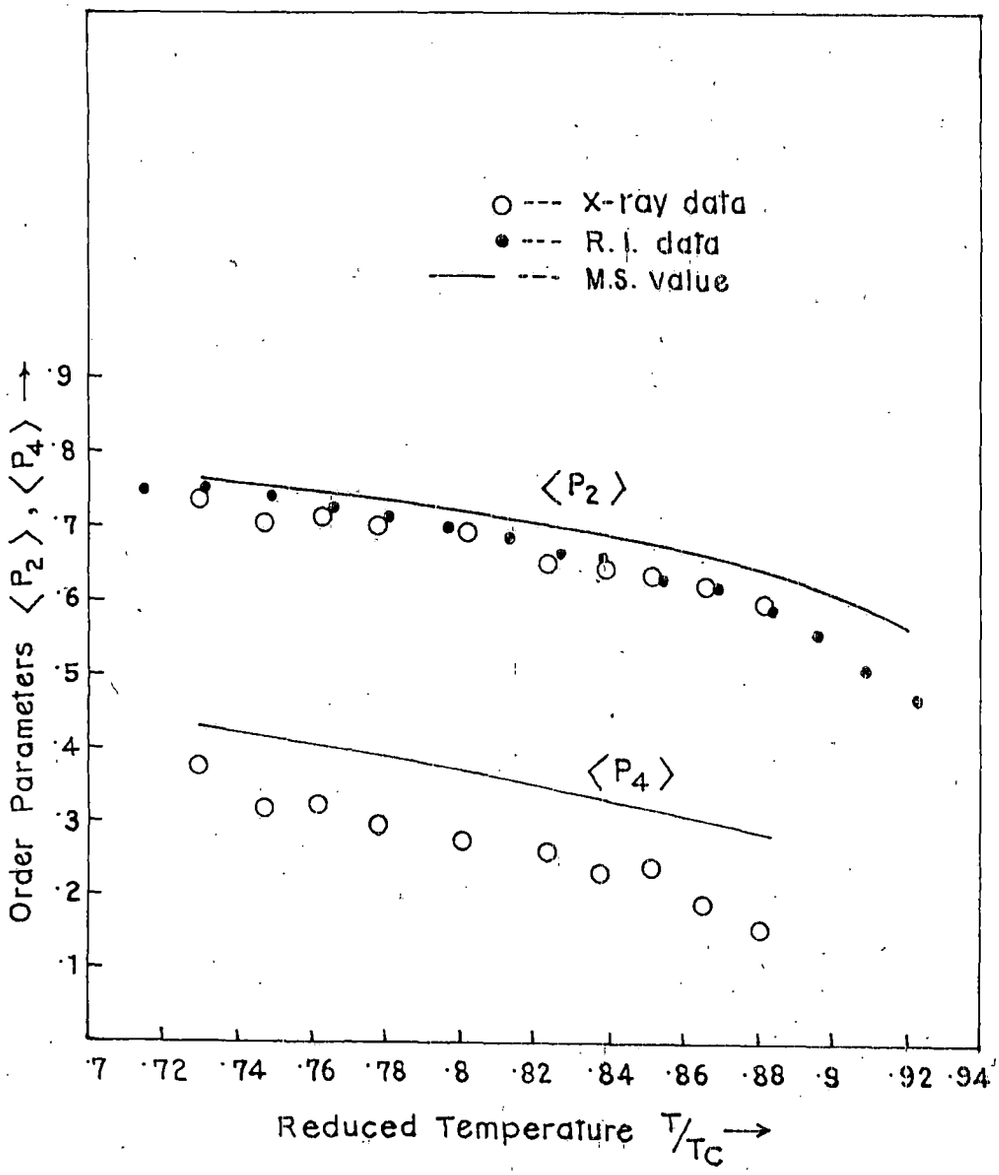
O --- X-ray data
• --- R.I. data
—— --- M.S. value
⟨P2⟩
⟨P4⟩
Order Parameters ⟨P2⟩, ⟨P4⟩ →
·9
·8
·7
·6
·5
·4
·3
·2
·1
·7
·72
·74
·76
·78
·8
·82
·84
·86
·88
·9
·92
·94
Reduced Temperature T/Tc →

Fig. 3.10

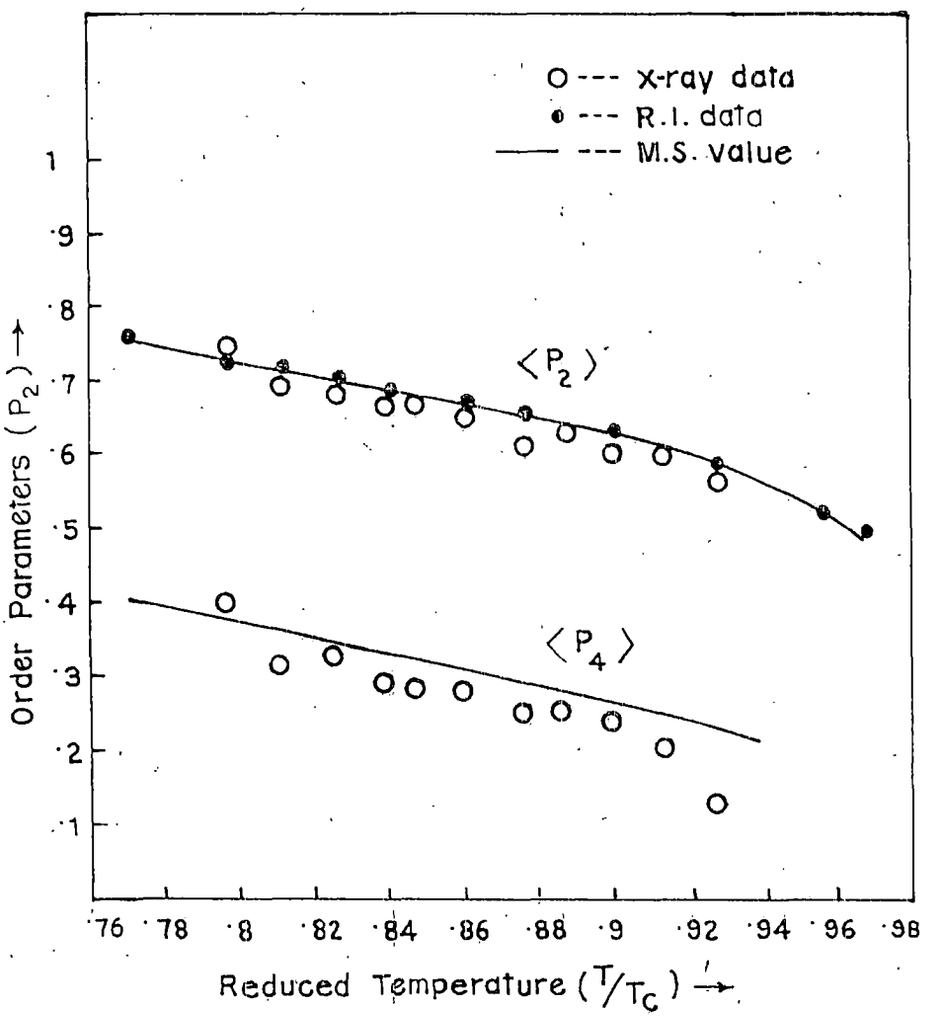
O --- X-ray data
• --- R.I. data
—— --- M.S. value
Order Parameters (P_2) →
1
·9
·8
·7
·6
·5
·4
·3
·2
·1
$\langle P_2 \rangle$
$\langle P_4 \rangle$
·76 ·78 ·8 ·82 ·84 ·86 ·88 ·9 ·92 ·94 ·96 ·98
Reduced Temperature (T/T_C) →

Fig. 3.11

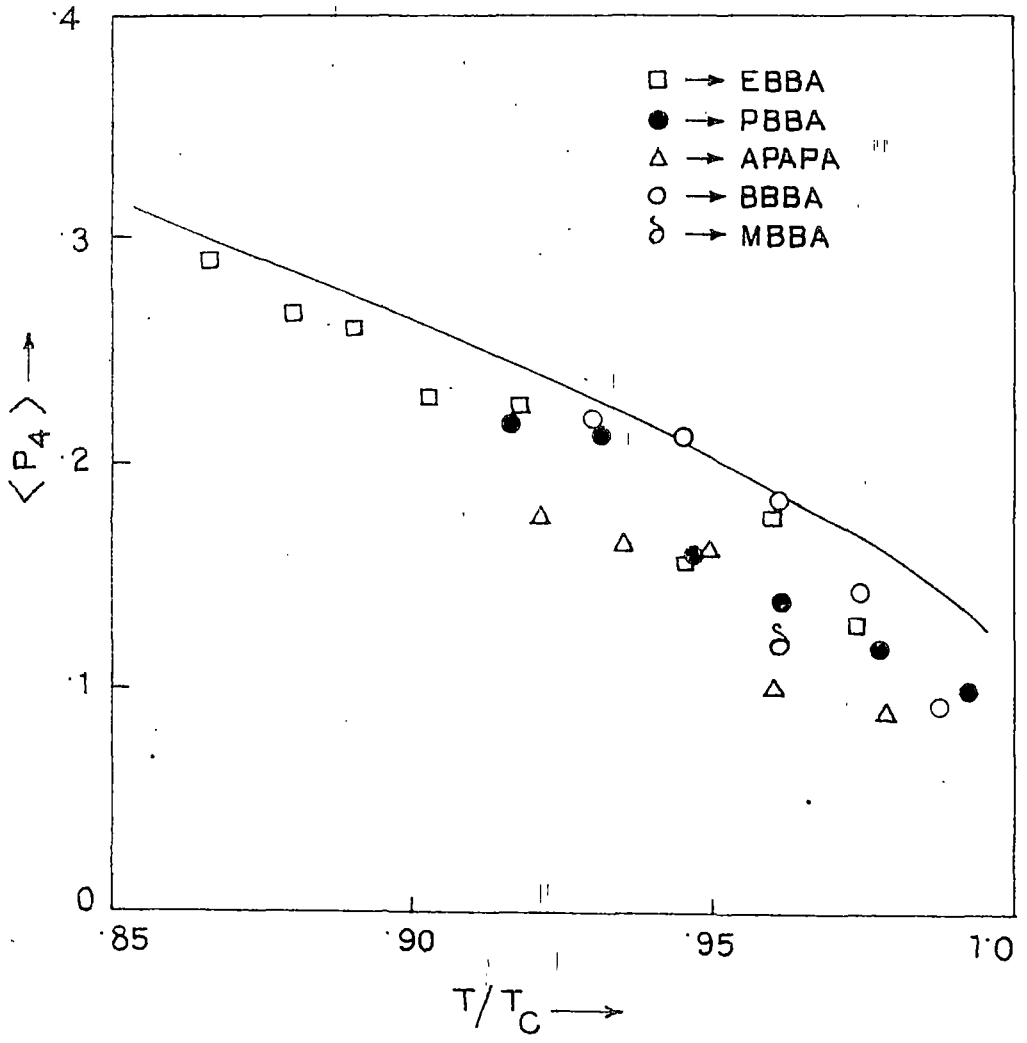

Fig 3.12

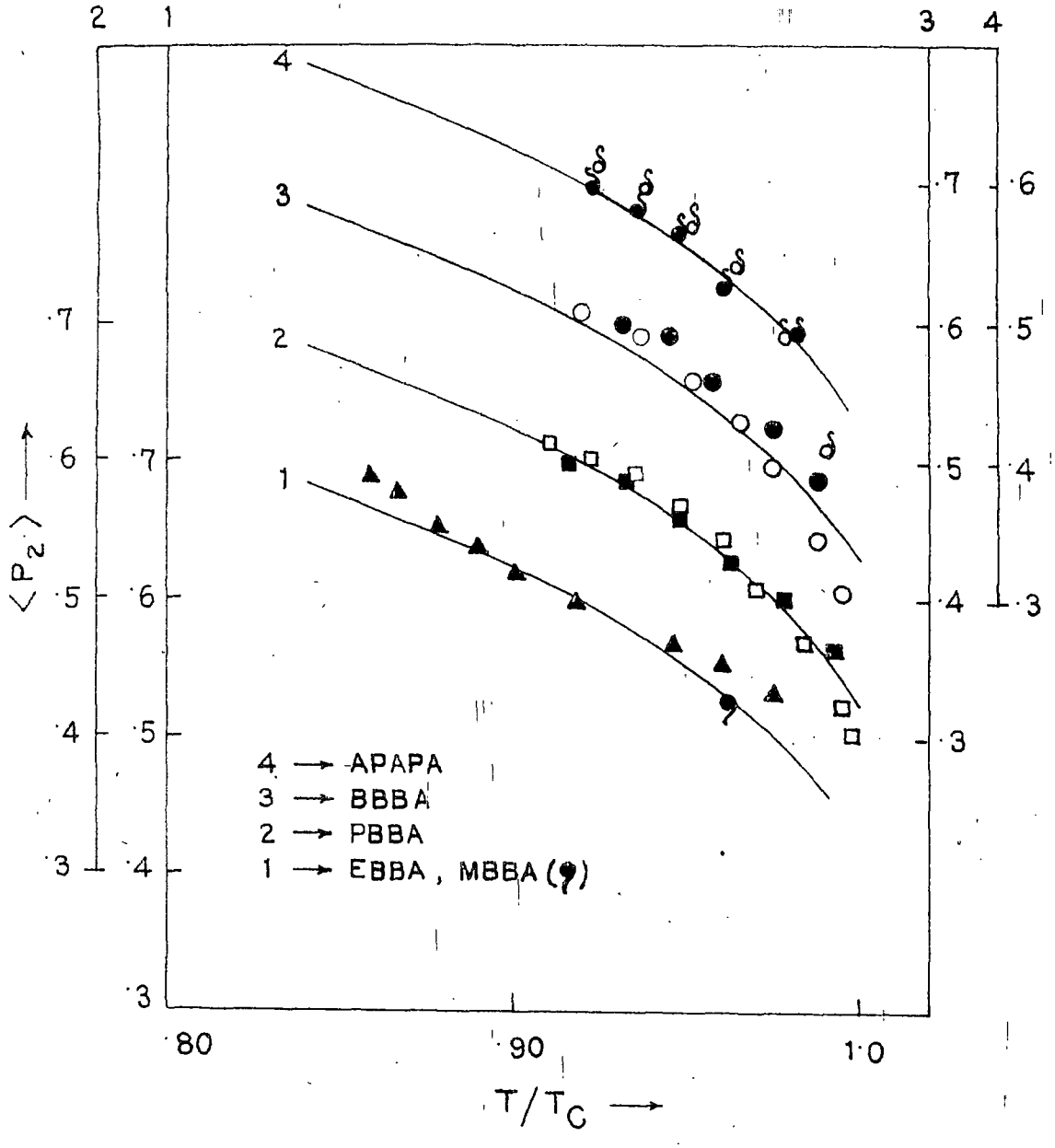
2 1
3 4
4
3
2
1
$\langle P_2 \rangle$
·7
·6
·5
·4
·3
·80
·90
1·0
T/T_C →
4 → APAPA
3 → BBBA
2 → PBBA
1 → EBBA , MBBA (?)

Fig 12a

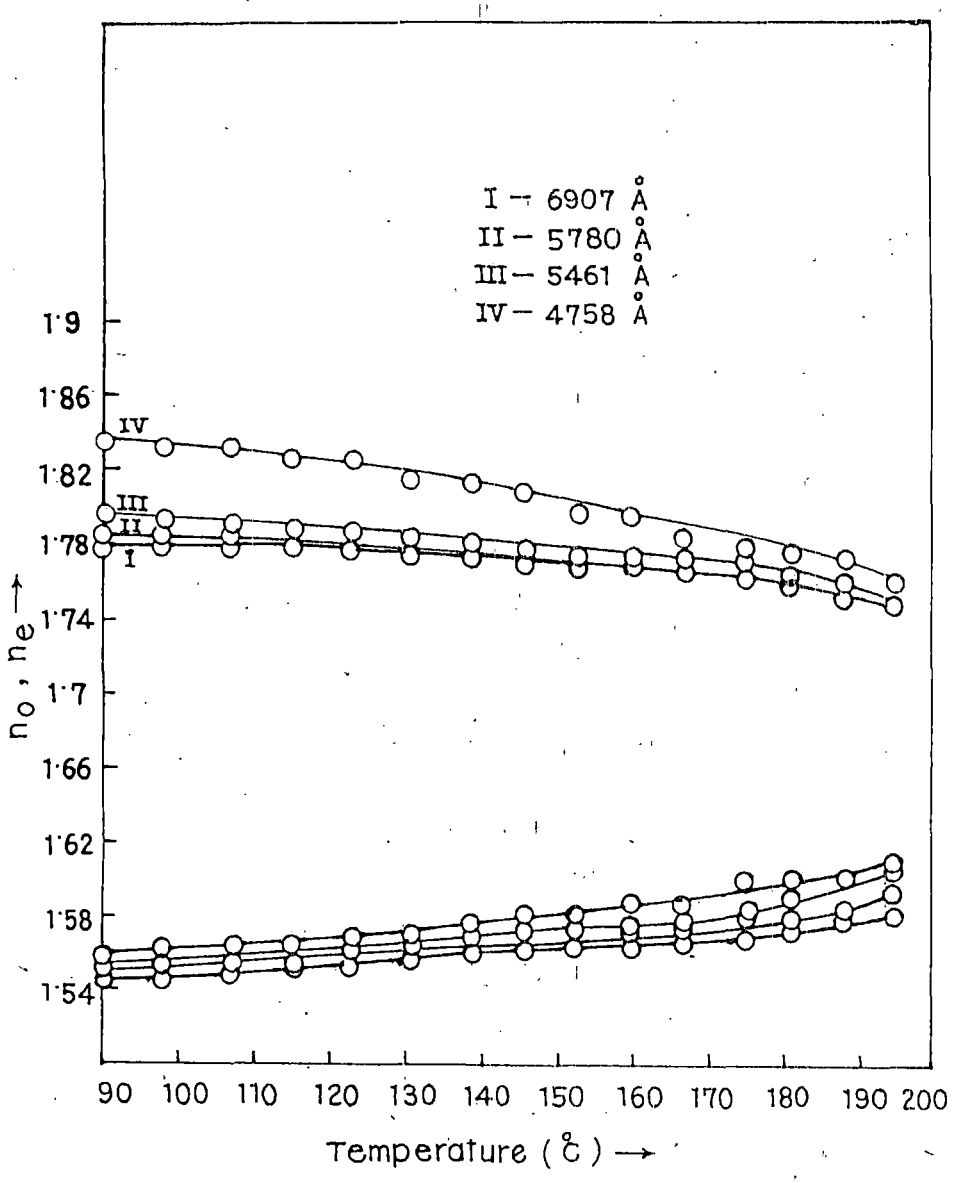
I – 6907 Å
II – 5780 Å
III – 5461 Å
IV – 4758 Å
1·9
1·86
1·82
1·78
1·74
1·7
1·66
1·62
1·58
1·54
IV
III
II
I
n_o , n_e →
90 100 110 120 130 140 150 160 170 180 190 200
Temperature (°C) →

Fig. 3.13

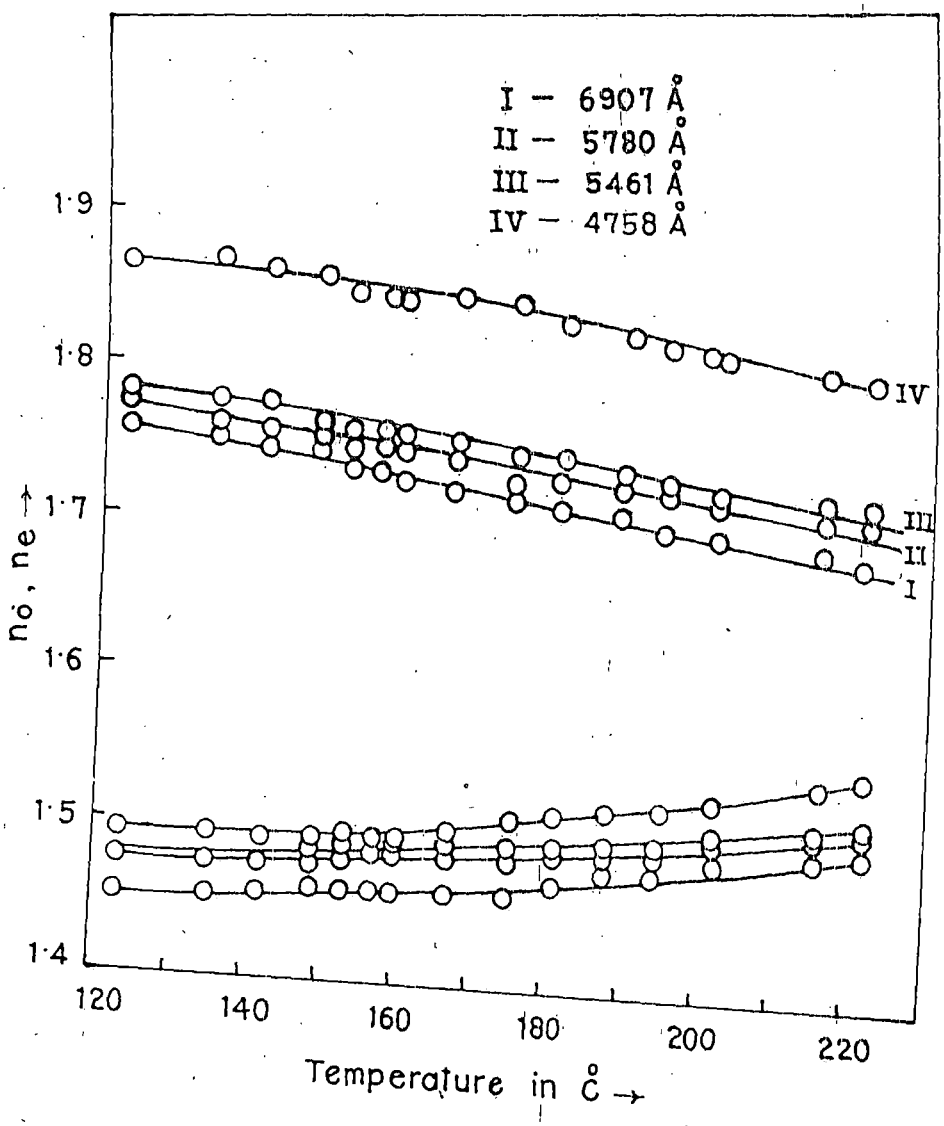
I – 6907 Å
II – 5780 Å
III – 5461 Å
IV – 4758 Å
1·9
1·8
1·7
1·6
1·5
1·4
no, ne
IV
III
II
I
120
140
160
180
200
220
Temperature in °C →

Fig. 3.14

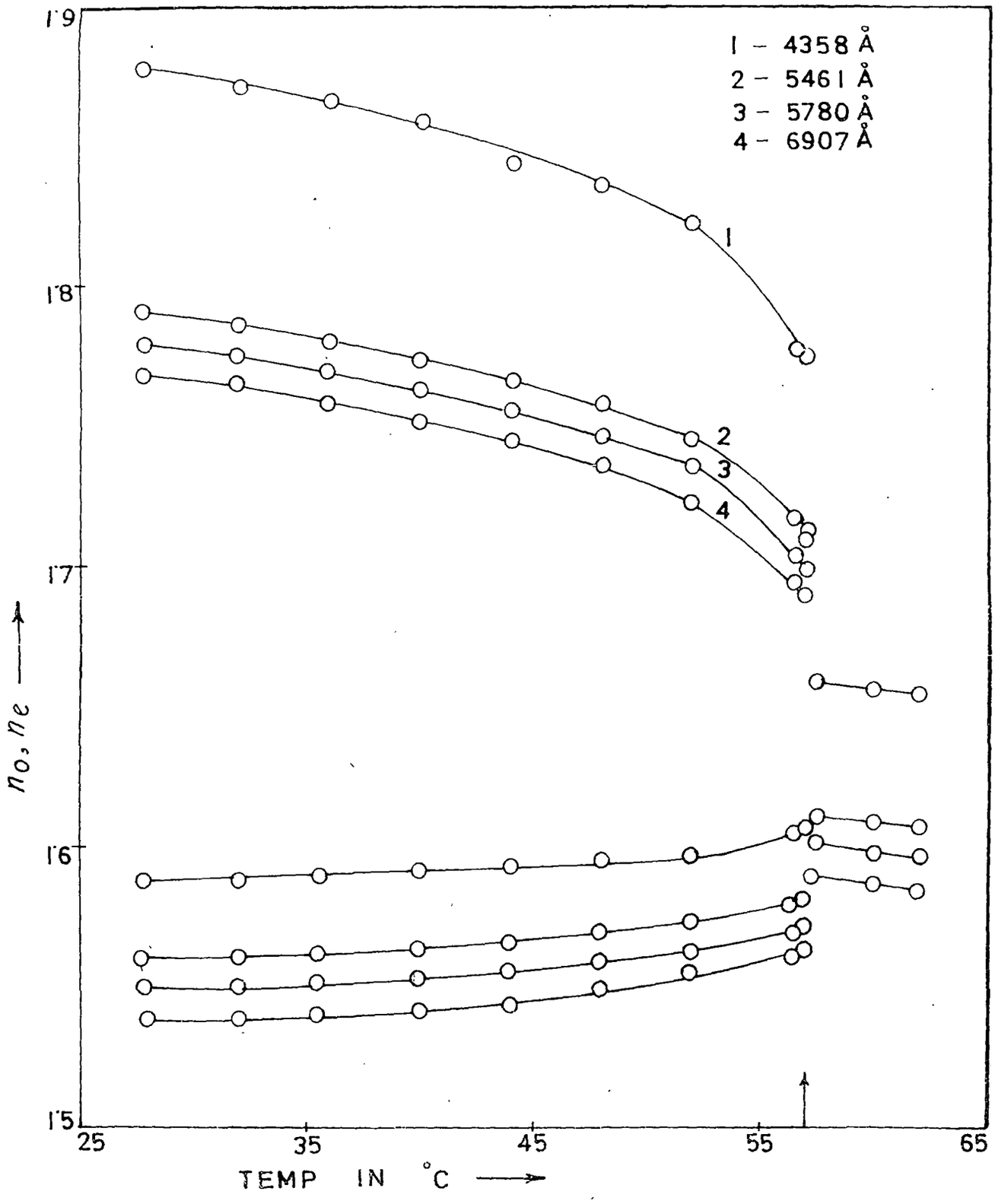
1 – 4358 Å
2 – 5461 Å
3 – 5780 Å
4 – 6907 Å
1
2
3
4
1·9
1·8
1·7
1·6
1·5
25
35
45
55
65
n_o, n_e
TEMP IN °C

Fig 1

Fig. 3.15

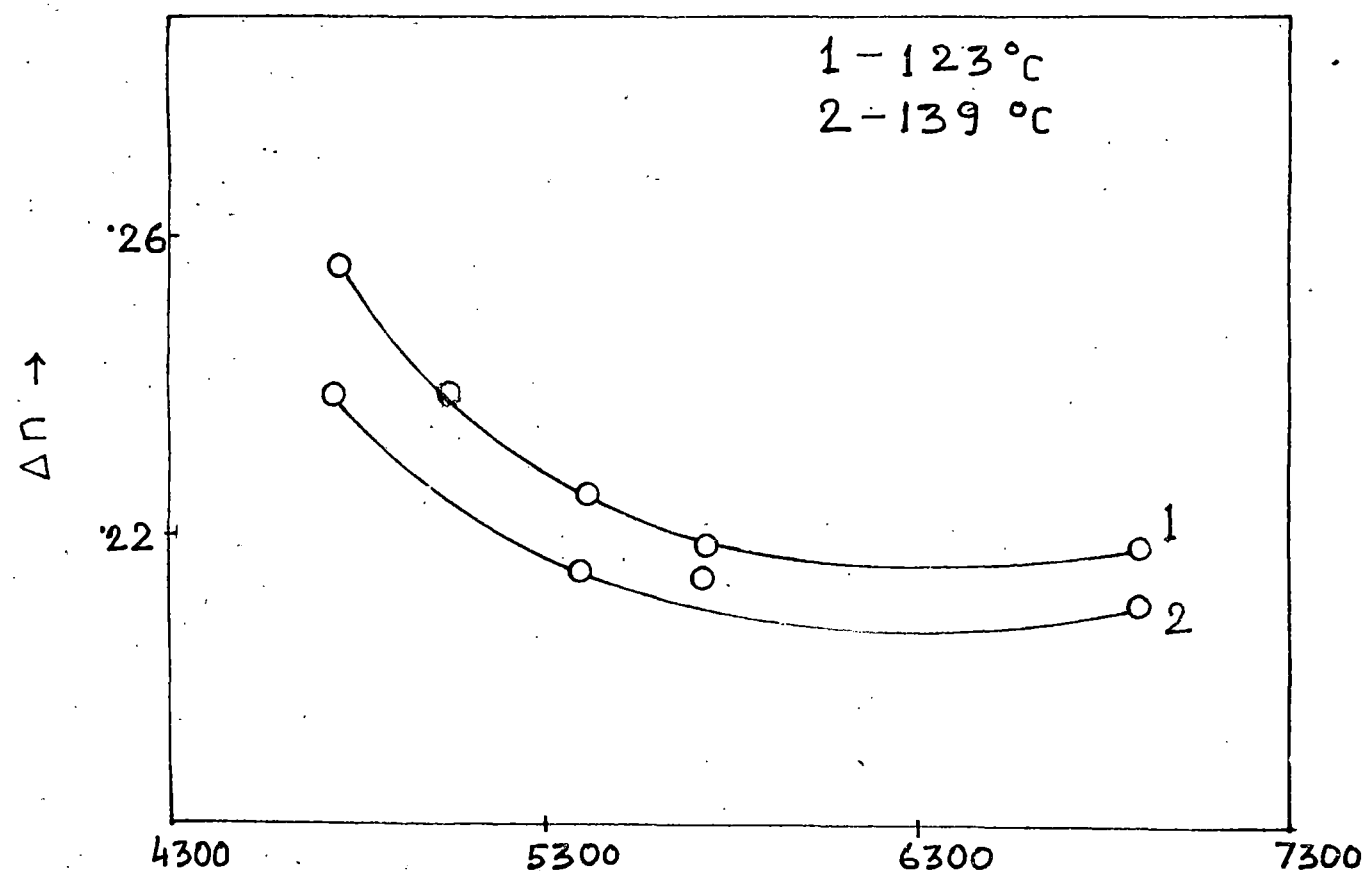

Fig. 3.16

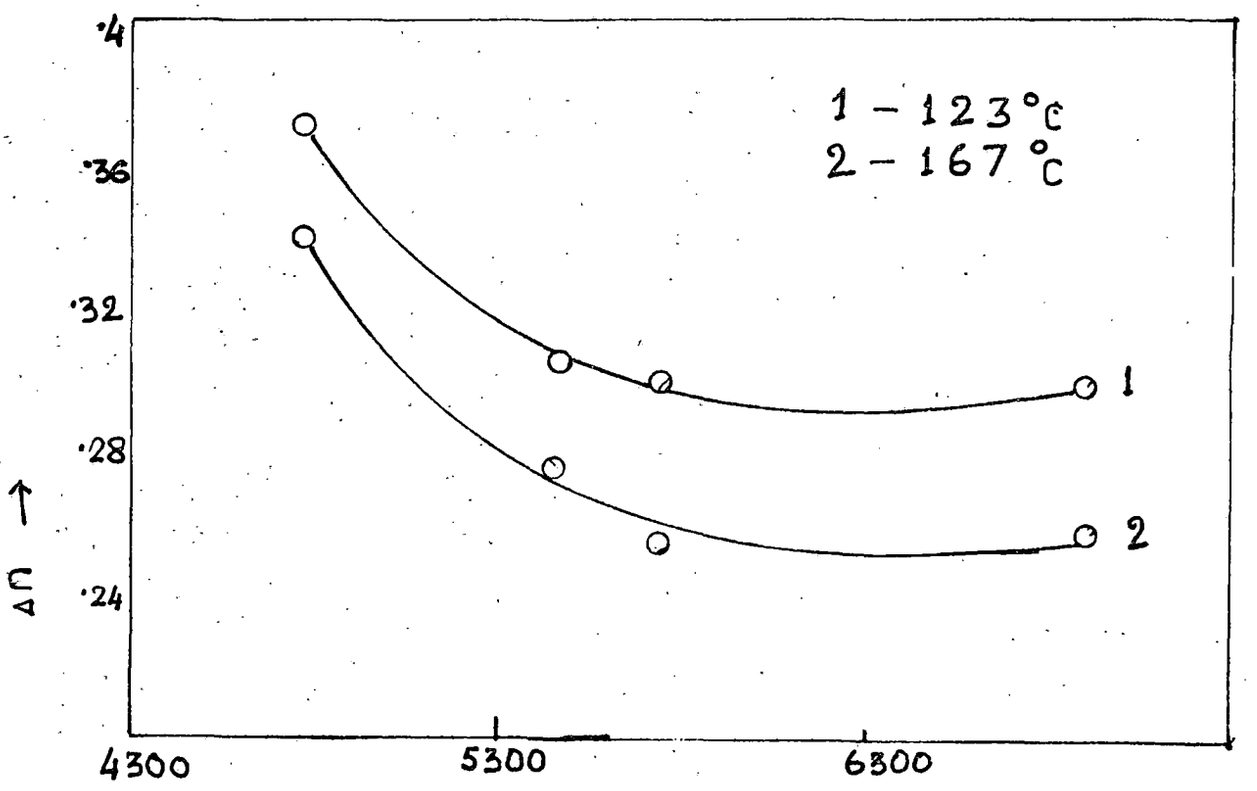

Fig. 3.17. Wavelength λ in Å →

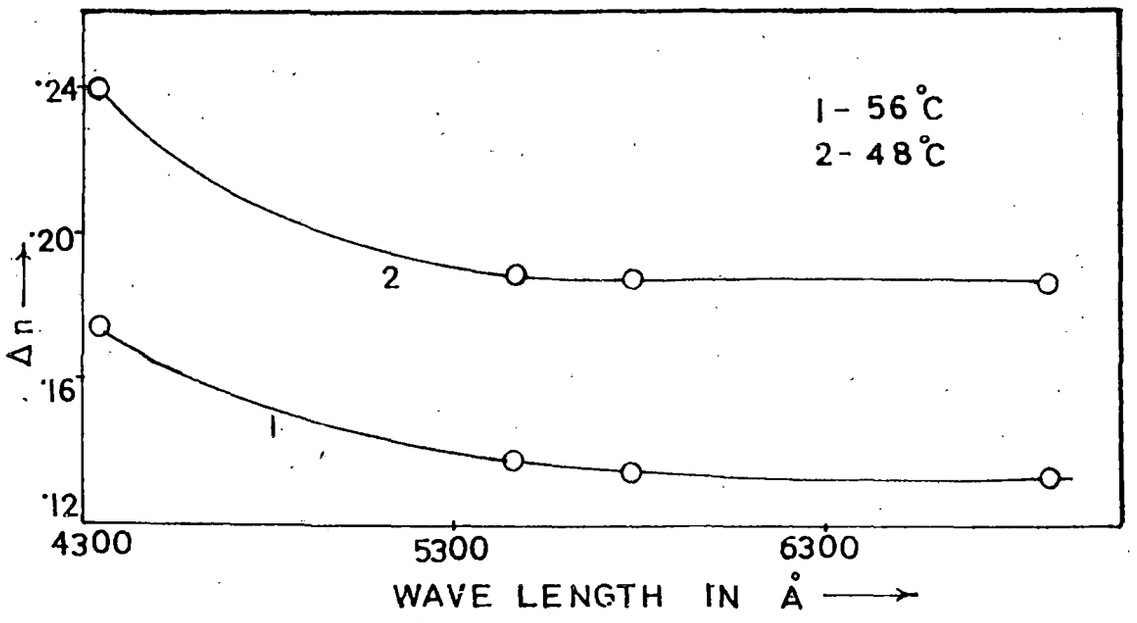

Fig - 3.18

3.2. X-ray Diffraction Studies on P-Ethoxy Benzylidene-p-n-Butylaniline (EBBA).

3.2.1. Introduction:

The structural formula of the sample EBBA is

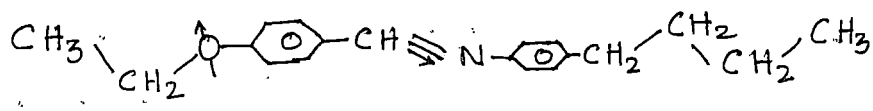

The X-ray work of the sample have been under taken as a part of the program of the study of the properties of Schiff's base compounds under taken by us. Leadbetter et al[17] have obtained the structure of the sample in meso-phases aligned by magnetic field. But the orientational order parameters have not been determined by them. Order parameter of oriented samples were obtained by NMR, Raman Scattering and IR dichroism measurement by different authors[18-20]. Leadbetter et al[21] have solved the crystal and molecular structure of EBBA. Here we have reported the order parameter values of EBBA from X-ray diffraction data. The apparent molecular length (l) and the average intermolecular spacings (D) have also been calculated and found to be in well agreement with that reported by Leadbetter et al[21].

The sample EBBA supplied to us by Prof.M.Wada of Tohoku University, Japan. The molecular arrangement in nematic phase determined by Wada[22]. The transition temperature according to them is

$$\text{Crystal} \underset{}{\overset{37^{\circ}C}{\rightleftharpoons}} \text{Nematic} \overset{79^{\circ}C}{\rightleftharpoons} \text{Isotropic}$$

The sample found to have a supercooling state, the transition temperature observed by us under polarising microscope and by X-ray photographs is

$$\text{Crystal} \underset{23^{\circ}C}{\overset{37^{\circ}C}{\rightleftharpoons}} \text{Nematic} \overset{79^{\circ}C}{\rightleftharpoons} \text{Isotropic.}$$

The same transition was also reported by Leadbetter et al.

3.2.2. Results and Discussions:-

The detailed of experimental procedures and theoretical backgrounds are discussed earlier. In table 3.21 and 3.22, the intensity values at different temperatures are given.

The normalised distribution function $f(\beta)$ as a function of β at different temperatures as obtained from experimental intensity values are given in Table 2r 3.23, and shown in Fig. 3.19 respectively. We expect as temperature decreases the function to become more packed at $\beta = 0^{\circ}C$. Our curves conforms to this idea. Orientational order parameters $\langle P_2 \rangle$ and $\langle P_4 \rangle$ at different tempe-

ratures are shown in Fig. 3.20. The order parameters are estimated to be accurate within $\pm$ 0.02. The experimental $\langle P_2 \rangle$ values are found to differ slightly from the M.F. theoretical values but within the experimental uncertainity. But lower $\langle P_4 \rangle$ values are obtained near the isotropic region. Such behaviour of $\langle P_4 \rangle$ was found by others also[10-13]. The case of this discrepancy has not been accounted with certainity.

Table 3.21

Sample: EBBA.

Experimental intensity values I (Ψ) at different temperature

Degree	Experimental intensity for temperature ^{o}K							
	302	305	309	313	318	323	333	338
0	83.00	62.00	34.50	30.75	82.50	47.50	66.00	60.50
5	80.00	58.00	33.00	37.48	80.75	46.75	60.25	57.00
10	67.10	50.20	30.25	32.50	74.00	43.58	55.50	52.00
15	54.25	42.10	25.75	27.13	62.50	37.75	47.25	46.75
20	42.50	34.50	21.00	21.30	51.52	31.00	44.25	41.10
25	33.25	25.25	16.50	17.75	42.25	25.25	38.00	35.25
30	26.25	19.50	13.55	13.80	32.0	19.00	31.35	28.50
35	19.40	15.50	9.15	18.28	23.75	14.00	24.75	22.10
40	14.00	10.10	5.60	7.18	19.25	9.50	18.50	16.25
45	10.25	6.50	3.40	4.83	12.90	8.00	13.75	11.00
50	8.15	4.00	2.65	3.38	9.60	5.90	10.00	7.35
55	6.00	2.35	1.90	2.25	7.00	4.25	6.25	5.30
60	4.25	1.15	1.30	1.48	4.35	3.10	4.25	3.60
65	3.10	0.60	0.75	0.88	2.50	2.50	2.50	3.15
70	2.25	0.50	0.40	0.55	1.80	1.90	1.60	2.60
75	1.25	0.10	0.40	0.33	1.10	1.25	0.65	2.15
80	0.85	00	0.25	0.18	0.65	0.65	0.50	1.40
85	0.60	0	0.00	0.05	0.25	0.25	0	0.90
90	0.00	0	.00	0.00	00	00	0	0.65

Table 3.22

Sample: EBBA.

Calculated
~~Experimental~~ intensity I (Ψ) at different temperature

Degree	Calculated intensity for temperature °K							
	302	305	309	313	318	323	333	338
0	83.57	61.21	34.54	38.91	83.00	47.84	64.55	59.66
5	79.04	58.41	33.24	37.16	80.37	46.59	61.81	57.65
10	67.63	51.15	29.88	32.69	73.28	43.07	55.29	52.60
15	54.14	41.98	25.57	27.21	63.53	37.80	46.33	46.53
20	42.41	33.27	21.29	22.12	52.80	31.52	42.81	40.74
25	33.40	26.02	17.03	17.77	42.13	24.96	37.92	35.11
30	26.05	20.02	12.94	13.88	32.18	18.87	32.03	28.94
~~35~~	~~20x02~~	~~12x94~~						
35	19.51	14.79	9.06	10.26	23.70	13.84	24.98	22.32
40	14.07	10.24	5.83	7.14	17.27	10.13	18.28	15.90
45	10.26	6.59	3.63	4.84	12.85	7.59	13.30	10.92
50	7.90	3.99	2.43	3.34	9.66	5.79	9.89	7.52
55	6.14	2.92	1.79	2.30	6.90	4.38	6.99	5.28
60	4.44	1.23	1.32	1.48	4.42	3.23	4.22	3.79
65	2.97	0.62	0.86	0.86	2.59	2.39	2.14	2.92
70	2.02	0.32	0.49	0.51	1.61	1.81	1.24	2.53
75	1.48	0.19	0.27	0.35	1.16	1.30	1.06	2.20
80	0.95	0.096	0.15	0.21	0.73	0.73	0.73	1.61
85	0.37	-0.011	0.07	0.52	0.22	0.21	0.06	0.87
90	0.10	-0.06	0.03	-0.003	-0.02	-0.016	-0.29	0.53

Table 3.23

Sample: EBBA.

Normalised Distribution Function Values f(β) at Different Temperature.

Degree	Distribution function f(β) at temp. ^{o}K							
	302	305	309	313	318	323	333	338
0	11.13	11.17	9.12	9.77	7.74	7.35	7.34	7.19
5	10.35	10.02	8.39	9.02	7.42	7.01	6.82	6.63
10	8.69	7.62	6.84	7.31	6.59	6.16	5.65	5.42
15	6.99	5.52	5.41	5.59	5.54	5.21	4.48	4.34
20	5.33	4.23	4.46	4.30	4.46	4.35	3.84	3.68
25	3.60	3.47	3.78	3.39	3.46	3.53	3.09	3.31
30	2.14	2.82	3.01	2.63	2.57	2.69	2.66	2.94
35	1.25	2.06	2.07	1.92	1.83	1.88	2.19	2.34
40	0.81	1.29	1.21	1.29	1.26	1.21	1.66	1.58
45	0.59	0.73	0.66	0.82	0.87	0.78	1.16	0.95
50	0.43	0.42	0.39	0.52	0.60	0.54	0.77	0.57
55	0.29	0.25	0.27	0.34	0.42	0.41	0.50	0.38
60	0.19	0.15	0.21	0.22	0.29	0.33	0.32	0.28
65	0.14	0.08	0.15	0.14	0.18	0.25	0.19	0.22
70	0.10	0.04	0.08	0.08	0.10	0.17	0.10	0.16
75	0.06	0.01	0.04	0.04	0.05	0.09	0.05	0.11
80	0.03	0.004	0.01	0.02	0.03	0.05	0.02	0.08
85	0.01	0.002	0.007	0.01	0.02	0.03	0.01	0.05
90	0	0	0	0	0	0	0	0.04

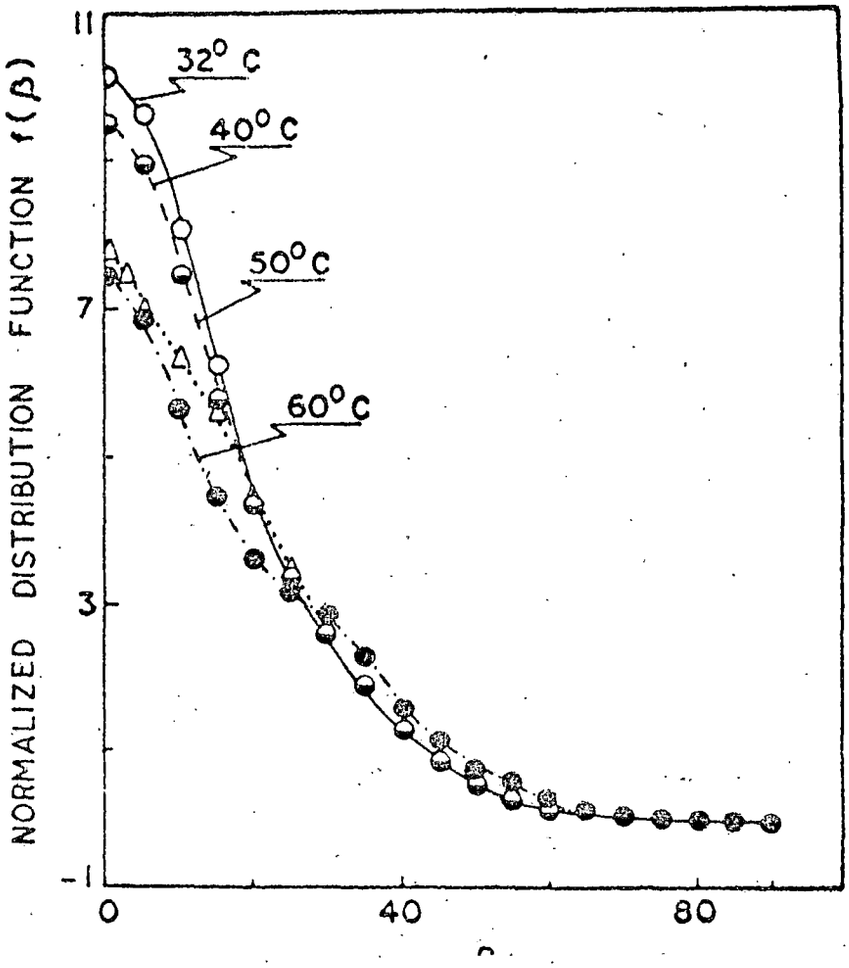
NORMALIZED DISTRIBUTION FUNCTION f(β)
11
7
3
-1
0
40
80
β
32° C
40° C
50° C
60° C

Fig. 3.19

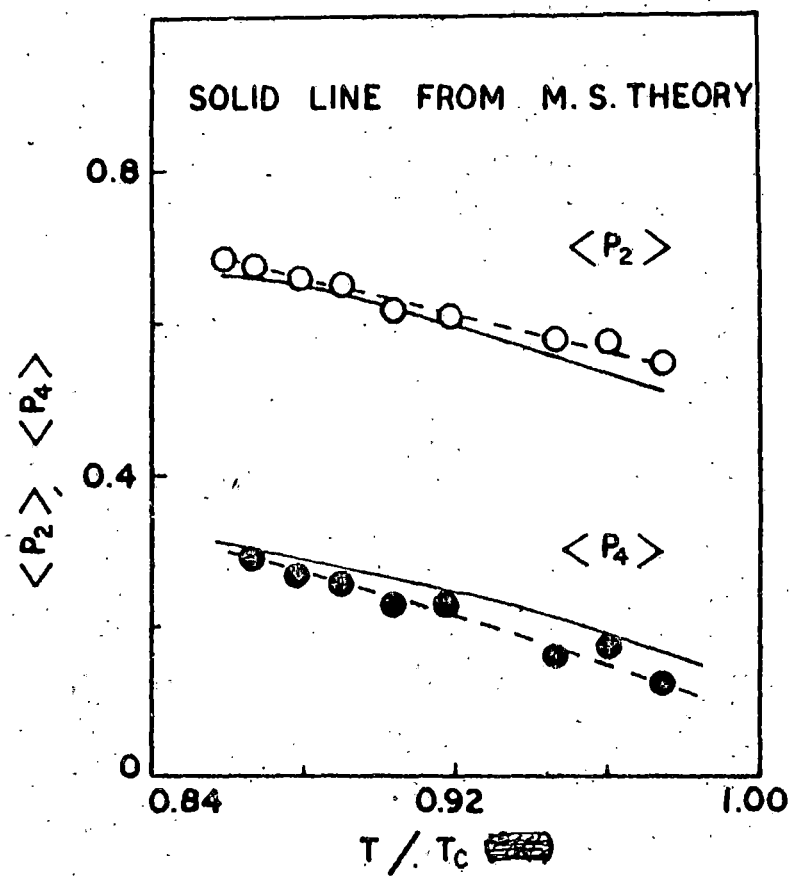
SOLID LINE FROM M. S. THEORY
0.8
0.4
0
$\langle P_2 \rangle$
$\langle P_4 \rangle$
$\langle P_2 \rangle, \langle P_4 \rangle$
0.84
0.92
1.00
T / Tc

Fig- 3.20

3.3. Optical bi-refringence studies on 5OCB and BPCPP

In this section the optical birefringence studies of the following samples are reported.

1. 4'-pentyloxy-4-cyanobiphenyl(5OCB in short)

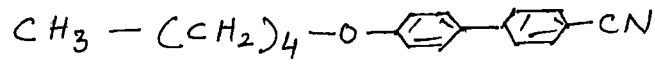

Solid $\underset{31.5^{\circ}C}{\overset{47.5^{\circ}C}{\rightleftharpoons}}$ Nematic $\rightleftharpoons^{67.5^{\circ}C}$ Isotropic

2. 5-(4-n-Butylphenyl)-2-(4-cyanophenyl)-Pyrimidene (BPCPP in short).

X-ray diffraction studies of the samples 1 and 2 were done in our laboratory by Bhattacharjee et al[23] and B.Jha et al[24] respectively. Orientational order parameters, apparent molecular length average intermolecular distance and the angular part of the mean field potential in the nematic phase of both the sample were studied by them. Crystal structure analysis of the sample 2 with the help of the X-ray diffraction were done by P.Mandal and S.Paul[25] of our laboratory.

The refractive index measurement and the determination of order parameters from bi-refringence study for these compounds are being reported here.

Results and Discussion:-

The experimental details are described earlier. The values of refractive indices (n_o , n_e) at different temperatures and for different wave lengths are given in the Table 3.24, and 3.25 and shown in Fig. 3.25 - 3.26 respectively for the samples. The density, polarizability from Vuk's approach and order parameters calculated are given in the Table 3.26 and 3.27. The results of Neugebaur's approach are given in Table ~~2x~~ 3.28 and 3.29 respectively.

The orientational order parameter $\langle P_2 \rangle$ ~~x~~ was calculated using the relation $\langle P_2 \rangle = (\alpha_e - \alpha_o)/(\alpha_{\parallel} - \alpha_{\perp})$ The values of $(\alpha_{\parallel} - \alpha_{\perp})$ is determined from Haller's extrapolation is described incase of the sample 1 only. The Fig. 3.27 shows the plot of $ln(\alpha_e - \alpha_o)$ Vs. $ln(T_c - T)$ of sample I which is a straight line. The straight line is extrapolated to T = 0°K.

The values of $(\alpha_{\parallel} - \alpha_{\perp}) = \alpha_a$ for Vuk's and Neugebauer's approach are tested by calculating α_a for both the samples by using additive rule of the bond polarizability values available in the literature[5,6,7]. The mean polarizability valuesalso calculated. The table 3.30 shows the α_a and α values of both the sample by different methods. This is clear from the table that the values obtained from Neugebauer's data is very close to that calculated from bond polarizability whereas the α_a values calculated from Vuk's formula is significantly different.

In case of compounds PCCPP, PCTP, PBBA we have found the same results. Discrepancies have also been found in other nematic liquid crystals[26]. Although the Haller's plot is not fully justifiable in all cases and the additive rule of the bond polarizability to estimate the molecular polarizability anisotropy (α_a) may be more realistic, but we have not used the bond polarizability values in any further calculations since the difference between two sets of α_a valuesx one from ~~the~~ bond polarizability and one from Neugebauer's approach, is marginal.

The order parameter values calculated using Vuk's formula and Neugebauer's relations agree well for the compounds in their respective nematic phases. This may be due to the fact that although α_e and α_o vary considerably in the two approaches the variation of $(\alpha_e - \alpha_o)$ with temperature is more or less the same in two cases.

The Fig. 3.28, and 3.29 shows the $\langle P_2 \rangle$ values of the samples obtained from different methods. It is found that the $\langle P_2 \rangle$ values obtained from R.I. data agree well with the M.S. theoretical values expect in the nematic - isotropic transition region. The higher temperature values in case of the sample 2 could not be taken because of experimental limitations. The $\langle P_2 \rangle$ values at the transition region are significantly lower than the theoretical values. Such behaviour near T_c has also been found by others[8,9] $\langle P_2 \rangle$ values from X-ray diffraction techniques are higher than the theoretical values. Different approximations involved in different cases may be the cause of such differences.

In the refractive indices study we rely on surface anchoring only for the formation of monodomain sample as the magnetic field cannot be applied during the measurements hence it is likely that near the nematic isotropic transitions temperature, the samples may not remain ideally monodomain.

Table 3.30

α and $(\alpha_{\parallel} - \alpha_{\perp})$

Sample	$\alpha \times 10^{24}$ cm		$(\alpha_{\parallel} - \alpha_{\perp}) \times 10^{24} cm^3$		
	Calculated from bond polarizability	Vuk's/ Neugebauers approach (Isotropic liquid)	Calculated from bond polarizability	Haller's process (Vuks' data)	Haller's process (Neugebauers' data)
1. 50CB	34.14	34.61	18.42	22.80	18.30
2. DPCPP	43.14		32.09	47.8	33

Table 3.24

Refractive indices (n_o , n_e) at different temperature of sample 5003

Temp °C	6907 Å		5780 Å		5461 Å		4758 Å	
	n_o	n_e	n_o	n_e	n_o	n_e	n_o	n_e
32.5	1.522	1.725	1.533	1.741	1.538	1.752	1.571	1.810
36	1.522	1.720	1.533	1.736	1.538	1.747	1.571	1.805
40	1.522	1.715	1.533	1.731	1.538	1.742	1.571	1.799
44.5	1.522	1.709	1.533	1.725	1.538	1.736	1.571	1.793
48	1.522	1.702	1.533	1.718	1.538	1.729	1.571	1.786
5255	1.525	1.695	1.536	1.711	1.541	1.722	1.575	1.778
57	1.529	1.685	1.540	1.701	1.545	1.712	1.579	1.768
61.5	1.534	1.673	1.545	1.689	1.550	1.700	1.585	1.755
66	1.540	1.658	1.551	1.673	1.556	1.684	1.592	1.738
67	1.545	1.651	1.556	1.666	1.561	1.677	1.599	1.730
70	1.5981		1.593		1.600		1.638	
75	1.580		1.592		1.599		1.637	

Table 3.25

Refractive indices (n) of sample BPCPP at different wavelength (λ)

Temp. in °C	6907 Å		5780 Å		5461 Å		4758 Å	
	n_o	n_e	n_o	n_e	n_o	n_e	n_o	n_e
100	1.483	1.846	1.499	1.862	1.511	1.874	1.546	1.909
110	1.483	1.842	1.499	11858	1.511	1.870	1.546	1.905
120	1.483	1.837	1.499	1.853	1.511	1.865	1.546	1.900
130	1.486	1.831	1.502	1.847	1.514	1.860	1.549	1.895
140	1.490	1.826	1.506	1.842	1.518	1.854	1.553	1.889
150	1.494	1.820	1.510	1.836	1.522	1.848	1.557	1.883
160	1.498	1.814	1.514	1.830	1.526	1.842	1.561	1.877
170	1.502	1.808	1.518	1.824	1.530	1.836	1.565	1.871
180	1.506	1.802	1.522	1.818	1.534	1.830	1.569	1.865
190	1.511	1.796	1.527	1.812	1.539	1.824	1.574	1.859
200	1.516	1.790	1.532	1.806	1.544	1.818	1.579	1.853

TABLE 3.26

Density (ρ), polarizability (α) and orientational order parameter ($\langle P_2 \rangle$) of 5OCB

$\lambda \rightarrow$		6907 Å			5761 Å			5461 Å			4358 Å		
Temp. (°c)	ρ (gm/cm^3)	α_o	α_e	$\langle P_2 \rangle$	α_o	α_e	$\langle P_2 \rangle$	α_o	α_e	$\langle P_2 \rangle$	α_o	α_e	$\langle P_2 \rangle$
32.5	1.067	28.84	45.13	.6325	29.30	45.93	.6325	29.48	46.53	.6321	30.73	49.60	.6310
36	1.0665	28.89	44.83	.6190	29.35	45.63	.6192	29.53	46.23	.6191	30.79	49.28	.6194
40	1.066	28.94	44.53	.6054	29.40	45.34	.6059	29.59	45.87	.6036	30.85	48.92	.6054
44.5	1.0642	29.03	44.22	.5898	29.49	45.03	.5907	29.67	45.63	.5914	30.94	48.69	.5945
48	1.0628	29.11	43.96	.5767	29.57	44.77	.5779	29.75	45.37	.5789	31.02	48.44	.5834
52.5	1.0608	29.42	43.58	.5498	29.88	44.39	.5516	30.06	44.99	.5533	31.40	47.91	.5532
57	1.0573	29.85	43.05	.5124	30.32	43.86	.5150	30.50	44.47	.5177	31.86	47.21	.5140
61.5	1.0523	30.39	42.50	.4699	30.86	43.31	.4734	31.04	43.92	.4772	32.47	46.40	.4657
66	1.0414	31.37	41.78	.4040	31.84	42.60	.4091	32.02	43.21	.4147	33.55	45.57	.4024
67	1.0310	32.01	41.71	.3767	32.48	42.54	.3825	32.67	43.16	.3889	34.33	45.43	.3720

α_o and α_e are in units 10^{-24}cm^3

Table 3.27

Density (ρ) and orientational order parameters ($\langle P_2 \rangle$) of sample BPCPP(Vuks' approach)

Temp. in ^oC	Density (ρ) in gm/cm.	6907 Å		5780 Å		5461 Å		4753 Å		Mean $\langle P_2 \rangle_{AV}$
		α_o	α_e	α_o	α_e	α_o	α_e	α_o	α_e	
100	.885	36.58	73.45	37.62	74.42	38.38	75.14	40.59	77.20	.768
110	.881	36.81	73.39	37.83	74.39	38.60	75.11	40.80	77.05	.763
120	.877	37.01	73.27	38.05	74.26	38.83	74.99	41.05	77.08	.756
130	.873	37.46	72.95	38.51	73.94	39.28	74.77	41.52	76.87	.741
140	.868	38.03	72.77	39.09	73.77	39.87	74.51	42.12	76.63	.723
150	.863	38.62	72.49	39.69	73.50	40.47	74.25	42.73	76.38	.705
160	.857	39.27	72.30	40.33	73.32	41.13	74.07	43.40	76.22	.689
170	.851	39.92	72.11	40.99	73.13	41.79	73.89	44.08	76.06	.671
180	.846	40.53	71.83	41.61	72.86	42.42	73.63	44.72	75.81	.652
190	.840	41.28	71.60	42.37	72.64	43.14	45.49	45.49	75.62	45x632
200	.833	41.88	69.48	42.18	70.81	42.97	71.57	45.25	73.74	.612

α_o and α_e are in units 10^{-24} cm^3

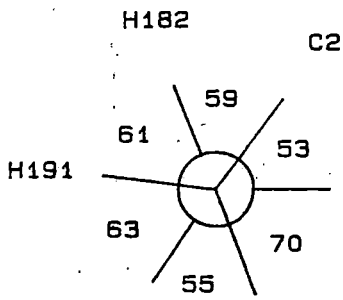

C14 H192
(C19 – C18)

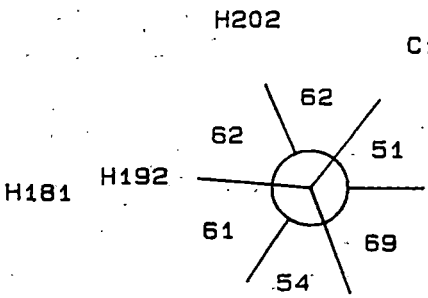

C21 H191
(C19 – C20)

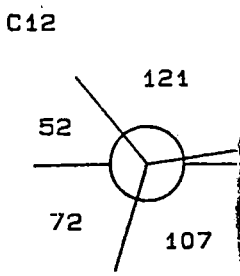

C16
(C11 – C9)

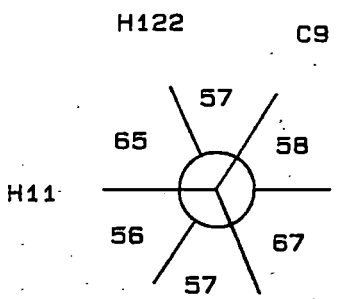

C13 C16
(C11 – C12)

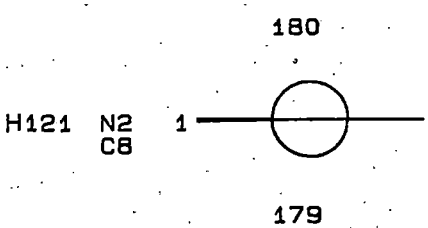

(C9 – C10)

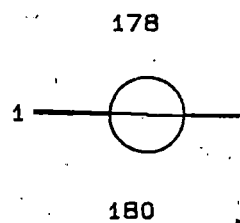

(C9 – C8)

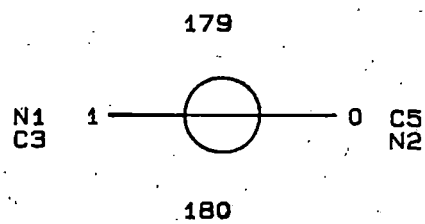

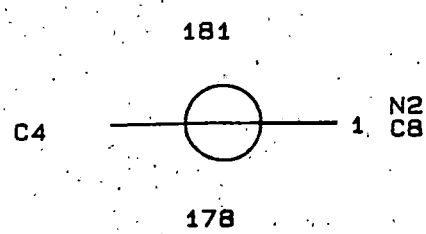

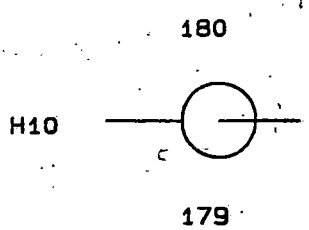

Table 3.29

Polarizability at different temperature from Neugebauer Method of Sample - BPCPP

Temp. in °C	λ → 6907 Å		5780 Å		5461 Å		4758 Å	
	α_o	α_e	α_o	α_e	α_o	α_e	α_o	α_e
100	38.97	68.67	40.06	69.54	40.87	70.18	43.19	72.00
110	39.18	68.66	40.25	69.54	41.06	70.19	43.2	72.0
120	39.34	68.59	40.45	69.47	41.26	70.12	43.61	71.98
130	39.75	68.36	40.86	69.25	41.68	69.99	44.03	71.86
140	40.28	68.27	41.39	69.17	42.21	69.83	44.57	71.73
150	40.82	68.09	41.93	69.01	42.76	69.68	45.13	71.60
160	41.41	68.01	42.53	68.92	43.36	69.60	45.74	71.55
170	42.01	67.91	43.14	68.84	43.97	69.53	46.35	71.50
180	42.57	67.75	43.70	68.69	44.54	69.38	46.94	71.37
190	43.26	67.64	44.40	68.59	45.24	69.29	47.65	71.31
200	43.71	65.82	44.10	66.97	44.92	67.66	47.29	69.66

α_o and α_e are in units 10^{-24} cm^3

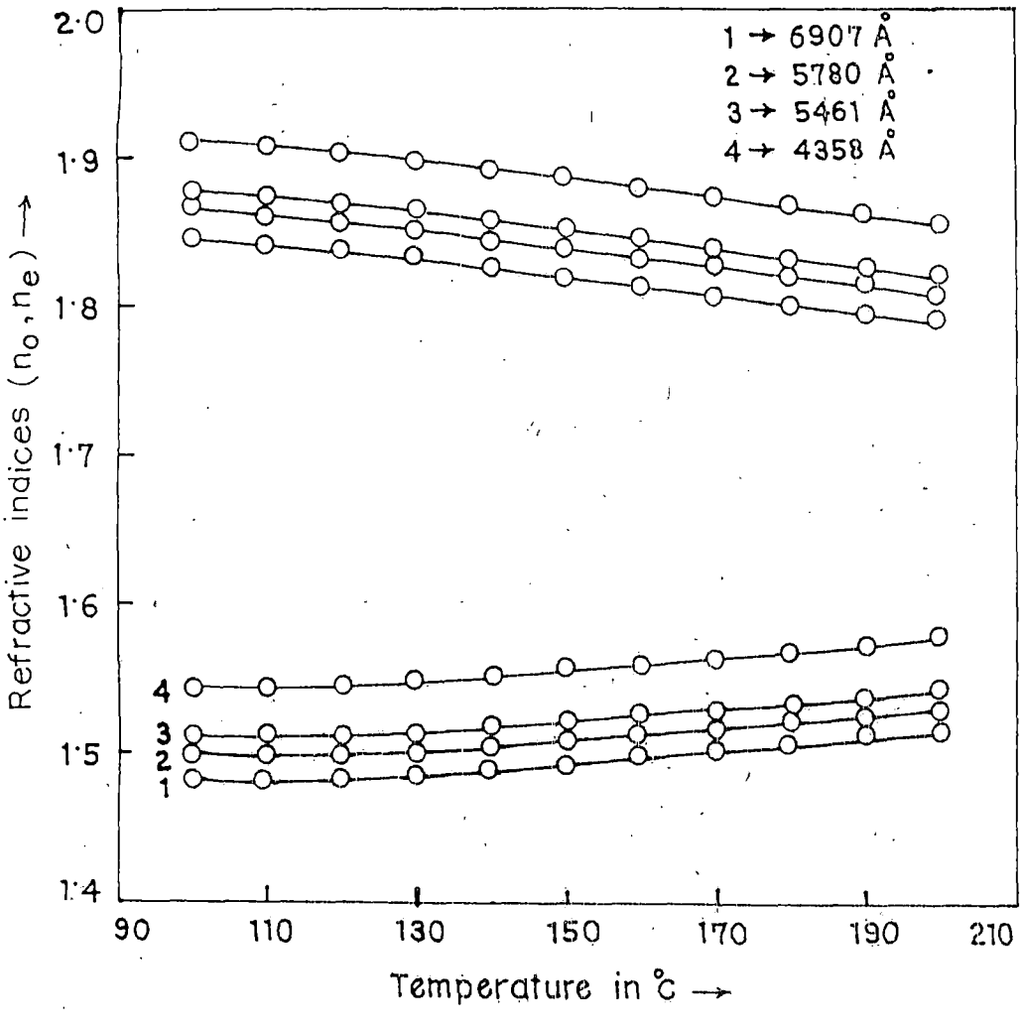
1 → 6907 Å
2 → 5780 Å
3 → 5461 Å
4 → 4358 Å
2·0
1·9
1·8
1·7
1·6
1·5
1·4
Refractive indices (n_o, n_e) →
4
3
2
1
90
110
130
150
170
190
210
Temperature in °C →

Fig. 3.29

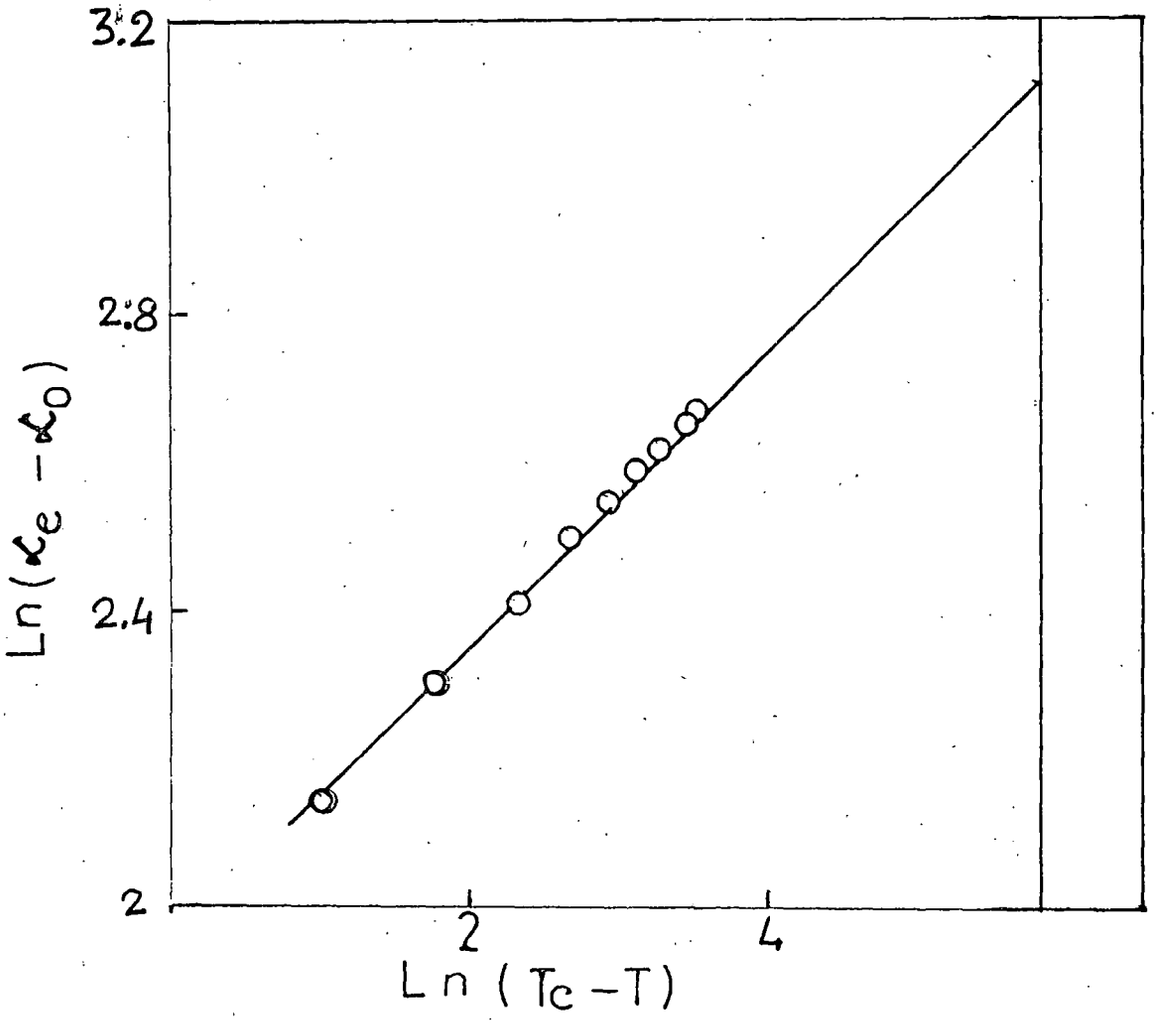

Fig. 3.27

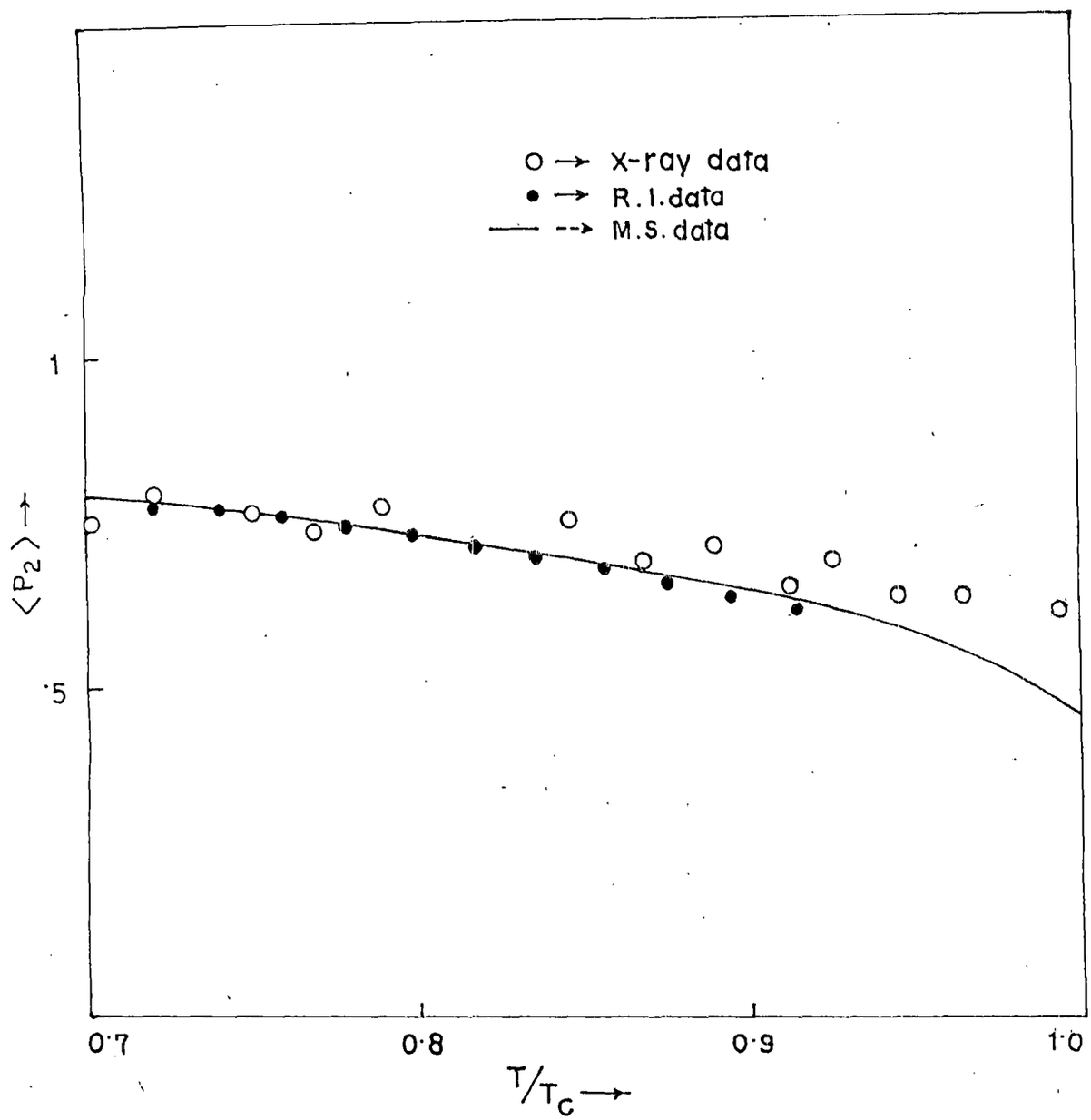

Fig. 3.25

References

1. B.Bhattacharjee, S.Paul and R.Paul, Mol.Cryst.Liq. Cryst. 89, 181 (1982).
2. W.Haase, H.Paulus and H.T.Muller, Mol.Cryst.Liq. Cryst. 97, 131 (1983).
3. A.J.Leadbetter, R.M.Richardson and C.N.Cooling, J.Phys. (Paris), 36, 37 (1975).
4. Ref. 26 of Chapter - 2.
5. C.G.Le Fevre and R.J.W. Le F Fevre: Rev.Pure Appl. Chem. 5, 261 (1955).
6. R.J.W. Le Fevre: Adv.Phys.Org.Chem. 3, 1 (1965).
7. D.A.Dunmur and A.E.Tomes, Mol.Cryst.Liq.Cryst.97, 241 (1983).
8. N.V.Madhusudana, R.Shashidhar and S.Chandrasekhar, Mol.Cryst.Liq.Cryst. 13, 61 (1971).
9. I.H.Ibrahim and W.Haase; J.De Physique. Collogue, C3 40, C3-164 (1979).
10. B.Bhattacharjee, S.Paul and R.Paul, Mol.Cryst.Liq. Cryst. 89, 181 (1982).
11. S.Jou, N.A.Clark, F.G.Perahan and E.B. Priestley, Phys. Rev.Lett. 31, 1552 (1973).
12. S.Kobinata, Y.Nakajima, H.Yoshida and S.Waeda, Mol. Cryst.Liq.Cryst., 66, 387 (1981).
13. J.P.Heagen; J.Phys.Lett. (Paris), 36, 209 (1975).
14. B.Bhattacharjee, R.Paul and S.Paul, Jpn. J.Appl. Phys. 18, 985 (1979).

15. P.Mandal, M.Mitra, S.Paul and R.Paul: Liquid Crystals, 2, 183 (1987).

16. P.Mandal, M.Mitra, K.Bhattacharjee, R.Paul and S.Paul, Mol.Cryst.Liq.Cryst. 149, 203 (1987).

17. A.J.Leadbetter, R.M.Richardson and C.N. Colling, J.Phys. (Paris) c-1, 36 37 (1975).

18. J.S.Prasad; J.Chem.Phys. 65, 941 (1976).

19. M.Yasuniwa, S.Taki and T.Takesmura; Mol.Cryst. Liq.Cryst. 60, 111 (1980).

20. N.Kirov and M.Fortann; Mol.Cryst.Liq.Cryst.Lett. 56 195 (1980).

21. A.J.Leadbetter and P.G.Wrighton; J.Phys. Collogue, 40, C3-234 (1979).

22. Tatsuo Ushida, Hideo Watanabe and Masanobk Wada; Jap.J. of Appl.Phys. 11, 1559 (1972).

23. B.Bhattacharjee, S.Paul and R.Paul, Mol.Cryst. Liq.Cryst. 89, 181 (1982).

24. Biswanath Jha, Aparna Nandi, Sukla Paul and Ranjit Paul, Mol.Cryst.Liq.Cryst. 104 289 (1984).

25. P.Mandal and S.Paul; Mol.Cryst.Liq.Cryst. 131 223 (1985).

CHAPTER IV

THE CRYSTAL STRUCTURE

4.1. Introduction

In this section, the complete crystal structure determination of 5-(4"-n-pentyl-cyclohexyl)-2-(4'-Cyanophenyl)-Pyrimidine (PCCPP) by means of X-ray crystallography is described. Attempts have been made to investigate the relationship between the molecular organization in the crystalline and liquid crystalline state. Study of the mesophase of this compound utilizing X-ray diffraction has been described in Chapter III. Optical birefringence study in the liquid crystalline phase is also given in the same chapter.

The molecular structure of this compound is given below

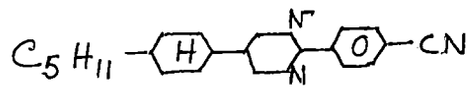

4.2. The geometry of diffraction

The phenomenon of diffraction by crystals results from a scattering process in which X-ray are scattered by the electrons of the atoms without change in wavelength. A diffraction a beam is produced by such scattering only when certain geometrical conditions are satisfied, which may be in either of the two forms, the Braggs' Law or Laues' equations.

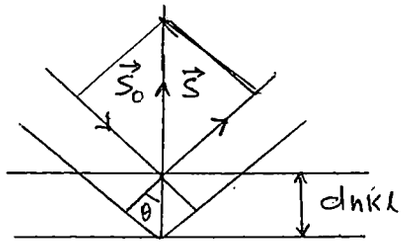

(Laue's equations)

$$\vec{a}.\vec{S} = h, \quad \vec{b}.\vec{S} = \vec{K}, \quad \vec{c}.\vec{S} = l$$

$$2 d_{hkl} \sin\theta_{hkl} = n\lambda$$

(Bragg's equations)

h, k, l are integers θ is the angle of reflection, d_{hkl} is interplanar spacing λ the wavelength, n is an integer determining the order of reflection

$$|\vec{S}| = \left|\frac{S - S_0}{\lambda}\right| = \frac{2\sin\theta}{\lambda} = \frac{1}{d} \qquad \ldots(4.1)$$

The resulting diffraction pattern of a crystal comparising both the positions and intensities of the diffraction effects, is a fundamental physical property of the substance which is used for the complete elucidation of the structure. Analysis of the positions of the diffraction effects leads immediately to a knowledge of the size, shape and orientation of the unit cell. To locate the positions of individual atoms in the cell, the intensities must be measured and analysed. Most important in relating the positions of the atoms to the diffraction intensities is the structure factor equation

$$\vec{F}_{hkl} = \sum_{j=1}^{N} f_j \exp 2\pi i (hx_j + ky_j + lz_j) \qquad \ldots(4.2)$$

The quantity $\vec{F}_{hkl}$ a function of h k l is called the structure factor which expresses the resultant scattering effect from the atom contents of the unit cell as compared to that of a single electron at the origin. $|\vec{F}_{hkl}|$ called the structure amplitude is thus a pure number-

number of electrons. f_j is the atomic scattering factor or form factor of the j th atom, N the unit cells contents, x_j , y_j and z_j are the fractional cordinates of the j th atom.

Now the atoms in the unit cell are the positions of the high electron density $\rho(xyz)$ so $\vec{F}_{hkl}$ can be expressed as

$$\vec{F}_{hkl} = \int_V \rho(xyz) \exp 2\pi i(hx+ky+lz)\, dv \qquad \ldots(4.3)$$

where V is the volume of the unit cell. Then by Fourier transformation we have

$$\rho(xyz) = \frac{1}{V} \sum_h \sum_k \sum_l F_{hkl} \exp 2\pi i (hx+ky+lz) \qquad \ldots(4.4)$$

If we could obtain a larger number of $\vec{F}_{hkl}$ by diffraction experiment, we could have directly derive the crystal structure by making a Fourier summation.

The complex form of the expression for the structure factor merely means that the phase of the scattered wave is not simply related to that of the incident wave. The phase however is not an observable quantity the only observable quantity being the intensity which is proportional to $|F|^2$

Without a knowledge of the phase a straightforward Fourier summation to evaluate $\rho(xyz)$ is not possible This is the well known phase problem of X-ray crystallography.

From the intensity data I_{hkl} we determine $|F_{hkl}|$ and direct mathematical relationships are being used to give phase information.

4.3. Crystal Data Collection:

Transparent plate like crystals were obtained from a solution of acetone by slow evaporation. Lattice parameters and space group were determined by taking oscillation and Weissenberg photographs along different axes. The crystal belong to the monoclinic system. The space group $P2/a$ was uniquely determined from the observed systematic absence of hol reflections with $h = 2n + 1$. By floatation technique the density of the crystal was found to be 1.18 $gm.cm^{-3}$. Taking four molecules per unit cell (i.e. $Z = 4$) the calculated density became 1.15 $gm.cm^{-3}$ which is very close to the observed value.

A crystal of dimension 0.035 x 0.3 x 0.4 mm^3 was used in the collection of intensity data. It was mounted on the tip of a glass fibre and the fibre was in turn fastened to a goniometer head. Accurate cell parameters were determined by a least square fit of Sin θ values of 25 reflections within $20^0 < \theta < 23^0$ measured on an 'Enraf Nonius' Cad-4 computer controlled diffractometer, CuK_α radiation monochromated by a graphite monochromator was used throughout. The name of the 4-circle, diffractometer arises from its possession of four arc which may be used to adjust the orientation of the crystal as to bring any desired (h k l) plane into reflecting position and the detector to the corresponding diffraction position. A schematic diagram of CAD4 single crystal orienter[1] is given in Fig. 4.1. The intensity data were collected by $\omega - 2\theta$ scan mode. A total of 3277 reflec-

tions were collected in the interval 4^0 (2 0 of which 2246 reflections were taken as observed and had intensities greater than $2\sigma(I)$. The important crystallographic data are given in table 1. The measured value of the intensity is given by

$$I_{raw} = \frac{A}{n}(C - R.B) \qquad \ldots(4.5)$$

where A = attenuation factor (26.55 for Cu $K\alpha$)

n = an integer varying from 8 to 24 to suit the particular case.

C = total count.

R = Ratio of scan time to background

B = Total background count.

The standard deviation $\sigma(I)$ calculated on the basis of counting statistics is given by

$$\sigma(I_{raw}) = \frac{20.166}{n} \cdot A\,(C + R^2B)^{1/2} \qquad \ldots(4.6)$$

Applying appropriate Lorentz polarization factor correction L_p (described below) we get I_{corr} and $\sigma(I_{corr})$

$$I_{corr} = \frac{I_{raw}}{L_p} \text{ and } \sigma(I_{corr}) = \frac{\sigma(raw)}{L_p} \qquad \ldots(4.7)$$

This intensity value is then converted to Fo, the observed structure factor with

$$|\vec{F_o}| = K\,(I_{corr})^{1/2} \qquad \ldots(4.8)$$

K being scaling constant and the corresponding standard deviation is

$$\sigma|\vec{F}_o| = \frac{\sigma(I_{corr})}{2|\vec{F}_o|} \qquad \ldots(4.9)$$

4.4. Intensity data reduction

The intensities collected are subjected to corrections for certain geometrical and physical factors before being used in the structure determination. These are described below:

Lorentz factor

For each reciprocal lattice point to pass through the surface of the sphere of reflection the required length of time varies as a function of its position in reciprocal space and the direction of its approach to the sphere. Because the intensity of a reflection is proportional to this time a correction is needed. Such correction is called the Lorentz factor L^2 and it varies with diffraction geometry. For single crystal of normal beam equation geometry, it is given by

$$L_{hkl} = \frac{1}{\sin 2\theta_{hkl}} \qquad \ldots(4.10)$$

Polarisation factor

In the usual experimental arrangements, the X-ray beam is unpolarised which means that the azimuth of the electric vector assumes all directions with time. The effective amplitude of the radiation after it is reflected by the crystal at the angle 2° consists of only

the components of these azimuthals after reflection. This feature has the effect of reducing the intensity of the X-ray beam by a factor p, known as the polarisation factor.

$$P = \tfrac{1}{2}(1 + \cos^2 2\theta)$$

...(4.11)

In our case the incident beam is partially polarized during monochromatisation by reflection from the based plane of a graphite crystal and P takes the form

$$P_{hkl} = P_{erf}\frac{\cos^2 2\theta_m + \cos^2 2\theta_{hkl}}{1 + \cos^2 2\theta_m} + (1 - P_{erf})\frac{\cos^2 2\theta_m + \cos^2 2\theta_{hkl}}{1 + \cos^2 2\theta_m}$$

...(4.12)

where P_{erf} = a constant depending on the crystal used in the monochromator (0.5 in our expt.)

θ_m = Bragg angle of reflection from the monochromator crystal.

These two correction factors L and P are combinedly termed as Lorentz Polarization factor L_p because of the dependence of both on the scattering angle θ.

Extinction correction:

Attenuation of diffracted beams may also be caused when the crystal is set at the Bragg angle. Darwin[4] first treated the effect mathematically and termed this as primary and secondary extinction effect. Primary extinction involves the loss of intensity of the incident beam

by an inteference process following multiple reflections as the beam penetrates deeper and deeper into the crystal. Secondary extinction may, however, be considered in case of strong reflections. In this case as the incident beam itself travels inside the crystal, it goes on losing considerable fractions of its energy by reflection in the planes it encounters. Thus the plane lying deeper receive less and less incident intensity. Consequently the diffracted intensity is attenuated. This effect is predominantly observed in low angle region. Correction for this effect has been derived[5-6]. Kato[7] derived a method based on dynamical theory for correction to both the effects.

2. Temperature factor

While introducing the idea of atomic scattering factor, 'f' we have not taken into consideration the finite size of the atom i.e. of the electron cloud about the atomic atomic nucleus and also the thermal vibration of the atom which increases the effective volume of the electron cloud, Because of the first effect, the scattered intensity falls off with increasing Sin θ and the second factor acts for more rapid fall. The first effect is corrected by taking 'f' values from standard f Vs. Sin θ curve[5,8,9] and the effect of thermal vibration, assuming it isotropic, can be taken care by multiplying f_o, the form factor for an

atom at rest, by a temperature factor[10]

$$f = f_0 \exp(-B\sin^2\theta/\lambda^2)$$

...(4.13)

where the parameter B, called isotropic temperature factor is equal to $8\pi^2\bar{U}^2$, $\bar{U}^2$ being the mean square displacement of the atoms from their mean positions.

A method introduced by A.J.C.Wilson[11] enables us to obtain an overall value of B, and at the same time, places all the observed intensities on an approximately absolute basis.

He showed that average absolute structure factor depends only on what is in the cell and not where the atoms are located and hence for a random distribution of N atoms in the unit cell

$$\langle |\vec{F}|^2 \rangle = \sum_{j=1}^{N} f_j^2$$

...(4.14)

Dividing the entire reciprocal space observed into annular zones of equal S^2 ($S = \sin\theta/\lambda$)

$\langle |\vec{F_{obs}}|^2 \rangle$ is determined for each of them and then $\sum_{j=1}^{N} f_{oj}^2 (S_{mid})$ is calculated using the mean value of S^2 for each zone. Since $|\vec{F_{obs}}|^2$ is usually known on an arbitrary scale, we may write

$$\langle |F_{obs}| \rangle = K \langle |\vec{F}|^2 \rangle$$

...(4.15)

where $\langle |\vec{F}| \rangle$ is the average absolute structure factor. To separate out thermal motion in the crystal, we write,

$$\langle |\vec{F}|^2 \rangle = \sum_{j=1}^{N} f_j^2 = \sum_{j=1}^{N} f_{oj}^2 \exp(-2B_j s^2) \qquad \ldots(4.16)$$

Assuming B same for all atoms

$$\langle |\vec{F}|^2 \rangle = \exp(-2Bs^2) \sum_{j=1}^{N} f_{oj}^2 \qquad \ldots(4.17)$$

Substituting this in equation (19) we get

$$\langle |\vec{F}_{obs}|^2 \rangle = K \exp(-2Bs^2) \sum_{j=1}^{N} f_{oj}^2$$

$$= \ln K - 2\frac{B \sin^2\theta}{\lambda^2} \qquad \ldots(4.18)$$

The plot of $\ln \langle |\vec{F}_{obs}|^2 \rangle \Big/ \sum_{j=1}^{N} f_{oj}^2$ against $\sin 2\theta/\lambda^2$ called the Wilson plot is therefore a straight line except for the scatter due to experimental errors and furnishes x us with intercept of $\ln K$ and a slope of $-2B$

When instead of random distribution of atoms, groups of atoms with known geometry (such as benzene ring) are present in the structure, they may be included in the expression for average intensity even known nothing about their positions and orientations. When G groups of known geometry are present, the k^{th} of which contains

M_k atoms, we may write using the scattering formula of Debye[12]

$$\langle |\vec{F}|^2 \rangle = \sum_{K=1}^{G} \sum_{i=1}^{M_K} \sum_{j=1}^{M} f_i f_j \frac{\sin 2\pi r_{ij} S}{2\pi r_{ij} S} + \sum_{j=1}^{N} f_j^2$$

...(4.19)

where r_{ij} is the distance between the i^{th} and j th. atoms of the k th group and $S = S_{mid}$ as before. The plot in this case is known by Debye plot and gives a better straight line fit for obtaining B and K.

It is often advantageous to use a K- curve To do this, K (mid) is computed for each zone of S^2 mentioned above, as

$$K(S_{mid}) = \frac{\sum \epsilon \sum_{I=1}^{N} f_{oj}(S)}{\sum |\vec{F}_o|^2 (S)}$$

...(4.20)

where ϵ is a small integer depending on the space group[13] A least squares procedure is used to fit a best smooth analytical functions, usually $\ln K = A + B S^C$ to experimental points. When C = 2.0, the curve is the same as Wilson's plot.

After scaling the data and ~~x~~ estimating the temperature factors we try to postulate, a trial structure by direct methods.

4.5. Determination of the trial structure

The trial structure was determined by direct method. Direct methods of crystal structure determination are usually associated with techniques in which phases for a set of structure factors are determined from the corresponding experimental amplitude by probabilistic calculations.

A large number of operating procedures for direct phase determination have been proposed. Most of these are based on the same fundamental principles, but differs in the manner of handling the data and extracting the phases. We shall consider only the fundamentals of the method and the technique which has been used in the present case.

Unitary and Normalised Structure Factors

For direct methods it is an advantage to work with structure factors for which the fall off with increasing scattering angle has been removed. The unitary structure factor is defined as

$$U(\vec{h}) = F(\vec{h}) / \sum_{j=1}^{N} f_j$$

So that $|U(\vec{h})| \leq 1$

writing the unitary scattering factor as

$$n_j = f_j / \sum_{j=1}^{N} f_j$$

We may write

$$U(\vec{h}) = \sum_{j=1}^{N} n_j \exp 2\pi i \vec{h} \cdot \vec{r_j} \qquad \ldots(4.21)$$

Another corrected structure factor, of great theoretical importance is the normalised structure factor given by

$$|E_{\vec{h}}|^2 = \frac{|F_{\vec{h}}|^2}{\epsilon_{\vec{h}} \sum_{j=1}^{N} f_j^2}$$

where $\epsilon_{\vec{h}}$ takes into account the effect of space group symmetry. Now if $\hat{f}$ be the common shape for all atoms then $f_j = Z_j \hat{f}$

$$E_{\vec{h}} = \epsilon_{\vec{h}}^{-\frac{1}{2}} \frac{F_{\vec{h}}}{\left(\sum_{j=1}^{N} Z_j^2 \hat{f}^2\right)^{1/2}}$$

$$= \epsilon_{\vec{h}}^{-\frac{1}{2}} \sum_{j=1}^{N} \left(Z_j / \sigma_2^{1/2} \right) \exp 2\pi i (\vec{h} \cdot \vec{r}_j) \quad \ldots(4.22)$$

where $\sigma_m = \sum_{j=1}^{N} Z_j^m$

$\vec{E}_h$ is called the normalised structure factors because of its property. This relationship shows that the averaging of E^2 can be carried out regardless of θ. The same is not true, however, of either and this simplification is one of the main reasons why 'E's are preferred for use in direct methods.

Structure invariant and semi-invariant

A structure invariant is defined as a quantity which is independent of the shift of the origin of the unit cell.

It can be shown that the intensities of reflection i.e. , are structure invariants.

However, the structure factor itself is not structure invariant. Otherwise the phase problem would not exist in crystallography. The structure factor $F_{\vec{h}}$ is given by

$$F_{\vec{h}} = |F_{\vec{h}}| \exp i(\vec{\phi}_{\vec{h}}) = \sum_{j=1}^{N} f_j \exp(2\pi i \vec{h} \cdot \vec{r}_j) \qquad \ldots(4.23)$$

whith shift $\Delta\vec{r}$ of the origin, the equation changes to

$$F'_{\vec{h}} = \sum_{j=1}^{N} f_j \exp[2\pi i \vec{h} \cdot (\vec{r}_j \cdot \Delta\vec{r})]$$

$$= |F_{\vec{h}}| \exp(-2\pi i \vec{h} \cdot \Delta\vec{r}) \qquad \ldots(4.24)$$

Thus we see that the phase changes by $-2\pi\vec{h} \cdot \Delta\vec{r}$ while the amplitude is x invariant.

In a similar xx way it can be shown that $|F_{\vec{h}}|^2$ is structure invariant

$$|F_{\vec{h}}|^2 = F_{\vec{h}} F'_{-\vec{h}} = \exp(-2\pi i \vec{h} \cdot \Delta\vec{r}) F_{\vec{h}} \exp(2\pi i \vec{h} \Delta\vec{r}) F_{-\vec{h}}$$

$$= F_{\vec{h}} F_{-\vec{h}}$$

$\ldots(4.25)$

It can be shown that although the values of the individual phases depend on the structure and choice of origin, some combinations of them is a structure invariant. For example if $\vec{h}_1 + \vec{h}_2 + \vec{h}_3 = 0$ then $\Phi_{\vec{h}_1} + \Phi_{\vec{h}_2} + \Phi_{\vec{h}_3}$ is a structure invariant for every space group. It follows directly from the fact that $F_{\vec{h}} F_{\vec{k}} F_{-\vec{h}} F_{-\vec{k}}$

is an invariant.

$$F'_{\vec{h}}\, F'_{\vec{k}}\, F'_{-\vec{h}-\vec{k}} = F_{\vec{h}} \exp(-2\pi i \vec{h}\cdot\Delta\vec{r})\, F_{\vec{k}} \exp(-2\pi i \vec{k}\cdot\Delta\vec{r})\, F_{-\vec{h}-\vec{k}} \exp(2\pi i \vec{h}\cdot\Delta\vec{r} + 2\pi i \vec{k}\cdot\Delta\vec{r}) = F_{\vec{h}}\, F_{\vec{k}}\, F_{-\vec{h}-\vec{k}}$$

...(4.26)

Since the moduli of the structure factors are invariant themselves, the angular part of $F_{\vec{h}}\, F_{\vec{k}}\, F_{-\vec{h}-\vec{k}}$ is also invariant i.e. $\Phi_{\vec{h}} + \Phi_{\vec{k}} + \Phi_{-\vec{h}-\vec{k}}$ is an invariant, however, this does not imply that its value is known.

The structure seminvariants[14] are those linear combinations of the phases whose values are uniquely determined by the crystal structure alone, when the choice of origin is restricted within permissible values. Semi-invariants originate from space group symmetry. For each space group they have to be derived separately. The structure invariants and semi-invariants have been tabulated for all space groups in reference[15].

In any space group any structure invariant is also a structure seminvariant, but in general the converse is not true. A complete theory concerning this subject it is given in a series of papers by Hauptman and Karle[16,17] and recently by Schenk[18,19].

Some relations involving the magnitudes and the phases

Harker-Kasper Inequalities:-

In 1948 Harker and Kasper[20] using Cauchy inequality relation derived the following inequality relation between magnitudes and phases of unitary structure factors.

$$U(\vec{h})^2 \leq \frac{1}{2}\{1 + U_{2\vec{h}}\}$$

...(4.27)

If we denote the sign of $U(\vec{h})$ by $S(\vec{h})$ which can have the values either + 1 or - 1, then this relationship can be written as

$$S(\vec{h})\,S(\vec{h}')\,S(\vec{h}+\vec{h}') = 1$$

A development made by Karle and Hauptman[21] in the form of an inequality does depend on the non-negativity of electron density. For a centro symmetric structure where $U(\vec{h}) = U(\vec{h})$ this gives $1 - U(\vec{h})^2 - U(\vec{K})^2$

$$U(\vec{h}-\vec{K}) + 2\,U(\vec{h})\,U(\vec{K})\,U(\vec{h}-\vec{K}) \geq 0$$

from which, if the U's are a sufficiently large, it may be shown that

$$S(\vec{h})\,S(\vec{K})\,S(\vec{h}-\vec{K}) = 1$$

A significant step in the development of direct methods was the one by Sayre[22]. This is the most funda-

mental and developed, what we refer to as Sayre's equation. The electron density is given by the summation

$$P(\vec{r}) = \frac{1}{V} \sum_{\vec{H}} F(\vec{H}) \exp(-2\pi i \vec{h} \cdot \vec{r})$$

and we may also write

$$P(\vec{r})^2 = \frac{1}{V} \sum G(\vec{h}) \exp(-2\pi i \vec{h} \cdot \vec{r})$$

where $G(\vec{h})$ is the Fourier coefficient of the squared density.

If the structure consists of equal resolved atoms, then both $P(\vec{r})$ and $P(\vec{r})^2$ will show equal resolved peaks. If the scattering factors of the squared atoms is represented by g and that of the normal atoms by f then

$$F(\vec{h}) = \frac{f}{gV} \sum_{\vec{h}'} F(\vec{h}') F(\vec{h} - \vec{h}') \qquad \ldots(4.28)$$

This is Sayre's equation and is an exact relationship between structure factors for equal and resolved atoms.

For a centrosymmetric structure it might be assumed that a large product on the right hand side of (28) was likely to have the same sign as $F(\vec{h})$ This leads to the relationship that for large structure factors

$$S(\vec{h}) S(\vec{h}') S(\vec{h} - \vec{h}') \approx +1 \qquad \ldots(4.29)$$

where $\approx$ means probably equals. This was the sign relationship given in the papers by Cochran[23] and Zachariasen[24] Expressions for the probability of (4.29) have been found by a number of authors, one which is sufficiently accurate for most purposes and is of convenient form, was given by Cochran and Woolfson[25]. This is for an equal atom structure

$$P_+ = \frac{1}{2} + \frac{1}{2} \tanh \{ N^{\frac{1}{2}} / E(\vec{h}), E(\vec{h}) E'(\vec{h}-\vec{h}) \}$$

...(4.30)

where P_+ is the probability that the product of signs in (4.29) is positive.

This expression also gives the probability that $S(\vec{h})$ equals the signs $S(\vec{h}) S(\vec{h}-\vec{h}')$. If there are several pairs of known signs all contributing to the indication of new one then the probability for the new sign being +ve will be

$$P_+(\vec{h}) = \frac{1}{2} + \frac{1}{2} \tanh [N^{-\frac{1}{2}} |E_h| \sum_{\vec{h}'} E(\vec{h}) E(\vec{h}-\vec{h})]$$

...(4.31)

In (4.30) and (4.31) if the atoms are not equal then $N^{-\frac{1}{2}}$ is replaced by $\sigma_3 \sigma_2^{-\frac{3}{2}}$ where $\sigma_n = \sum_{j=1}^{N} z_j^n$ where z_j is the atomic number of the j th. atom. The approximate phases thus obtained have to be refined

and that this may be convinient-by done by using following tangent formula of Karle and Hamptman

$$\tan \Phi_{\vec{h}} = \frac{\sum_{K} |K(\vec{h}\vec{K})| \sin(\Phi_{\vec{h}-\vec{K}} + \Phi_{\vec{K}})}{\sum_{K} |K(\vec{h}\cdot\vec{K})| \cos(\Phi_{\vec{h}\cdot\vec{K}} + \Phi_{\vec{K}})} \qquad \ldots(4.32)$$

A quantity $\mathcal{L}_{\vec{n}}$ which gives a measure of the reliability with which $\Phi_{\vec{h}}$ may be determined was defined by Karle and Karle

$$\mathcal{L}_{\vec{n}}^{2} = \Big[\sum_{\vec{K}} K(\vec{h}\vec{K}) \sin(\Phi_{\vec{h}-\vec{K}} + \Phi_{\vec{K}}\Big]^{2} + \Big[\sum_{\vec{K}} K(\vec{h}\cdot\vec{K}) \cos(\Phi_{\vec{h}-\vec{K}} + \Phi_{\vec{K}})\Big]^{2} \qquad \ldots(4.33)$$

All the theory given above is the launching pad from which modern direct methods have grown to the present form.

In our trial structure determination we have used the complete direct method program SIMPEL[26]. There are other direct method program 'viz.' SHELX[27], MULTAN[28], XTAL[29] SAPI[30], X-RAY[31].

The program system Simpel is a complete direct methods system, which may be entered with /F/-values and may produce an E-map of the structure. The unique part of SIMPEL is formed by a series of routines, successively gathering the relation-ships and determininga starting set, carrying out a symbolic addition, finding the correct numerical values x for the symbols and finally executing a numerical phase extension and refinement.

The program system SIMPEL is completely devoted to the symbolic addition method.

In a symbolic addition the following expressions play important roles.

The triplet relation

$$\Phi_{\vec{H}} \simeq \Phi_{\vec{K}} + \Phi_{\vec{H}-\vec{K}}$$

for large

$$E_3 = 1/N^{\frac{1}{2}} \, | E_{\vec{H}} E_{\vec{K}} H_{H-K} |$$

and its centrosymmetric analogue.

$$S_{\vec{H}} \approx S_{\vec{K}} S_{\vec{H}-\vec{K}}$$

in which S is the sign of a reflection.

These formulae have their counter parts when more than one relation is available.

$$\Phi_{\vec{H}} = \frac{\sum_K E_3 (\Phi_{\vec{K}} + \Phi_{\vec{H}-\vec{K}})}{\sum_K E_3}$$

and

$$S_{\vec{H}} = A \sum_{K} E_3 S_{\vec{K}} S_{\vec{H}-\vec{K}}$$

In general, in the final stage of a symbolic addition also numerical phases have to be refined. This is carried out by means of the tangent formula or rather, because phases must be known on the interval $0 \leq \varphi \leq 2\pi$ by its exponential analogue.

$$\exp i \varphi_{\vec{H}} = \frac{\sum_{K} E_3 \exp i (\varphi_{\vec{H}} + \varphi_{\vec{H}-\vec{K}})}{|\sum E_3 \exp i (\varphi_{\vec{H}} + \varphi_{\vec{H}-\vec{K}})|}$$

<u>Elements of a symbolic addition:-</u>

<u>Calculation of the normalised structure factors</u>

In the first step the experimental structure factor data are corrected for thermal motion (Wilson plot, Debye curve, K curve), brought to absolute scale and finally converted into normalised structure factors /E/.

<u>Generation of the phase relationships</u>

The phase relationships are collected. In the program system SIMPEL not only triplet relations are generated, but also positive and negative quartets, relationship. Harker Kuopor relations and quintets are generated.

<u>Σ_1 relation[32]</u>

$$S E_{2h,0,2l} \approx s \sum_{K} (1)^{K+l} \left(\sum_{hKl}^{2} - 1 \right)$$

The positive quarter relation is formulated as

$$\Phi_{\vec{H}} + \Phi_{\vec{K}} + \Phi_{\vec{L}} + \Phi_{\vec{H}-\vec{K}-\vec{L}} \approx 0$$

for large value of $E_4 = N^{-1} | E_{\vec{H}} E_{\vec{K}} E_{\vec{L}} E_{-\vec{H}-\vec{K}-\vec{L}} |$ and large $| E_{\vec{H}+\vec{K}} |$, $| E_{\vec{H}+\vec{L}} |$ and $| E_{\vec{K}+\vec{L}} |$ [33]

Negative quartet relation

For reasonably large values of E_4 and small $| E_{\vec{H}+\vec{K}} |$, $| E_{\vec{H}+\vec{L}} |$ and $| E_{\vec{K}+\vec{L}} |$ [34]

Harker Kasper relations[35]

Using the probability that the product $S(\vec{H}+\vec{K}) \times S(\vec{H}-\vec{K})$ is negative, the larger $| E_{\vec{H}} |$, $| E_{\vec{H}+\vec{K}} |$ and $| E_{\vec{H}-\vec{K}} |$ and the smaller $| E_{\vec{K}} |$ and $| E_{2\vec{H}} |$. Of course this is the result of a special negative quartet, the main terms being $E_{\vec{H}}$, $E_{\vec{K}}$, $E_{\vec{H}+\vec{K}}$ and $E_{\vec{H}-\vec{K}}$.

Quintets

From the general Hughes formula derived by Simerska[36] the quintet phase relation can be wrriten as

$$\Phi_{\vec{H}} + \Phi_{\vec{K}} + \Phi_{\vec{L}} + \Phi_{\vec{M}} + \Phi_{-\vec{H}-\vec{K}-\vec{L}-\vec{M}} \simeq \varphi$$

In a first approximation φ is expected to be zero for

large values of

$$E_5 = N^{-\frac{3}{2}} | E_{\vec{H}} E_{\vec{K}} E_{\vec{L}} E_{\vec{M}} E_{-\vec{H}-\vec{K}-\vec{L}-\vec{M}} |$$

Starting set determination

The determination of the starting set begins with a convergence procedure similar to that devised by Germain, Main and Woolfson (1970)[37]. This procedure searches for that reflection which is the weakest linked to the other reflections by means of the phase relations and then this reflection is removed from the set of reflections. At the same time all its phase relations are removed from the collection of phase relation ships. This process is repeated until no reflections are left in the set. Any time a reflection is removed without having phase relationships linking it with other phases, this reflection has taken to be starting set. Since a starting set reflections with large /E/ are preferred, the use f of triplets and quartets generally leads to very good starting set. The second step is a few cycles of symbolic addition using quartets and triplets, a employing very strict acceptance criteria not allowing relations among the symbolic phases. This leads to a much larger starting set.

The next step is the extension of the starting set. This is done in 'SIMPEL' using triplet relations only. It is verys essential no errors are included during this process and therefore, the criteria used to accept a symbolic phase for a reflection are very strict, in particular in the beginning. In general, no single indication will be accepted unless it belongs to the ten to fifteen strongest triplet relationships. For multiple indications giving rise to the same symbolic phase, high acceptance limits are applied. In general these precautions make sure that the resulting set of symbolic phases contain the correct solution, that is to say that when the correct values for the symbols are substituted the phases of the reflections are good enough to image the structure.

Numerical values for the symbols:

Figures of Merit.

With the extended group of phased reflections as input numerical values for the symbols are calculated using a number of figures of merit (FOM'S).

In general figures of merit can be based on any quantity which can be expected to be extreme for the set of correct signs. In 'SIMPEL' several FOM'S may be used.

1) The Σ_2 - consistency FOM Q (Schenk, 1971)[38]
2) The positive quartet criterion (PQC), Schenk and Kiers (1984)[39].
3) The Negative Quartet Criterion (NQC), (1974).

4) The ~~Negative~~ Σ_1- criterion (Overback and Schenk, 1976)[40]

5) The Harker-Kasper criterion (HKC, Schenk, De Jong)[41].

Apart from the separate FOM's also a combined FOM is calculated, which mostly discriminates the correct solution without difficulties.

After determining the symbols all symbolically phased reflections can get a numerical phase. These phases are then used as starting point for a numerical phase extension, because in general the number of phased reflections is yet sufficient to calculate a good E-map. In the centrosymmetric case this is achieved by means of a fast Σ_2 refinement and extension, in the non symmetric case by means of a usual tangent refinement.

In the SIMPEL produces a set of h, k, l, E values with phases, which can be fed into an E map calculating ps program with subsequent interpretation.

Eventually the atomic positions can be tested on the correctness and be refined by a fast diagonal least squares program.

4.6. Structure determination and refinement.

The structure was determined by the direct methods program SIMPEL-83[26] (C.T.Kiers and H.Schenk) using all reflections in order to employ all positive and negative quartet relation ships, all sigma1 relations and all special two dimensional quartets apart from triplets. The 300 strongest reflections were phased using 4 symbols. The E map with the highest a combined figure of merit revealed the structure

completely. Eventually the atomic positions were tested. The trial structure showed a R value of 22.9 . The structure was refined by four cycles of fast diagonal least squares program having an over all temperature factor and scale factor, the then individual 17.6

$$R = \frac{\Sigma |F_o| - |F_c|}{\Sigma |F_c|}$$

For the space group ~~P_2/a~~ $P2/a$

$$F_{hkl} = \Sigma f_r A_r$$

$$Ar = \text{?} \; 4 \cos 2\pi \left(\frac{h}{4} x_r + k y_r + l z_r \right) \cos 2\pi \left(k y_r - \frac{h}{4} \right)$$

x_r, y_r, z_r , are the co-ordinates of the rth. atom in the molecule. Summation is over the number of atoms in the asymmetric unit

$$\rho = \frac{4}{V_c} \sum_0^{\infty} \sum_0^{\infty} \sum_0^{\infty} \Big[\sum^{h=2n} F_{hkl} \cos 2\pi (hx + lz) + F(hkl) \cos 2\pi (hx - lz) \Big] \cos 2\pi k y - \sum_0^{\infty} \sum_0^{\infty} \sum_0^{\infty} \sum^{h=2n+1} F(hkl) \sin 2\pi (hx + lz) + F(hkl) \sin 2\pi (hx - lz) \sin 2\pi k y \Big]$$

isotropic temperature factors. The R value came down to Three cycles of block diagonal least squares calculation with anisotropic temperature factors reduced the R value to . At this stage a difference fourier was computed to locate the positions of the hydrogen atoms. All the hydrogen atoms could be located. For further refinement. For further refinement all reflections with $I \leq 2.5\,\sigma(I)$ were removed. The structure was now refined through several cycles of block diagonal least squares allowing the non-hydrogen atoms, to vibrate anisotropically and hydrogen atoms having an overall fixed temperature factor.

A weighting scheme with

$$W = (5.96 + F_{obs} + 0.0031\,F_{obs})^2 - 1$$ was applied. Extinction was taken into account with exp.R = 0.85. The R value converged to R = 0.049. $Rw = \left\{\frac{\Sigma(w\Delta^2)}{\Sigma F_o^2}\right\}^{\frac{1}{2}} = 0.048$ The calculations were carried out with X-Ray-76 (Stewart et al)[43]. The scattering factors were taken from Cromer and Mann[44].

4.7. Newman Projection

Newman projections along different C-C bonds are shown in the fig. 4.2. We can get an estimate of the dihedral ring angle from it.

4.8. Results and Discussions:

Molecular geometry and conformation.

In table - 1, important crystallographic data of the sample are given, in Fig. 4.3 shows the perpective drawing of the molecule viewed normal to the least squares plane. Final positions and thermal parameters of all the atoms are listed in Tables 4.2, 4.3 and 4.4 using the numbering scheme shown in Fig. 4.3.

Bond length and angles are given in Table 4.5. The average C-C bond length in the phenyl ring ($C_1 - C_6$) is 1.385 (2) Å the expected value[45] being 1.395 Å. The C-C bond lengths in the pyrimidine ring (C_7-N_2) are 1.374(2)Å and 1.381 (2) Å whereas the C-N bonds have the average value 1.336(2) Å which are comparable to those found in other pyrimidine compounds[46-48]. The cyclohexyl group ($C_{11} - C_{16}$) has the average C-C bond length 1.530(3) Å which is reasonable. The average C-C, single bond length in the alkyl chain (C14-22) is 1.516(3) Å which is lower by about 8 than the expected[45] value 1.541 Å. The cyano-group bond length (C17-N3) is 1.142 (3) Å which is close to the values found in other mesogenic compounds[49-52]. The average internal (C-C-C) bond angles in the phenyl ring is 120.0(2)°. In the pyrimidine ring the internal angles (N1-C-N2), C9-10-N2 and C1-C8-C9) have average value 124.5(2)° and the remaining three angles have average value 115.4(2)°. The internal (C-C-C) angles in the cyclohexane ring vary from 108.9° to 112.2° with an

average of 110.9(2) which in close to the reported values. The external non-hydrogen angles in the phenyl ring have an average value of 120.4(2)° as expected. But the angles C4-C7-N1 and C4-C7-N2 have values 113.4(2)° and 111.6(2)° respectively indicating some strain between the pyrimidine and cyclohexane rings. The tetrahedral C-C-C bond angles in the alkyl chain range from 113.1° to 115.9° with a mean value 114.2(2)° which exceeds the expected value by about 5°. The bond angle C1-C7-N3 is 178.2(2)°. Deviation from the linearity of the cyanobond was found in other cyanocompounds[49-52]. The C-H distances ranges from 0.96 A° to 1.14 Å with a mean value of 1.03(2) Å.

The length of the fully extended molecule estimated from a stereo model is found to 21.2 Å whereas the length of the molecule (in the crystalline state is 20.7 Å. This indicates that in the crystalline state the molecule is in nearly most extended form.

The least squares planes for different parts of the molecule have been calculated. The equation of the consistituent atoms have been listed in table 4.6. As expected, the phenyl ring and the pyrimidine ring show a high degree of planarity. The dihedral angle between the phenyl ring and the pyrimidine ring is 2°. The cyano-group atoms C7 and N 3 are displaced slightly upward from the plane of the phenyl ring. The equation of the plane of the cyclohexane ring is given in table 4.6. The cyclo-hexane ring is in chair form. Three atoms are displaced

upward from the plane and three are displaced downward. The displacements for C11 and C14 are approximately ± 0.2 Å, for C12 and C15 ± 0.4 Å and for C13 and C16 ± 0.5 Å. The dihedral angle between the cyclohexane ring and the pyrimidine ring is 78.4°.

Molecular Packing

Packing of PCCPP molecules in ab and ac plane are shown in Figure 4.4 and Figure 4.5 respectively. From these figures it is clear that the phenyl and pyrimidines are almost in the ac plane whereas the cyclohexane ring is almost at right angles to this plane. Pairs of molecules related by a centre of symmetry give rise to a sheet of parallel molecules in ac plane and these sheets of paired parallel molecules are stacked in an impricated mode along the b-axis. The crystalline modification of PCCPP therefore corresponds to the commonly found molecular packing in a nematogenic precursor. With the increase in thermal energy, a transformation in the liquid crystalline state is presumably accomplished by the breakdown of the molecular stacking along b-axis. This gives rise to three translational degrees of freedom of the pair of parallel molecules accompanied by rotation about the long molecular axis. The transition is thus displacive type.

All interatomic contact distances less than 4 Å involving non-hydrogen atoms only have been listed in table 4.7. We note that the only distance between C6 of molecule at x, y, z and N3 of molecule at $1+\frac{1}{2}$ - x, y, z is close to the sum of the Vander Waal's radii of the atoms. The length of these pair of molecules which are in head to head configuration is 39.8 Å. On the otherhand the apparent length of the molecule in nematic state is found to be 26.2 Å, which is 1-2 times the most extended molecular length. This is often found in cyanocompounds and to explain this a bimolecular association of the molecules, because of cyanogroup interaction, is involved[49,52-55]. We therefore infer that interaction between dipoles of cyanogroups exists both in crystalline and nematic phase. In crystalline state the overlap is small (in cyanoregion only) due to steric hindrance and in nematic state this is surpassed by increased thermal energy giving rise to large overlap (extending cyano to pyrimidine).

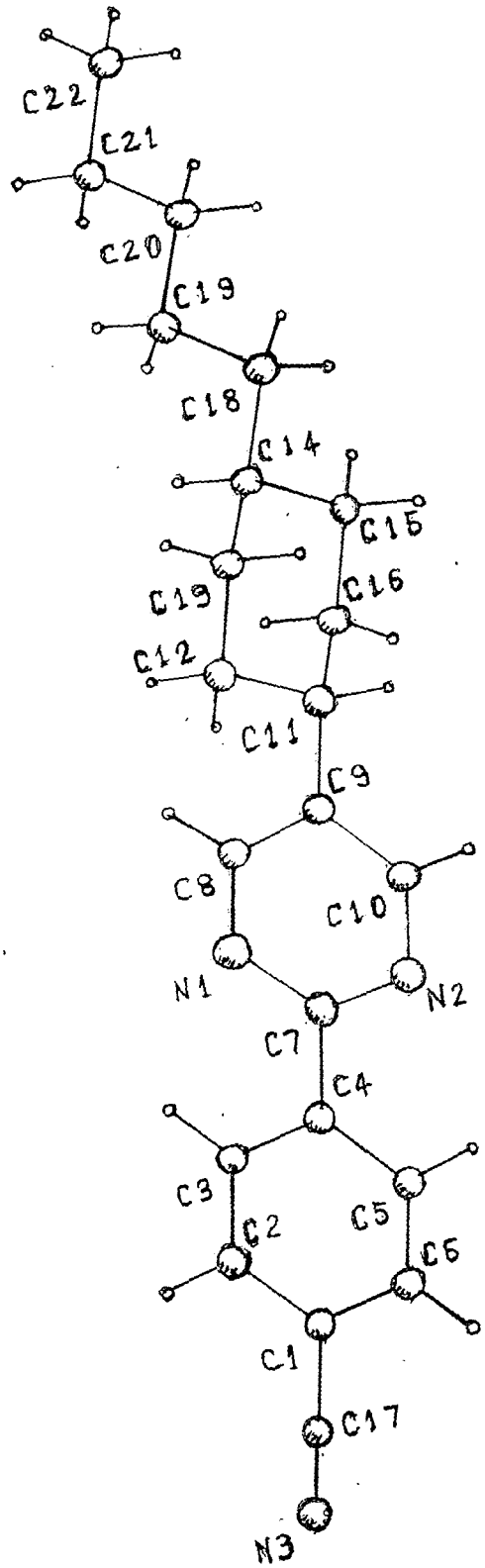
C22
C21
C20
C19
C18
C14
C15
C16
C13
C12
C11
C9
C8
C10
N1
N2
C7
C4
C3
C2
C5
C6
C1
C17
N3

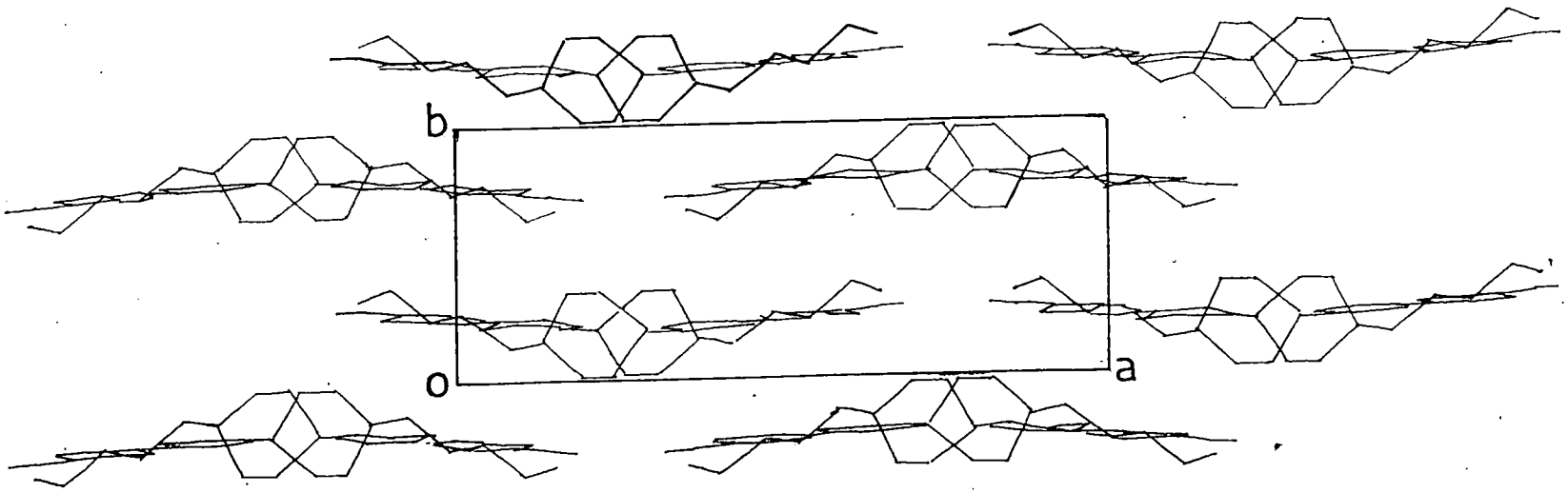

Fig. 4.4

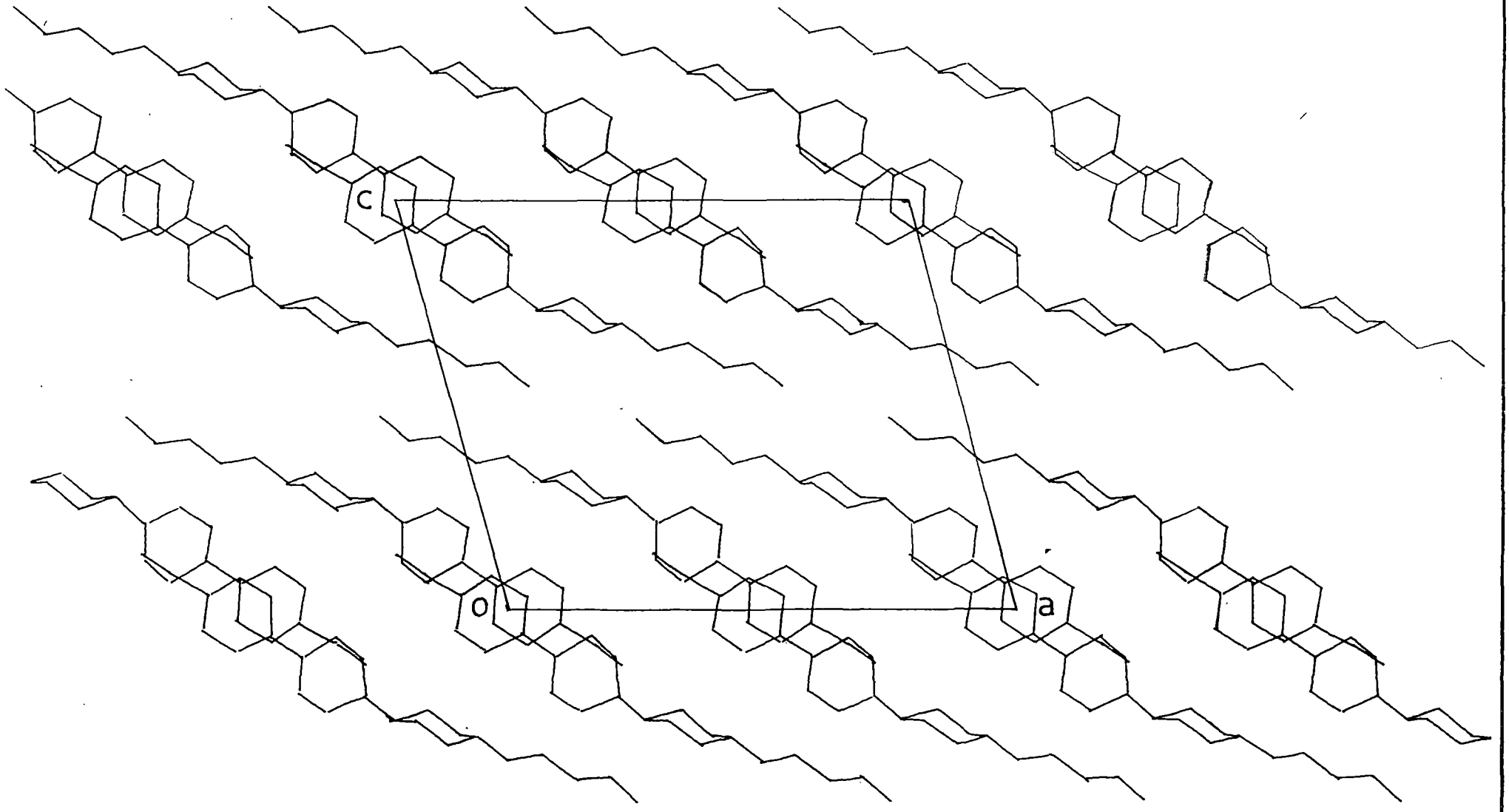

Fig. 4.5

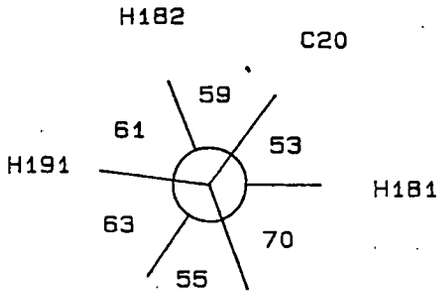

(C19 - C18)

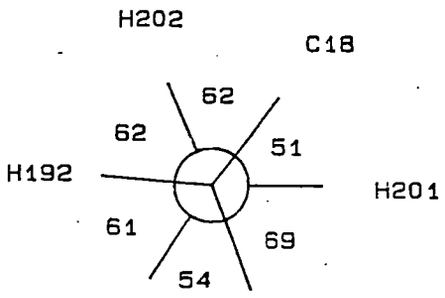

(C19 - C20)

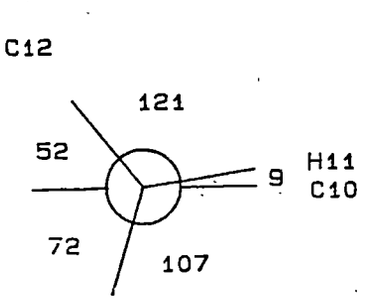

(C11 - C9)

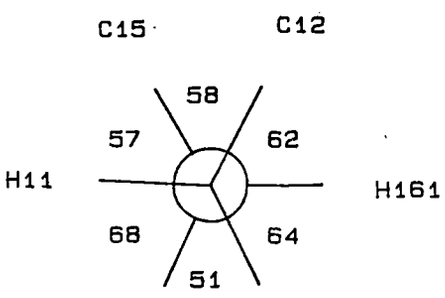

(C11 - C16)

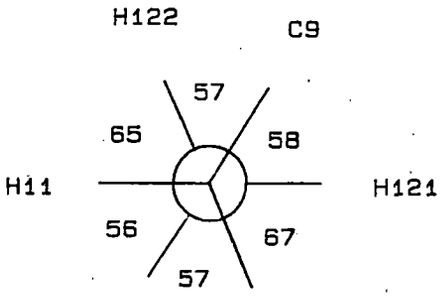

(C11 - C12)

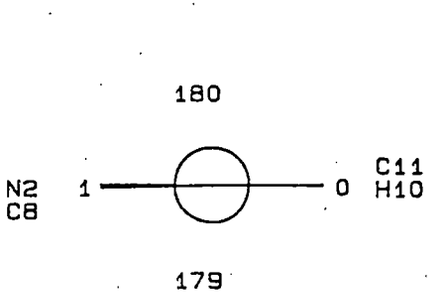

(C9 - C10)

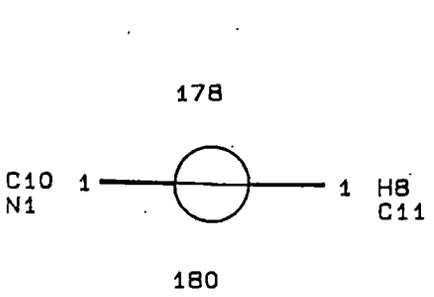

(C9 - C8)

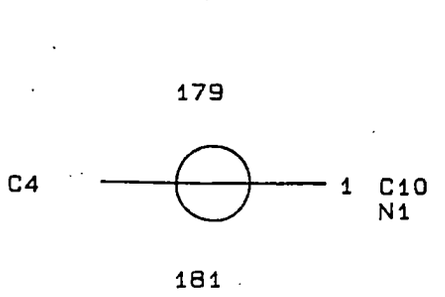

(C7 - N2)

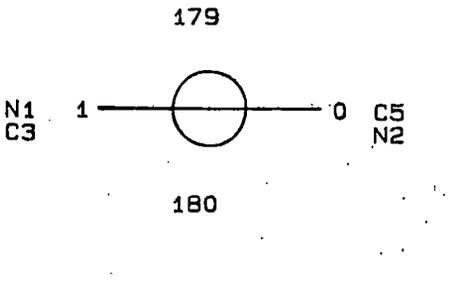

(C7 - C4)

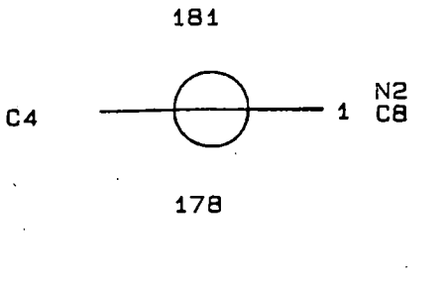

(C7 - N1)

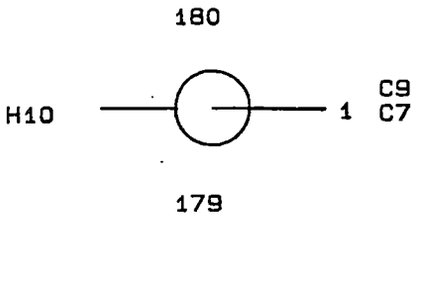

(N2 - C10)

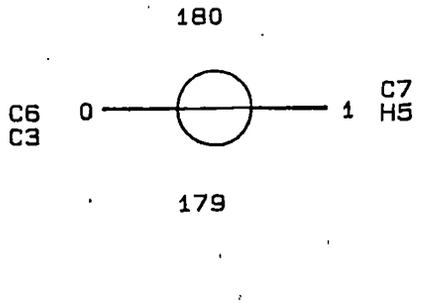

(C4 - C5)

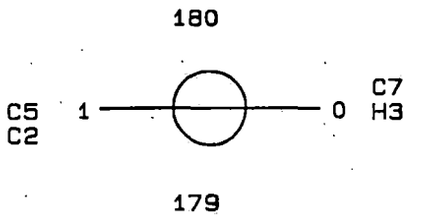

(C4 - C3)

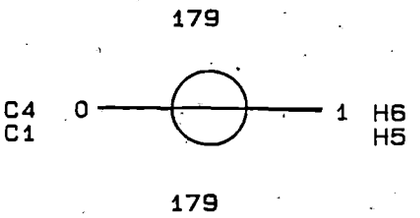

(C5 - C6)

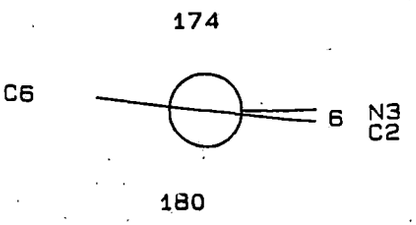

(C1 - C17)

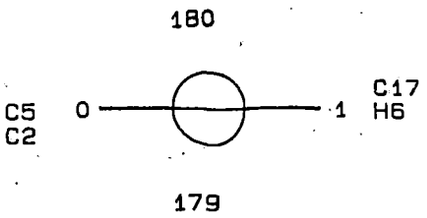

(C1 - C6)

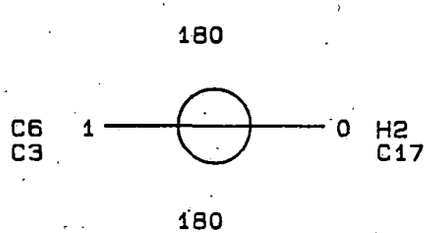

(C1 - C2)

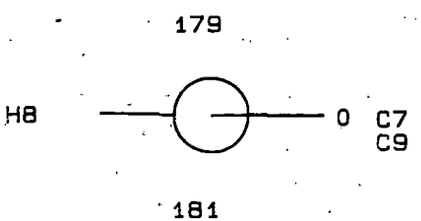

(N1 - C8)

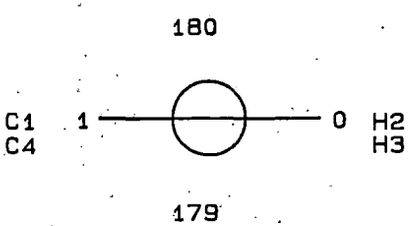

(C3 - C2)

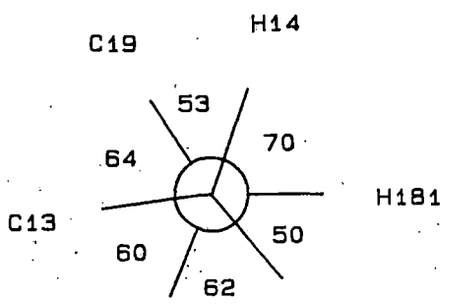

(C14 - C18)

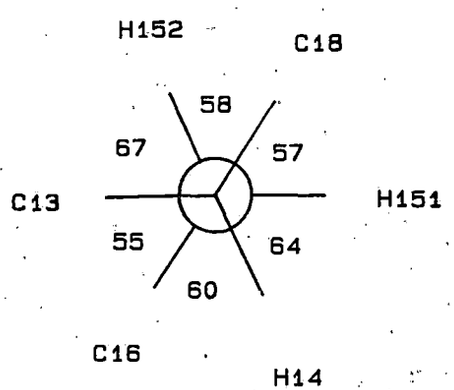

(C14 - C15)

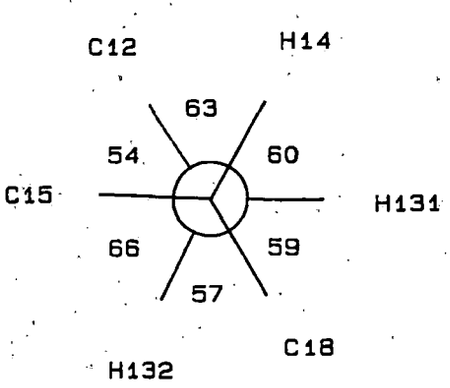

(C14 - C13)

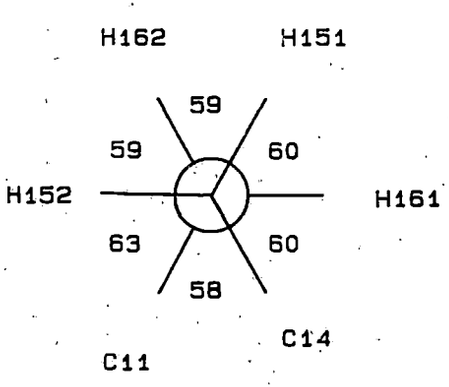

(C15 - C16)

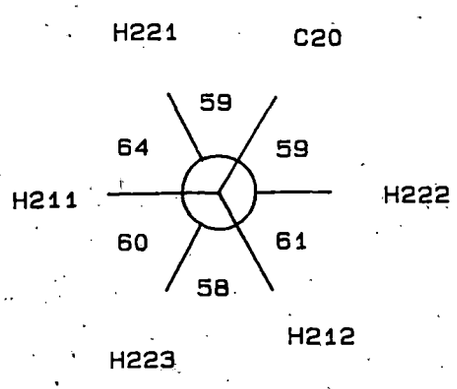

(C21 - C22)

Newman projections of

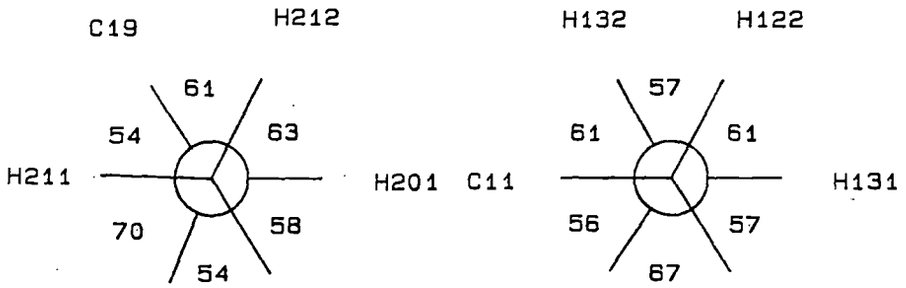

Table 4.1

Important Crystallographic Data

Mol. Formula	$C_{22}H_{27}N_3$
Mol. Weight	333.48 g/mol.
Crystal system	Monoclinic
Space group	P2/a
a = 18.437(1) Å	
b = 7.1027(5) Å	
c = 15.342(1) Å	
β = 106.35 (5)°	
V = 1927.83 Å^3	
D_c = 1.15 g.cm^{-3}	
D_m = 1.17 g.cm^{-3}	
Z = 4	
λ(Cu Kα) = 1.5418 Å	
Number of independent reflections	3277
Number of observed reflections	2246

Table 4.2

Fractional coordinates of the non-hydrogen atoms with e.s.d. in the parenthesis and equivalent isotropic thermal parameters.
Ueq = 1/3 $(U_{11} a^2 a^{*2} + U_{22} b^2 b^{*2} + U_{33} c^2 c^{*2} + U_{13} a a^* c c^* \cos\beta$

Atom	X(6)	Y(6)	Z(6)	Ueq
C1	0.5925 (1)	0.2702 (3)	-0.0344 (2)	0.060 (1)
C2	0.5153 (1)	0.2615 (4)	-0.0779 (2)	0.070 (1)
C3	0.4647 (1)	0.2477 (3)	-0.0269 (2)	0.064 (1)
C4	0.4889 (1)	0.2442 (3)	0.0664 (1)	0.055 (1)
C5	0.5667 (1)	0.2534 (4)	0.1096 (2)	0.068 (1)
C6	0.6177 (1)	0.2668 (4)	0.0590 (2)	0.069 (1)
C7	0.4341 (1)	0.2310 (3)	0.1210 (1)	0.056 (1)
C8	0.3122 (1)	0.2178 (4)	0.1262 (2)	0.070 (1)
C9	0.3338 (1)	0.2169 (3)	0.2195 (1)	0.060 (1)
C10	0.4111 (1)	0.2204 (4)	0.2581 (2)	0.071 (1)
C11	0.2803 (1)	0.2084 (3)	0.2776 (2)	0.064 (1)
C12	0.2178 (1)	0.3576 (3)	0.2528 (2)	0.071 (1)
C13	0.1664 (1)	0.3466 (4)	0.3155 (2)	0.075 (2)
C14	0.1311 (1)	0.1515 (4)	0.3155 (2)	0.066 (1)
C15	0.1935 (1)	0.0040 (4)	0.3380 (2)	0.079 (2)
C16	0.2440 (1)	0.0143 (4)	0.2740 (2)	0.075 (2)
C17	0.6449 (1)	0.2834 (3)	-0.0883 (2)	0.069 (1)
C18	0.0824 (1)	0.1378 (4)	0.3813 (2)	0.077 (2)
C19	0.0130 (1)	0.2619 (4)	0.3598 (2)	0.077 (2)
C20	-0.0347 (1)	0.2347 (4)	0.4256 (2)	0.073 (2)
C21	-0.1003 (1)	0.3684 (4)	0.4102 (2)	0.081 (2)
C22	-0.1487 (2)	0.3382 (5)	0.4736 (2)	0.095 (2)
N1	0.36050(10)	0.2251(3)	0.0753 (1)	0.066 (1)
N2	0.46167(10)	0.2282 (3)	0.2106 (1)	0.071 (1)
N3	0.6849 (1)	0.2933 (4)	-0.1530 (2)	0.092 (2)

Table 4.3

Anisotropic thermal parameters of the non hydrogen atoms with the e.s.d.s in parenthesis. The temperature factor is of the form

$$\exp[-2\pi^2(U_{11}h^2a^{*2} + U_{22}k^2b^{*2} + U_{33}l^2c^{*2} + 2U_{12}hka^*b^* + 2U_{23}klb^*c^*)].$$

Atom	U11	U22	U33	U12	U13	U23
C1	0.056 (1)	0.054 (1)	0.080 (1)	0.0026(10)	0.033 (1)	-0.001(1)
C2	0.059 (1)	0.087 (2)	0.069 (1)	-0.005 (1)	0.026 (1)	-0.006(1)
C3	0.050 (1)	0.077 (2)	0.071 (1)	-0.002 (1)	0.023 (1)	-0.003(1)
C4	0.049 (1)	0.048 (1)	0.072 (1)	0.0042(9)	0.0247(10)	0.000(1)
C5	0.051 (1)	0.084 (2)	0.073 (1)	0.007 (1)	0.022 (1)	0.003(1)
C6	0.049 (1)	0.079 (2)	0.085 (2)	0.005 (1)	0.027 (1)	0.003(1)
C7	0.050 (1)	0.054 (1)	0.069 (1)	0.0047(9)	0.0220(10)	-0.002(1)
C8	0.051 (1)	0.090 (2)	0.074 (1)	-0.001 (1)	0.027 (1)	-0.003(1)
C9	0.056 (1)	0.062 (1)	0.070 (1)	0.003 (1)	0.027 (1)	-0.003(1)
C10	0.056 (1)	0.097 (2)	0.067 (1)	0.009 (1)	0.025 (1)	0.000(1)
C11	0.053 (1)	0.079 (2)	0.068 (1)	0.003 (1)	0.026 (1)	-0.002(1)
C12	0.065 (1)	0.066 (1)	0.094 (2)	0.003 (1)	0.041 (1)	0.002(1)
C13	0.066 (1)	0.073 (2)	0.100 (2)	0.005 (1)	0.047 (1)	-0.001(1)
C14	0.055 (1)	0.077 (2)	0.072 (1)	0.001 (1)	0.026 (1)	0.006(1)
C15	0.076 (1)	0.007 (2)	0.099 (2)	0.010 (1)	0.048 (1)	0.014 (1)
C16	0.076 (1)	0.070 (2)	0.093 (2)	0.009 (1)	0.046 (1)	0.008 (1)
C17	0.063 (1)	0.068 (1)	0.088 (2)	0.002 (1)	0.038 (1)	-0.003 (1)
C18	0.063 (1)	0.093 (2)	0.085 (2)	0.007 (1)	0.038 (1)	0.013 (1)
C19	0.059 (1)	0.093 (2)	0.088 (2)	0.005 (1)	0.036 (1)	0.011 (1)
C20	0.062 (1)	0.082 (2)	0.085 (2)	0.002 (1)	0.035 (1)	0.003 (1)
C21	0.066 (1)	0.087 (2)	0.102 (2)	0.004 (1)	0.040 (1)	0.003 (2)
C22	0.082 (2)	0.109 (2)	0.111 (2)	0.010 (2)	0.054 (2)	0.001 (2)
N1	0.0492 (9)	0.083(1)	0.070(1)	-0.0015(9)	0.0242(9)	-0.003(1)
N2	0.0523(10)	0.096(2)	0.070(1)	0.008 (1)	0.0245(9)	0.001(1)
N3	0.079 (1)	0.102(2)	0.113(2)	0.001 (1)	0.058 (1)	0.000(1)

Table 4.4

Fractional coordinates of the hydrogen atoms and isotropic thermal parameters with e.s.d. in parenthesis. Atoms are numbered according to the heavy atoms to which they are attached.

Atom	x(δ)	y(δ)	z(δ)	U
H2	0.498 (1)	0.265 (3)	-0.148 (1)	0.078 (7)
H3	0.407 (1)	0.241 (3)	-0.057 (2)	0.090 (7)
H5	0.583 (1)	0.248 (3)	0.179 (1)	0.074 (6)
H6	0.673 (1)	0.274 (3)	0.092 (1)	0.083 (7)
H8	0.257 (1)	0.211 (3)	0.090 (2)	0.089 (7)
H10	0.433 (1)	0.217 (3)	0.326 (1)	0.076 (7)
H11	0.310 (1)	0.227 (3)	0.346 (1)	0.068 (6)
H14	0.098 (1)	0.130 (3)	0.249 (1)	0.062 (6)
H121	0.187 (1)	0.344 (3)	0.184 (2)	0.084 (7)
H122	0.244 (1)	0.483 (3)	0.258 (1)	0.083 (7)
H131	0.127 (1)	0.444 (4)	0.299 (2)	0.095 (8)
H132	0.198 (1)	0.371 (3)	0.385 (2)	0.092 (7)
H151	0.169 (1)	-0.118 (4)	0.336 (2)	0.104 (8)
H152	0.230 (1)	0.025 (4)	0.411 (2)	0.094 (8)
H161	0.211 (1)	-0.009 (3)	0.208 (1)	0.074 (6)
H162	0.284 (1)	-0.078 (4)	0.286 (2)	0.111 (9)
H181	0.065 (1)	-0.001 (4)	0.386 (2)	0.101 (8)
H182	0.117 (1)	0.166 (3)	0.447 (2)	0.085 (7)
H191	0.029 (1)	0.397 (4)	0.363 (2)	0.096 (8)
H192	-0.019 (1)	0.239 (3)	0.297 (1)	0.082 (7)
H201	0.001 (1)	0.247 (3)	0.496 (2)	0.088(7)
H202	-0.055 (1)	0.099 (4)	0.422 (2)	0.097 (8)
H211	-0.133 (1)	0.356 (4)	0.340 (2)	0.099 (8)
H212	-0.078 (2)	0.502 (4)	0.419 (2)	0.125 (10)
H221	-0.169 (1)	0.204 (4)	0.466 (2)	0.119 (9)
H222	-0.117 (1)	0.352 (4)	0.541 (2)	0.114 (9)
H223	-0.191 (2)	0.431 (4)	0.465 (2)	0.128 (10)

Table 4.5

Bond distances of the non hydrogen atoms in angstrom with standard deviations in parenthesis.

C1 - C2	1.393 (2)	C10 - N2	1.336 (2)
C1 - C6	1.377 (2)	C11 - C12	1.533 (2)
C1 - C17	1.441 (2)	C11 - C16	1.527 (2)
C2 - C3	1.380 (2)	C12 - C13	1.531 (3)
C3 - C4	1.374 (2)	C13 - C14	1.531 (3)
C4 - C5	1.402 (2)	C14 - C15	1.522 (3)
C4 - C7	1.486 (2)	C14 - C18	1.531 (2)
C5 - C6	1.381 (2)	C15 - C16	1.533 (3)
C7 - N1	1.341 (2)	C17 - N3	1.142 (3)
C7 - N2	1.325 (2)	C18 - C19	1.512 (3)
C8 - C9	1.374 (2)	C19 - C20	1.526 (3)
C8 - N1	1.341 (2)	C20 - C21	1.503 (3)
C9 - C10	1.381 (2)	C21 - C22	1.509 (3)
C9 - C11	1.505 (2)		

Bond distances of the hydrogen atoms in angstrom, with standard deviations in parenthesis.

C2 - H2	1.03 (1)	C16 - H161	1.04 (1)
C3 - H3	1.03 (2)	C16 - H162	0.96 (2)
C5 - H5	1.02 (1)	C18 - H181	1.05 (2)
C6 - H6	1.00 (2)	C18 - H182	1.05 (2)
C8 - H8	1.01 (2)	C19 - H191	1.00 (2)
C10 - H10	1.01 (1)	C19 - H192	0.99 (2)
C11 - H11	1.05 (1)	C20 - H201	1.10 (2)
C12 - H121	1.05 (2)	C20 - H202	1.03 (2)
C12 - H122	1.01 (2)	C21 - H211	1.08 (2)
C13 - H131	0.98 (2)	C21 - H212	1.03 (2)
C13 - H132	1.08 (2)	C22 - H221	1.02 (2)
C14 - H14	1.04 (1)	C22 - H222	1.04 (2)
C15 - H151	0.97 (2)	C22 - H223	1.00 (2)
C15 - H152	1.14 (2)		

Contd.....

(Table V contd...)

Bond angles of the non hydrogen atoms with standard deviations in parenthesis.

C2 - C1 - C6	119.9 (2)	C9 - C11 - C12	115.4 (2)
C2 - C1 - C17	119.2 (2)	C9 - C11 - C16	111.6 (2)
C6 - C1 - C17	120.9 (2)	C12 - C11 - C16	108.9 (2)
C1 - C2 - C3	119.6 (2)	C11 - C12 - C13	111.3 (2)
C2 - C3 - C4	121.3 (2)	C12 - C13 - C14	112.6 (2)
C3 - C4 - C5	118.7 (2)	C13 - C14 - C15	109.2 (2)
C3 - C4 - C7	121.0 (2)	C13 - C14 - C18	112.7 (2)
C5 - C4 - C7	120.3 (2)	C15 - C14 - C18	110.7 (2)
C4 - C5 - C6	120.4 (2)	C14 - C15 - C16	112.2 (2)
C1 - C6 - C5	120.2 (2)	C11 - C16 - C15	111.0 (2)
C4 - C7 - N1	117.1 (2)	C1 - C17 - N3	178.2 (2)
C4 - C7 - N2	117.6 (2)	C14 - C18 - C19	115.9 (2)
N1 - C7 - N2	125.3 (2)	C18 - C19 - C20	113.1 (2)
C9 - C8 - N1	124.2 (2)	C19 - C20 - C21	113.8 (2)
C8 - C9 - C10	114.1 (2)	C20 - C21 - C22	113.9 (2)
C8 - C9 - C11	124.8 (2)	C7 - N1 - C8	115.9 (2)
C10 - C9 - C11	121.1 (2)	C7 - N2 - C10	116.3 (2)
C9 - C10 - N2	124.1 (2)		

Bond angles of the hydrogen atoms with standard deviations in parenthesis.

C1 - C2 - H2	118(1)	H151 - C15 - H152	107 (2)
C3 - C2 - H2	122 (1)	C11 - C16 - H161	103 (1)
C2 - C3 - H3	122 (1)	C11 - C16 - H162	108 (2)
C4 - C3 - H3	117 (1)	C15 - C16- H161	109 (1)
C4 - C5 - H5	117 (1)	C15 - C16 - H162	114 (1)
C6 - C5 - H5	123 (1)	H161 - C16 - H162	107 (2)
C1 - C6 - H6	121 (1)	C14 - C18 - H181	111 (1)
C5 - C6 - H6	118 (1)	C14 - C18 - H182	108 (1)
C9 - C8 - H8	121 (1)	C19 - C18 - H181	108 (1)

Contd.....

Table - 4.6

Equations of least squares planes, the individual and r.m.s. displacements (△) of the atoms from them.

Equations of the planes	Atoms	△ in Å	r.m.s. △ in Å
1. $-.0677X + .9974Y + 0.246Z = 1.156$	C_1	- .0044	
	C_2	.0018	
	C_3	.006	.0025
	C_4	-.0024	
	C_5	.0032	
	C_6	.0012	
Other atoms	C_{17}		
	N_3		
2. $-.0365X + .992Y + .0131Z = 1.384$	C_7	.0058	
	C_8	-.0040	
	C_9	.0077	
	C_{10}	-.0059	
	N_1	-.0025	
	N_2	-.0012	
3. $.0106X + .1891Y + .9819Z = 4.5425$	C_{11}	- .2060	
	C_{12}	- .3757	
	C_{13}	. 3024	
	C_{14}	.2332	
	C_{15}	. 3702	
	C_{16}	-.5259	

Dihedral angle between plane 1 and plane 2 is 2.001°, plane 3 and plane 2 is 78.80°

Table 4.7

Intermolecular contact distances less than 4 Å (invälging non-hydrogen atoms)

C1 - x C3^{b}	3.779	C6 - C16^{e}	3.996
C1 - C4^{a}	3.928	C6 - N3^{d}	3.499
C1 - C4^{b}	3.738	C7 - C17^{a}	3.913
C1 - C7^{a}	3.783	C7 - C17^{b}	3.723
C1 - C7^{b}	3.767	C8 - C8^{c}	3.906
C1 - N1^{a}	3.718	C8 - C17^{a}	3.828
C1 - N1^{b}	3.782	C8 - C17^{b}	3.711
C2 - C3^{a}	3.933	C8 - N1^{c}	3.762
C2 - C3^{b}	3.813	C8 - N3^{a}	3.632
C2 - C4^{a}	3.598	C8 - N3^{b}	3.474
C2 - C4^{b}	3.517	C9 - N3^{a}	3.841
C2 - C5^{a}	3.935	C9 - N3^{b}	3.705
C2 - C5^{b}	3.739	C10 - C21^{f}	3.781
C2 - C7^{a}	3.727	C10 - C21^{g}	3.781
C2 - C7^{b}	3.827	C11 - C21^{f}	3.937
C2 - C14^{c}	3.955	C11 - C21^{g}	3.937
C3 - C3^{a}	3.762	C12 - N3^{b}	3.821
C3 - C3^{b}	3.823	C15 - C22^{e}	3.911
C3 - C4^{a}	3.688	C16 - N3^{a}	3.573
C3 - C4^{b}	3.797	C17 - N1^{a}	3.620
C3 - C5^{a}	3.768	C17 - N1^{b}	3.500
C3 - C5^{b}	3.753	C17 - N3^{d}	3.922
C3 - C6^{a}	3.935	C18 - N2^{e}	3.910
C3 - C6^{b}	3.744	N1 - N3^{a}	3.932
		N1 - N3^{b}	3.688

None: x y z a: 1-x, y, z b: 1-x, 1-y, z c: 1/2-x, y, z,
d: $1 + \frac{1}{2} - x$, y, z e: 1/2 + x, y, z f: 1/2+x-1, 1-y, z
g: 1/2 + x, 1-y, z.

REFERENCES

1. A. Seal, Ph.D. Dissertation, Indian Association for the Cultivation of Science, Calcutta - 32, India (1984).
2. C.H.Sout and L.H.Jensen, X-ray Structure Determination, Macmillan Pub.Co., Inc., N.Y., Page 195 (1968).
3. M.J. Buerger, Crystal Structure Analysis, Wiley, N.Y. Page 158 (1969).
4. M.M.Woolfson, A.Int. to X-ray Crystallography Cambridge University Press, London, p. 173 (1970).
5. P.J. Becker and P. Coppens, Acta Cryst. A30, 129 (1974).
6. B.Borie, Ibid, A 38, 248 (1982).
7. N.Kato, Acta Cryst., A 32, 453 (1976), A32, 458 (1976).
8. D.T.Cromer and J.T.Waber, Acta Cryst., 18, 194 (1965).
9. R.F.Stewart, E.R.Davidson and W.T.Simpson, J.Chem. Phys. 42, 3175 (1965).
10. H. Lipson and W.Cochran, The Determination of Crystal Structures, G.Bell and Sons Ltd., London, pp. 72, 301 (1968).
11. A.J.C. Wilson, Nature, 150, 152 (1942).
12. P.Debye, Ann. Phys. Lp., 46, 809 (1915).
13. J. Karle and H.Hauptman, Acta.Cryst. 475-476 (1973).
14. M.F.C. Ladd and R.A. Palmer, Theory and Practice of Direct Methods in Crystallography, Plenum Pub.Co.N.Y.(1980).
15. International Tables for X-ray Crystallography, Vol. II, eds. J.S.Kasper and K.Lonsdale, Kynoch Press, Birmingham, Englands, p. 355 (1959).
16. H.Hauptman and J.Karle, Act.Cryst. 9, 45 (1956), 12, 93 (1959).
17. J.Karle and H.Hauptman, Acta. & Cryst. 14, 217 (1961).

18. H.Schenk, Computing Methods in Crystallography, Editors, R.Diamond, S.Ramaseshan and K.Venkatesan, Indian Academy of Science (1980).

19. H.Schenk, A.A.Overbeek and C.T.Kiers, Lecture Notes Part II, 10th. International School on Direct Methods of Solving crystal structure, Grice (1984).

20. D.Harker and J.S.Kasper, Acta Cryst., 1, 374 (1948).

21. J.Karle and H.Hamptman, Acta Cryst., 3, 181 (1950).

22. D.Sayre, Acta Cryst. 5, 60 (1952).

23. W.Cochran, Acta. Cryst. 5, 65 (1952).

24. W.H.Zacharia Sen Acta Cryst. 5, 68 (1952).

25. W.Cochran and M.M.Woolfson Acta Cryst. 8, 1 (1955).

26. C.T.Kiers and H.Schenk, SIMPEL 83, An automatic Direct Method Program Package, University of Amsterdam, 1983, H.Schenk, Recl. Trav.Chim. Payebas, 102, 1 (1983).

27. G.M.Sheldrick, Crystallography Program System, University of Cambridge, England.

28. P. Main, S.E.Hull, L.Lessinger, G.Germain, J.P.Declerg and M.M.Woolfson, MULTAN-78, A System of computer programme for the Automatic Solution of crystal structures for X-ray Diffraction Data (University of York, England and Louvain, Belgium, 1978).

29. Hall, Stewart and Munn, Acta Cryst. A36, 979 (1980).

30. Yao, Jia-Xing, Zheng Chao de, Quan Jin-Zi, Han Fu-son, Gu Yuan.xin and Fan Hai-fu (9, - ''SAPI: A Computer Program for automatic solution of crystal structures from X-ray data'', Institute of Physics, Academia Sinica, Beijing, China.

31. S.F.Stewart, The X-RAY 76 System, Tech.Rep., TR-446 Computer Science Centre, Univ. of Maryland, College Park, Maryland (1968)

32. H.Hauptman and T.Karle: Solution of the Phase problem 1, The Centro symmetric crystal, A.C.A.Monography No. 3 (1953).

33. H.Schenk: Acta Cryst. A29 77 (1973a).

34. H.Schenk: Acta Cryst. A29, 480 (1973b)

35. H.Schenk and De K Jong: Acta Cryst, A29 31 (1973)

36. M.Simerska: Czech.J.Phys. 6 1 (1956).

37. G.Germain, P.Main and M.M.Woolfson, Acta Cryst. B 26, 274 (1970).

38. H.Schenk: Acta Cryst. B27 2039 (1971).

39. H.Schenk and C.T.Kiers, In Methods and Applications in Crystallographic Computing, Edited by S.R.Hall and T.Ashida, Clarendon Press, Oxford, p.96-105.

40. A.R.Overbeek and H.Schenk, Proc. K.Ned.Akad.Wet.B39, 341(1976).

41. H.Schenk and I.G.H. de Jong: Acta Cryst.A29, 480 (1973).

42.

43. Same as reference no. 31

44. D.T.Cromer and J.B.Mann, Acta Cryst. A24, 321 (1968).

45. International Tables for X-ray Crystallography, Vol. III, Kynoch Press Birmingham, 1962.

46. C.J.B. Clews andW.Cochran, Acta Cryst. 2, 46 (1949).

47. G.S.Parry, Acta, Cryst., 7, 313 (1954).

48. N.G.Beaton, G.R.Willey and M.G.B.Drew, J.Chem.Soc.Perkin Trans.II, No.4, 469 (1987).

49. P.Mandal and S.Paul, Mol.Cryst.Liq.Cryst.,131, 223 (1985).

50. P.Mandal, S.Paul, H.Schenk and K.Goubitz, Mol.Cryst.Liq. Cryst., 135, 35 (1986).

51. U.Dammeister, H.Hartung and M.Jaskolski, Mol.Cryst. Liq.Cryst. 88, 167 (1982), 69, 119 (1981).

52. W.Haase, H.Pauls and H.T.Muller, Mol.Cryst.Liq. Cryst., 97, 131 (1983).

53. B.Jha, A.Nandi, S.Paul and R.Paul, Mol.Cryst.Liq. Cryst. 104 289 (1984).

54. B.Bhattacharjee, S.Paul and R.Paul, Mol.Cryst. Liq.Cryst. 89, 181 (1981).

55. A.J.Leadbetter,R.M.Richardson and C.N.Colling, J.Phys. (Paris), 36, 37 (1975).

In the present work I have reported the optical birefringence and X-ray diffraction studies of liquid crystalline substances. The samples studied are PCCPP, PCTP, PBBA, EBBA, PPCPP, 50CB.

A hot stage was designed to study the textures and the phase transitions of the compounds under a polarizing microscope. A high temperature X-ray camera was designed and fabricated in our laboratory for taking flat plate photographs of liquid crystal samples in presence and absence of magnetic field.

From the observed textures under polarising microscope and diffraction photographs were samples PCTP, PBBA, EBBA and PCCPP were found to have nematic phase only.

X-ray diffraction photographs were analysed to obtain apparent molecular length (l), and average intermolecular distance (D) in the mesophase. In case of PBBA the apparent molecular length (l) in its most extended form determined by Princeton molecular model Kit is slightly higher than the length of the molecule (L). In case of PCCPP and PCTP the ratio of l to L is 1.25 and 1.28 respectively which are probably due to molecular association as in other cyano compounds. It is a common feature in the liquid crystalline samples. The l and D values of the sample EBBA were calculated and found to be almost equal to that obtained by Leadbetter et al[2]. As the results were already reported by them, so these are not repeated. The average intermolecular distances (D) are found to be in the expected range of 4.8 Å to 5.3 Å in all substances. The values are some time found to increase slightly with temperatures.

X-ray diffraction photographs of the samples were circularly scanned with a microdensitometer and the measured optical densities were converted to relative X-ray intensities using standard callibration method. From these intensity data normalised orientational distribution function $f(\beta)$ in a power series of $Cos^2\beta$ and the orientational order parameters $\langle P_2 \rangle$ and $\langle P_4 \rangle$ were calculated. In principle we could also obtain $\langle P_6 \rangle$, $\langle P_8 \rangle$ etc. from our data but experimental uncertainties and truncation errors involved in series representation would make the values of the these higher order parameters unreliable.

The experimentally obtained $\langle P_2 \rangle$ and $\langle P_4 \rangle$ values are compared with these obtained theoretical estimation. The $\langle P_2 \rangle$ values of the samples PCTP agree well with the M.S. theoretical values that of PBBA and EBBA also agrees well but slightly, lower near transition, but similar results found $\langle P_4 \rangle$ values of other also[3], near the nematic - isotropic transition temperature, where the experimental $\langle P_2 \rangle$ values are significantly lower than the theoretical values. In case of PCCPP the order parameters are slightly less than the theoretical values even at lower temperatures. Such behaviour of the transition temperature, have been found in the determination of $\langle P_2 \rangle$ by magnetic anisotropy measurements[5] Mitra and Paul, 1987 Low values of $\langle P_2 \rangle$ at near nematic isotropic transition temperatures have been reported[6] (Chang, 1975; Sen et al, 1983; Madhusudana et al, 1971; Dunmuer et al, 1978). As said earlier this may be due to the fluctuation of the director which is more pronounced.

Crystal and molecular structure of PCCPP in the solid phase have also been determined. This is a part of our program to determine the conformational behaviour of a mesogenic compound in the crystalline phase.

We have undertaken the study of the crystal and molecular structure of a homologous series 5-(4-Alkycyclohexyl)-2-(4-cyanophenyl) Pyrimidines all of them having nematic phase. In homologous series of thermal mesogens containing alkyl chains, the type of liquid crystalline phases formed, if any, depends on the chain length. The lowest members of the series may not yield liquid crystals those with intermediates chain lengths yield only nematic phases. Smectic phases of * 6 types A or C appears only when some critical chain length is reached. These properties clearly have a structural basis. The structures of ECCPP and HCCPP have also been determined which will be reported elsewhere.

The structures was solved by applying direct method package program 'SIMPEL-83' to X-ray diffraction intensity data. The crystal belong to monoclinic system with space group $P2/a$. I found a = 18'437 Å , b = 7.1027 Å, C = 15.342 Å and $\beta = 106.35^{\circ}$ with 4 molecules per unit cell. Least squares refinement leads to R = .049 and R_w = '048 for 2246 observed reflections. The molecules are find to be in their most extended conformation. As expected the phenyl ring and the pyrimidine ring show a high degree of planarity.

The dihedral angle between the phenyl ring and the pyrimidine ring is 2^{0}. And the dihedral angle between the cyclohexane ring and the pyrimidine ring is 78.4^{0}. The phenyl and pyrimidines are almost in the ac plane whereas the cyclohexane ring is almost at right angles to this plane. Pairs of molecules related by a centre of symmetry give rise to a sheet of parallel ~~mxts~~ molecules in ac plane and these sheets of paired molecules are stacked in an imbricated mode along the 6 - axis. The crystalline modification of the sample therefore corresponds to the commonly found molecular packing in a nematogenic precursor. With the increase in thermal a energy, a transformation in the liquid crystalline state is presumably accomplished by the breakdown of the molecular stacking along b-axis. It could transform from the solid phase to nematic phase by means of a single dispacive transition.

LISTFC FOR ** Q27SLA **

H,0,0

2	373	387
4	222	-227
6	335	328
8	50	-53
10	61	56
12	74	61
14	24	24
16	48	-45
18	78	-75
20	34	-32

H,0,1

20	45	-43
18	79	-74
16	68	63
14	75	86
12	51	49
10	77	-76
8	211	205
6	347	352
4	156	160
2	675	726
0	558	645
-2	41	50
-4	179	-200
-6	55	-52
-8	238	-256
-10	43	44
-12	92	-104
-14	24	-23
-16	108	113
-18	45	51
-20	29	29

H,0,2

-20	87	82
-18	166	-178
-16	148	-152
-14	32	-33
-12	124	-131
-10	107	111
-8	111	-103
-4	170	178
-2	169	189
0	182	-205
2	1677	1769
4	914	-946
6	339	346
8	519	517
10	39	-45
12	32	35
14	44	48
16	154	151
18	37	33

H,0,3

16	43	43
10	259	243
8	465	466
6	193	-200
4	352	-368
2	465	509
0	530	601
-2	326	-358
-4	522	548
-6	73	-72
-8	161	166
-10	21	25
-16	186	-178
-18	45	-48
-20	19	20

H,0,4

-18	36	38
-16	502	-516
-14	206	-211
-12	31	32
-10	253	-247
-8	769	746
-6	152	-167
-4	161	178
-2	114	115
0	312	-353
2	706	-782
4	133	140
6	298	-306
8	34	31
10	52	-56
12	124	-121
16	35	-29
18	43	38

H,0,5

18	17	-16
16	29	-25
10	75	71
8	32	29
6	223	-224
4	287	312
2	830	914
0	643	-705
-2	34	37
-4	48	-46
-6	326	-323
-8	508	-483
-10	118	112
-12	89	-84
-14	576	-580
-16	437	-437
-18	65	63
-20	29	30

H,0,6

-20	27	-27
-18	38	40
-16	194	191
-14	183	-199
-12	69	68
-10	28	-29
-8	468	-456
-6	748	743
-4	237	-235
0	633	-682
2	254	-274
4	60	59
8	39	-38
12	50	-52

H,0,7

12	68	-65
8	236	-241
6	219	-235
4	183	181
2	534	-539
0	222	-214
-2	23	-19
-4	60	-61
-6	598	-595
-8	102	-113
-10	63	65
-12	141	141
-14	268	-276
-16	47	-49
-18	38	40
-20	64	-62

H,0,8

-20	39	-41
-18	40	-41
-16	42	39
-14	88	92
-12	24	-26
-10	288	294
-8	58	52
-6	442	-439
-4	130	143
-2	82	-90
0	12	-10
2	168	-163
4	123	131
6	154	-159
8	415	-423
12	102	99
14	18	17

H,0,9

14	47	-45
12	29	-27

LISTFC FOR ** Q27SLA **

H,0,9

10	221	-217
8	278	-281
4	172	-169
2	33	40
0	49	46
-2	28	-24
-4	153	158
-6	485	471
-8	203	-193
-10	245	240
-12	58	-61
-14	17	18
-16	142	150
-18	49	-51
-20	17	11

H,0,10

-20	40	38
-16	112	127
-14	43	39
-12	188	-184
-8	113	113
-6	148	-145
-4	204	-218
2	43	41
4	44	40
6	57	57
8	87	-87
10	162	-163
12	29	25

H,0,11

10	25	-20
8	18	13
6	16	-14
4	17	-18
2	26	-20
0	57	-59
-2	33	-32
-4	332	353
-6	127	-125

-8	275	275
-10	17	-19
-12	20	24
-14	258	283
-16	63	62

H,0,12

-18	26	27
-14	108	114
-10	28	30
-8	321	320
-6	163	164
-4	34	-33
-2	34	-31
0	31	-34
4	31	-21
6	24	-24
10	18	13

H,0,13

10	19	-15
8	22	23
4	18	-19
2	27	-35
0	40	-45
-2	40	43
-4	187	-186
-6	396	393
-8	232	225
-10	78	-75
-12	43	49
-14	37	28
-16	57	-48
-18	44	42

H,0,14

-16	36	29
-14	31	-25
-10	67	-63
-8	73	68
-6	216	213
-4	177	171

-2	80	78
0	32	35
2	26	-29
4	29	29
6	32	34
8	47	42

H,0,15

4	16	-12
2	33	40
0	61	62
-2	149	-144
-4	28	30
-6	51	48
-8	45	-41
-10	28	-26
-12	68	56
-14	45	-39
-16	64	54

H,0,16

-14	36	26
-10	23	23
-8	41	-36
-4	36	-33
2	29	35

H,0,17

0	26	-24
-8	26	-23
-10	50	46
-12	35	-32

H,0,18

-6	32	-27

H,1,17

-11	33	28
-7	20	13
-5	62	-57

-4	21	16
-3	37	-33
-1	36	-37

H,1,16

3	22	-27
-1	34	31
-2	32	29
-3	54	46
-4	44	-38
-5	25	-21
-7	20	-21
-9	19	-18
-11	56	-49
-14	14	12

H,1,15

-11	71	-62
-9	27	-27
-7	21	-8
-5	60	58
-3	45	-41
1	55	-63
3	61	-66
4	20	15

H,1,14

1	90	-102
0	18	20
-1	73	-79
-2	31	-33
-3	25	-24
-4	58	59
-5	18	-14
-7	32	34
-10	23	-19
-11	29	-31
-12	22	-17
-13	24	-22

LISTFC FOR ** Q27SLA **

H,1,6

2	55	-63
0	43	39
-1	176	-187
-3	97	-104
-4	45	44
-5	262	259
-6	84	82
-7	840	805
-8	211	-205
-9	95	92
-10	74	70
-11	57	-56
-12	89	-87
-13	75	-73
-14	57	59
-15	168	-167
-16	27	28
-17	53	57
-18	19	-20
-19	49	46
-20	17	18
-21	21	20

H,1,5

-19	22	-19
-18	22	19
-17	78	80
-16	78	-85
-15	57	56
-14	92	97
-13	93	93
-12	24	19
-11	62	59
-10	97	-91
-9	319	308
-8	33	-26
-7	734	713
-6	16	18
-5	116	122
-4	46	50
-3	74	-74
-2	21	-20

-1	32	27
0	44	-45
1	150	155
2	182	191
3	227	-222
4	113	-117
5	23	-24
6	143	144
7	21	-20
8	109	-106
9	29	31
10	18	-18
11	55	57
12	24	23
15	27	22
17	34	35

H,1,4

17	107	104
15	50	47
12	20	16
11	55	-51
10	37	-35
9	78	70
8	51	43
7	166	-164
6	62	-59
5	231	-234
4	81	86
3	81	-85
2	50	56
1	277	-294
0	46	-47
-1	247	259
-2	49	-51
-3	172	-176
-4	37	34
-5	88	89
-6	37	36
-7	16	15
-8	203	200
-9	249	242
-10	17	-11
-11	38	41

-12	68	69
-14	173	-171
-15	98	105
-16	23	25
-17	92	-98
-18	36	39
-20	17	-17
-21	51	-48

H,1,3

-21	48	-50
-19	15	19
-18	108	-110
-17	236	232
-16	47	50
-15	382	391
-14	103	105
-11	130	-130
-10	23	-24
-9	221	211
-8	182	-170
-7	226	225
-6	19	19
-5	217	-220
-4	38	-40
-3	202	-210
-2	110	116
-1	202	-218
0	327	350
1	818	-887
2	459	-495
3	214	-229
5	30	-27
6	61	-58
7	73	-77
8	99	98
9	112	-100
10	49	48
11	80	-77
12	24	-24
13	30	30
14	25	-21
15	115	119
17	89	84

19	15	-13

H,1,2

18	31	29
17	29	-31
15	117	120
13	59	56
11	25	-18
9	127	-121
8	188	-180
6	36	34
5	216	-217
4	123	125
3	383	399
2	461	500
1	1955	1989
0	441	-471
-1	58	51
-2	233	-252
-3	353	-384
-5	155	-155
-6	145	154
-7	76	75
-8	79	74
-9	51	-48
-10	55	49
-11	65	-66
-12	54	-51
-13	26	-29
-14	63	63
-16	54	-56
-17	170	168
-18	27	27
-19	37	-36

H,1,1

-20	25	-26
-19	62	-59
-18	42	43
-17	18	-6
-15	29	-26
-14	46	-48

LISTFC FOR ** Q27SLA **

H,1,1

-13	35	-35
-12	53	49
-11	50	-52
-10	64	-56
-9	76	77
-8	20	-22
-6	51	-54
-5	55	-60
-4	69	-72
-3	19	13
-2	207	217
-1	39	-38
0	50	-56
1	98	104
2	96	-104
3	79	78
4	161	-165
5	286	-289
6	188	181
7	648	-624
8	137	131
9	445	-416
11	49	-48
12	25	-26
13	50	48
14	28	25
15	27	30
16	51	-48
17	62	58
19	64	62
20	39	37

H,1,0

19	20	-20
18	61	-55
16	66	63
15	95	-89
13	30	31
10	40	-37
9	88	-82
8	55	-50
7	317	-306
6	219	-217
5	368	-375
4	259	254
3	183	181
2	150	-149
1	641	-627
0	312	303

H,2,0

0	2622	-2381
1	621	-595
2	1069	-1011
3	647	-626
4	215	205
5	196	189
6	472	-449
7	242	232
8	31	26
9	22	15
14	51	-51
16	60	62
17	54	-52
18	20	18
19	43	44
20	40	40

H,2,1

19	24	21
18	56	51
16	69	-65
15	42	-43
14	60	-63
13	19	18
12	43	-40
11	30	28
10	27	-20
9	63	-66
8	33	-17
7	316	-299
6	423	-395
5	343	327
4	388	375
3	214	-200
2	864	-831
1	271	265
0	1329	-1266
-1	305	294
-2	507	505
-3	529	-533
-4	80	-75
-5	380	386
-6	366	371
-7	161	160
-8	126	131
-10	48	-47
-11	35	35
-12	23	28
-13	39	41
-15	109	-112
-16	73	-79
-17	19	20
-18	15	16
-19	53	57
-20	55	-55

H,2,2

-20	39	-35
-19	52	-55
-18	118	127
-17	40	-40
-16	45	47
-15	135	145
-14	105	114
-12	68	65
-11	26	-25
-10	25	24
-9	61	-61
-8	35	-34
-7	47	-49
-6	57	-57
-5	152	-156
-4	217	-221
-3	64	-67
-2	177	171
-1	425	428
0	488	-483
1	48	-47
2	491	-482
4	123	127
5	113	119
7	28	-25
8	481	-463
9	43	-41
11	19	-18
12	24	-25
14	46	-47
15	19	25
16	133	-129
19	43	-42

H,2,3

18	29	-26
17	18	-19
16	33	-32
11	24	-22
10	113	-108
8	477	-447
7	405	391
6	105	104
5	200	-195
4	182	184
3	161	-161
2	390	-388
1	161	167
0	173	179
-1	96	-96
-2	235	-229
-3	55	53
-4	208	-218
-5	49	53
-6	40	42
-7	67	-64
-8	109	-108
-10	75	-75
-11	122	127
-12	44	48
-13	110	-113
-14	57	-58
-15	78	75
-16	255	256

LISTFC FOR ** Q27SLA **

H,2,3

-17	31	32
-19	22	-24
-20	17	-13

H,2,4

-20	13	-13
-17	43	-46
-16	416	414
-15	37	-37
-14	155	156
-13	102	103
-12	53	53
-10	57	-57
-9	118	118
-8	231	-230
-7	27	23
-5	56	54
-4	28	-24
-3	32	31
-1	168	-163
0	230	242
1	144	152
2	39	-46
3	30	27
4	216	220
5	116	112
6	151	150
7	53	-47
8	125	123
9	127	-127
10	42	-42
11	26	23
12	74	76
13	27	25
16	26	25
17	15	14
18	29	-27

H,2,5

16	18	16
12	57	50
11	20	-19
10	62	-59
9	156	158
8	58	-62
7	28	-25
6	97	98
5	121	-124
4	321	-318
3	142	-140
2	180	-185
1	160	164
0	331	348
-1	22	-10
-2	66	57
-4	30	34
-6	18	19
-7	94	-97
-8	153	155
-9	36	-35
-10	220	217
-11	138	-138
-12	33	-34
-13	271	270
-14	582	578
-16	233	231
-17	169	-169
-19	23	26

H,2,6

-21	15	-14
-19	20	20
-18	95	-92
-17	31	35
-15	21	-21
-14	166	172
-13	222	-216
-12	107	-108
-9	118	120
-8	114	105
-7	147	152
-6	20	8
-4	21	0
-2	57	48
-1	103	-100
0	459	443
1	21	28
2	154	152
3	205	207
4	152	-156
5	66	-67
6	142	140
7	49	46
8	25	-25
10	47	52
11	51	-51
13	24	25
14	18	19

H,2,7

12	37	37
9	28	-26
8	256	254
7	43	45
6	136	136
5	54	-47
4	25	-24
3	106	99
2	293	277
1	29	-30
0	244	250
-1	33	-32
-2	32	28
-3	25	-28
-4	33	27
-5	32	31
-6	203	200
-7	20	-19
-8	363	361
-9	301	-296
-10	222	-217
-11	154	156
-12	117	113
-13	106	104
-14	70	68
-15	88	-91
-16	44	44
-20	57	56

H,2,8

-20	25	28
-18	48	47
-17	23	23
-16	88	-84
-15	41	-40
-14	28	28
-13	78	77
-12	82	-79
-11	49	-49
-10	166	-169
-9	26	-29
-8	42	38
-7	25	-25
-6	118	115
-5	52	-51
-4	76	77
-3	53	58
-2	18	-21
-1	17	-21
0	32	34
1	59	-61
2	180	175
3	25	-23
4	58	-55
5	45	-45
6	86	90
7	113	-109
8	337	328
9	133	131
11	59	59
12	30	-27
13	42	-44
14	23	-25

H,2,9

14	34	32
11	16	-15
10	215	211
8	244	239
7	55	-53
6	62	63

LISTFC FOR ** Q27SLA **

H,2,9

5	60	58
4	43	41
2	31	-34
0	65	-64
-2	35	30
-3	67	-68
-4	137	-140
-5	27	29
-6	68	-62
-7	43	43
-8	141	-137
-9	87	81
-10	74	-74
-11	44	-40
-12	39	-37
-13	67	-65
-14	23	24
-16	108	-108
-17	22	21
-18	28	26
-19	24	-24
-20	17	-14

H,2,10

-18	16	13
-17	25	24
-16	94	-95
-14	116	-115
-13	69	-73
-12	215	208
-11	194	194
-10	40	-36
-9	48	-45
-8	50	45
-7	144	-141
-6	74	75
-5	24	21
-4	26	-25
-2	66	65
-1	51	53
5	29	-30
6	53	-48
7	28	-30
8	61	66
9	46	-46
10	129	126
11	36	38
12	21	-18

H,2,11

0	52	55
-2	31	-34
-3	43	-45
-4	72	-68
-5	41	40
-6	61	-61
-7	66	63
-8	162	-158
-9	38	-35
-10	84	-80
-11	75	-76
-13	48	-48
-14	186	-196
-15	38	39
-16	39	-46
-18	16	-14
-19	20	18

H,2,12

-15	42	37
-14	100	-99
-12	41	-41
-11	18	-17
-10	57	54
-9	130	129
-8	335	-327
-7	89	-86
-6	76	-77
-5	81	-83
-3	44	48
-1	43	-42
0	62	62
1	38	41
3	16	-10
4	27	26

H,2,13

8	25	-22
3	29	-29
2	56	64
-2	33	31
-5	59	-59
-6	255	-249
-8	208	-200
-9	82	76
-10	49	47
-12	30	-32

H,2,14

-14	24	20
-10	24	22
-9	28	-24
-8	39	-35
-7	92	87
-6	269	-255
-5	27	27
-4	66	-65
-3	35	-35
-2	51	-48
0	47	-47
1	42	-42
3	40	42
4	31	-31
6	21	-18

H,2,15

4	17	25
2	32	-36
0	16	-18
-1	44	42
-2	52	51
-5	43	-38
-6	33	-31
-7	39	41
-8	37	37
-10	31	28
-12	36	-28
-13	25	20
-14	17	-15

H,2,16

-13	21	-18
-10	22	-20
-9	20	-17
-5	23	19
-3	20	18
-2	38	34
0	15	-16
2	24	-28

H,2,17

-2	18	17
-4	19	16
-8	27	20
-9	14	-8
-10	17	-18

H,3,16

-6	22	23
-8	26	-25
-11	32	31

H,3,15

-13	19	20
-11	36	33
-9	21	23
-5	22	-24
-2	17	-14
1	59	65
2	17	-18
3	41	46

H,3,14

2	37	37
1	78	84
0	20	-22

LISTFC FOR ** Q27SLA **

H,3,14

-1	27	28
-5	22	23
-6	66	-64
-8	61	61
-9	26	28
-11	15	11
-12	23	20
-15	41	-38

H,3,13

-16	38	-33
-13	20	-25
-12	21	18
-11	24	-24
-10	57	-57
-9	41	-36
-8	67	-66
-7	47	43
-6	72	66
-5	47	47
-1	53	55
0	21	-22
1	29	37
2	31	38
4	23	21

H,3,12

9	18	-14
5	17	-19
3	28	25
2	40	-38
1	48	48
0	46	50
-1	85	88
-4	23	25
-5	66	62
-7	276	268
-8	122	-116
-9	112	108
-10	72	69
-11	20	19

-12	28	-28
-13	59	-58
-15	36	-40
-17	39	-39

H,3,11

-18	13	-13
-17	23	-24
-15	25	-25
-14	16	13
-12	22	-18
-11	37	-39
-10	114	-105
-9	130	125
-8	105	103
-7	117	114
-6	48	46
-5	31	-29
-4	33	37
-3	27	-24
-2	49	-53
-1	19	-18
1	28	-24
2	48	47
3	40	-37
5	35	-35
9	50	45

H,3,10

10	52	50
9	44	44
8	34	-32
6	30	-30
5	20	-19
1	39	32
0	49	-49
-2	49	49
-4	43	-47
-5	23	-25
-6	49	46
-8	120	119
-9	145	131
-10	146	-143

-11	79	-77
-12	66	62
-15	20	21

H,3,9

-17	25	25
-15	33	33
-14	31	34
-13	84	-84
-11	39	37
-10	155	154
-9	39	41
-8	182	-180
-7	70	68
-6	23	21
-3	27	-27
-2	27	-25
-1	36	38
0	25	-24
1	102	95
3	44	41
7	68	63

H,3,8

10	70	-68
9	88	-89
8	60	56
6	30	32
4	55	51
3	89	87
2	25	25
1	149	141
-1	101	100
-2	86	-86
-3	48	-45
-4	36	40
-5	29	-22
-7	39	-42
-8	126	125
-9	191	-192
-10	53	53
-11	84	-81
-12	251	-251

-13	121	-114
-14	60	60
-15	26	-24
-16	40	39
-17	20	-20
-19	33	-35

H,3,7

-20	15	16
-19	24	-25
-17	23	-23
-16	30	-30
-15	28	-29
-14	78	-77
-13	130	125
-12	198	195
-11	52	61
-10	178	-178
-9	134	136
-8	48	47
-7	104	-95
-6	21	-23
-5	118	-116
-3	25	25
-2	58	-55
-1	201	198
1	166	154
3	20	16
5	59	-53
7	253	-243
8	21	-19
9	122	-121
11	32	32
14	20	-23

H,3,6

13	20	23
12	22	24
11	45	40
10	34	-35
9	63	63
8	195	-186

LISTFC FOR ** Q27SLA **

	H,3,6		-2	88	80	-19	34	35	13	39	-38
			-1	65	-60	-20	17	14	12	18	20
7	61	-57	0	100	-91				11	40	37
6	112	105	2	22	-20		H,3,3		9	158	149
5	50	48	3	173	170				8	90	87
4	44	39	4	24	-19	-18	79	82	7	42	-44
3	41	31	5	73	-74	-17	120	-118	6	179	175
1	21	17	6	90	-90	-16	40	40	5	99	-90
0	64	63	7	29	-23	-15	210	-217	4	449	-435
-1	101	86	8	95	93	-14	215	-225	3	352	-335
-2	30	35	9	22	-22	-12	76	74	2	68	68
-3	74	74	15	23	-25	-11	94	-95	1	381	-358
-4	137	-148	16	21	20	-10	40	43	0	114	110
-5	173	-173				-9	69	-65	-1	105	-102
-6	46	55		H,3,4		-8	18	21	-2	309	301
-7	340	-329				-7	92	-84	-3	22	-22
-8	39	40	17	58	-61	-6	50	-47	-4	65	-63
-9	122	-117	15	44	-44	-5	197	182	-5	27	-23
-10	82	82	11	29	33	-4	244	223	-6	222	-220
-11	41	-41	9	31	-31	-3	170	170	-7	34	-32
-12	72	70	8	85	80	-2	286	-270	-10	25	28
-13	97	95	7	80	76	-1	203	193	-11	60	64
-14	109	-106	6	126	-120	0	71	64	-12	53	-53
-15	77	72	5	56	55	1	16	20	-13	63	61
-17	14	-14	4	132	127	2	184	172	-15	54	-53
-18	18	-16	3	179	181	3	24	-18	-16	23	-18
-19	26	-26	2	106	-104	4	20	20	-17	116	-117
			1	88	87	5	261	243	-18	20	16
	H,3,5		0	19	-21	6	88	83			
			-1	66	-60	7	82	76		H,3,1	
-20	17	-17	-2	47	43	8	193	-183			
-19	40	-39	-3	42	41	9	65	57	-19	26	29
-18	22	20	-4	118	-106	12	26	23	-17	20	-20
-17	16	-15	-5	62	-53	14	24	26	-16	41	-44
-15	21	23	-6	117	-125	15	90	-87	-14	52	55
-14	66	64	-7	211	-209	16	16	-16	-12	29	-30
-13	103	-106	-8	23	-18	17	59	-62	-11	56	58
-12	172	-173	-9	132	-118	18	23	-22	-10	41	43
-10	238	239	-10	129	-139				-9	99	-96
-9	336	-328	-11	105	107		H,3,2		-8	26	-28
-7	294	-288	-12	30	34				-6	282	282
-6	108	-109	-14	97	101	17	21	-15	-5	35	-28
-5	70	-72	-15	123	-124	16	41	-40	-4	254	-244
-4	38	-27	-17	22	-19	15	80	-75	-3	326	320
-3	42	38	-18	19	-20	14	33	29			

LISTFC FOR ** Q27SLA **

	H,3,1		3	245	230				-2	66	63
			4	265	266	-16	63	-64	-4	115	107
-2	272	258	5	135	-127	-15	49	-51	-5	29	-34
-1	343	-315	6	115	109	-13	20	16	-6	17	-13
0	79	-79	8	20	-17	-12	130	-138	-7	39	36
1	441	-415	10	22	-17	-9	16	18	-8	23	14
2	67	-62	13	17	-16	-8	17	15	-9	17	17
3	185	183	14	24	-22	-6	27	32	-10	90	94
4	210	207	15	20	24	-5	47	44	-11	78	-79
5	241	236	16	42	37	-4	62	62	-12	26	-26
6	431	-403	17	22	19	-3	76	71	-13	31	34
7	467	440	18	39	-38	-2	69	65	-14	41	-36
8	48	39				-1	195	-181	-15	100	-104
9	175	169		H,4,1		0	162	147	-16	115	-115
10	39	40				1	155	-147	-18	63	-68
11	20	23	17	33	28	2	280	251			
13	69	-68	16	27	27	3	106	101		H,4,4	
14	39	-30	15	30	28	4	130	-133			
16	34	33	14	76	72	5	85	-82	-18	30	-33
19	26	-28	9	48	46	6	131	122	-17	100	104
			8	116	112	7	72	-73	-16	194	-196
	H,3,0		7	143	139	8	137	127	-15	39	-38
			6	66	65	9	89	86	-14	203	-205
18	20	18	5	183	-173	10	50	45	-13	86	-86
15	28	33	4	243	-243	11	19	-15	-12	96	100
14	34	-34	3	247	217	14	49	51	-11	20	-15
13	16	16	2	496	458	15	16	-15	-10	22	-18
12	49	49	1	42	-37	16	40	42	-9	78	-78
11	17	20	0	660	617	17	26	28	-8	102	100
10	54	49	-1	383	-360				-7	54	55
9	68	64	-2	102	-94		H,4,3		-5	57	-52
8	25	27	-3	159	130				-3	30	-28
7	221	201	-4	195	-195	16	38	36	-2	89	-73
6	131	129	-5	156	-150	15	38	-35	0	68	-65
5	93	91	-6	83	-88	13	34	-28	1	86	-83
4	74	69	-8	38	-38	11	41	35	2	109	105
2	381	-355	-9	38	38	10	68	64	3	33	34
1	35	33	-11	41	-38	8	192	182	4	80	-79
0	238	220	-12	57	67	7	220	-214	6	248	-237
			-13	63	-60	5	42	41	8	35	35
	H,4,0		-15	32	38	4	110	100	14	16	-20
			-16	16	-14	3	72	70	15	29	21
0	858	799	-17	17	-21	2	21	-24			
1	388	369				1	106	-98			
2	326	306		H,4,2		-1	52	52			

LISTFC FOR ** Q27SLA **

H,4,5

12	27	-25
9	52	-55
6	156	142
5	83	84
3	17	17
2	48	48
1	152	-141
0	159	-156
-1	50	66
-2	32	-29
-3	39	34
-6	17	22
-7	19	-19
-9	24	-21
-10	163	-172
-11	104	98
-12	118	-120
-13	176	-174
-14	201	-198
-15	60	61
-16	179	-181
-17	111	113
-18	32	33
-19	19	-20

H,4,6

-18	43	44
-16	52	-54
-15	69	71
-14	143	-135
-13	37	36
-10	195	207
-8	131	-127
-7	79	-80
-6	60	-60
-4	23	-16
-3	34	-35
-3	34	-35
-2	51	-35
-1	63	65
0	191	-191
1	66	-69

H,4,7

2	90	-80
3	111	-109
4	82	85
5	67	68
6	77	-77
7	41	-43
8	75	-73
10	34	32
11	17	16
12	29	-29
10	36	-37
9	50	-50
8	91	-86
6	192	-187
5	52	52
4	54	54
3	92	-91
2	126	-124
1	34	32
0	136	-135
-1	59	59
-2	36	-35
-5	23	-26
-6	87	-89
-8	151	-150
-9	192	197
-10	31	-35
-11	79	-80
-14	65	-65
-15	58	56
-16	38	39
-18	41	-40

H,4,8

-15	29	28
-13	46	-45
-12	48	49
-10	26	29
-7	47	47
-6	70	-72
-4	23	-23

-2	23	-24
-1	27	29
1	69	72
2	61	-68
4	45	-43
5	29	30
6	24	-20
7	88	88
8	138	-138
9	95	-98
10	55	-57
11	34	-34
12	17	15
13	16	19

H,4,9

11	33	-37
10	80	-88
8	221	-223
7	74	71
6	18	-22
0	32	30
-1	39	-41
-2	41	42
-3	29	26
-4	23	-21
-8	66	67
-9	39	-37
-10	126	131
-13	21	20
-15	40	39
-16	40	41
-17	29	-28

H,4,10

-17	43	-44
-16	59	61
-14	67	67
-13	88	89
-12	44	-43
-11	104	-105
-10	44	-47
-9	42	42

-8	74	-75
-7	39	38
-4	66	65
-3	19	24
-2	42	-44
0	45	-44
1	17	17
4	15	13
7	27	38
9	44	46
10	53	-60

H,4,11

9	21	23
6	17	-12
1	25	-26
0	19	23
-2	33	-34
-3	21	22
-4	27	28
-6	22	26
-8	160	160
-10	65	65
-13	51	55
-14	78	81
-15	38	-40
-16	37	42

H,4,12

-15	45	-45
-14	60	64
-12	17	20
-11	22	24
-9	116	-118
-8	135	133
-7	81	84
-6	85	84
-5	56	55
-2	28	33
-1	23	23
0	32	-33
1	26	-28

LISTFC FOR ** Q27SLA **

H,4,13

1	16	13
0	66	-66
-4	15	17
-5	73	73
-6	135	137
-7	28	-24
-8	115	116
-9	74	-77
-10	18	-17
-12	19	15
-13	15	-14

H,4,14

-8	68	70
-7	80	-82
-6	132	138
-5	19	20
-4	52	50
-2	28	-28
-1	15	-8
0	60	62
3	20	-19

H,4,15

0	22	21
-1	28	-30
-6	16	20
-7	37	-42
-8	33	-32

H,5,14

-4	16	19

H,5,13

-9	16	14
-8	24	28
-6	36	35
-4	35	-39
-3	25	-24
-2	40	41
-1	27	-31
0	29	-30

H,5,12

1	35	-36
-1	77	-77
-2	20	24
-3	32	33
-5	36	-34
-6	41	-43
-7	139	-139
-8	24	26
-9	64	-68
-10	50	46
-13	24	26

H,5,11

-13	19	16
-10	28	33
-9	58	-57
-8	19	23
-7	47	-44
-6	103	-101
-5	24	-27
-4	42	42
-2	36	-33
-1	38	35
2	24	-23
5	19	16

H,5,10

8	21	23
-3	39	-42
-5	26	25
-6	22	-20
-7	30	-30
-8	60	-59
-9	65	-61
-11	33	35
-12	20	21
-14	37	-38

H,5,9

-14	28	-29
-13	30	29
-10	36	35
-9	57	-54
-8	63	-59
-7	55	-52
-6	46	48
-4	44	-45
-3	22	22
-2	51	48
-1	46	-48
0	29	28
1	39	-44
6	30	25
7	35	-38
8	34	-35

H,5,8

10	19	23
9	24	29
6	20	-20
5	19	22
3	38	-41
2	18	-20
1	88	-90
-1	25	-25
-3	40	44
-5	32	-33
-6	49	-50
-7	29	29
-8	29	29
-9	108	113
-10	31	-31
-11	43	43
-13	30	30
-14	25	26
-16	28	-29

H,5,7

-15	23	-22
-14	34	37
-13	36	-31
-12	45	43
-11	52	-56
-10	43	-46
-9	75	-80
-7	90	92
-6	61	-68
-5	74	72
-4	60	64
-3	49	-58
-2	67	68
-1	69	-70
0	36	33
1	64	-61
2	55	-52
3	39	-39
5	21	15
6	72	-62
7	154	162
8	48	53
9	46	45
10	39	39

H,5,6

11	19	-20
8	49	47
5	46	-48
4	27	-27
2	19	18
1	38	-32
0	65	-62
-1	69	-63
-4	26	18
-5	84	90
-6	78	83
-7	109	107
-8	101	-112
-9	70	70
-11	48	53
-12	39	-37
-13	63	-67
-16	56	62

LISTEC FOR ** Q27SLA **

H,5,5

-16	16	-20
-13	39	42
-12	43	-40
-11	21	19
-10	51	-51
-9	161	166
-7	121	123
-6	73	79
-5	19	18
-1	16	19
1	31	-30
2	81	79
3	61	-55
4	81	-78
5	80	78
6	62	63
9	27	27

H,5,4

9	30	-28
6	26	-21
4	32	32
3	97	-95
2	68	-66
0	81	76
-1	29	20
-4	53	58
-5	28	24
-6	48	50
-7	102	107
-8	57	63
-9	75	70
-10	52	-60
-11	85	-91
-12	64	66
-13	20	20
-14	21	17
-15	52	52
-16	45	-48
-17	44	48

H,5,3

-17	59	68
-15	79	84
-14	38	44
-13	27	29
-12	24	-21
-11	85	93
-10	25	-17
-9	28	25
-8	27	23
-7	31	29
-6	34	33
-5	28	-24
-3	89	-87
-2	57	-56
-1	91	-87
1	82	77
2	111	-111
3	52	52
4	70	72
5	188	-186
7	23	-22
9	26	-24
10	31	29
12	17	-14
14	20	-19
15	46	48

H,5,2

15	30	28
14	35	-31
13	35	33
12	32	-29
11	30	-28
9	58	-59
7	54	-51
6	64	57
5	125	124
4	33	-32
3	151	149
2	90	91
1	47	40
0	206	-195
-1	92	88

-2	58	57
-3	64	64
-7	23	18
-13	53	-56
-14	52	56
-15	65	72
-16	24	28
-17	33	40

H,5,1

-13	18	18
-11	18	-19
-10	33	-35
-9	25	22
-8	31	-26
-7	57	54
-5	24	17
-4	46	-48
-3	153	-156
-2	66	-65
-1	155	148
0	69	-73
1	189	183
2	115	110
3	121	-131
4	97	93
5	91	-93
6	29	30
7	180	-174
9	73	-76
10	54	-55
13	37	39
14	46	43
15	18	14

H,5,0

14	20	-19
13	21	-26
12	22	-21
9	64	-64
8	56	-52
7	77	-72
6	37	-40

5	58	-56
4	98	92
2	86	-83
1	35	34
0	194	199

H,6,0

0	142	-142
1	194	-195
2	245	-241
3	19	19
4	55	-54
5	18	15
7	50	-48

H,6,1

14	26	-28
9	33	-37
8	24	-28
6	54	-51
4	83	83
3	155	-154
2	158	-158
0	224	-223
-1	214	208
-2	42	45
-3	76	75
-6	41	41
-9	21	-24
-11	20	23
-13	30	30

H,6,2

-14	37	41
-13	17	-18
-12	16	16
-11	23	28
-9	19	-22
-2	19	-26
-1	25	23
0	154	-153

LISTFC FOR ** Q27SLA **

H,6,2

1	149	143
3	110	-112
4	59	-58
5	78	79
7	41	40
8	56	-60
9	54	-55
10	22	-27

H,6,3

10	21	-25
9	19	-16
8	66	-68
7	49	53
5	16	13
4	51	-48
3	18	14
2	42	-44
1	32	26
0	27	30
-2	73	-70
-3	40	-40
-5	38	41
-7	30	-34
-8	26	-24
-10	34	-32
-12	27	25
-13	39	39
-15	59	63

H,6,4

-15	47	51
-14	71	78
-13	51	58
-10	41	-44
-9	50	51
-8	19	21
-7	38	-41
-6	32	-36
-5	19	25
-2	48	43

-1	81	72
0	48	46
1	24	24
2	57	-55
4	83	86
5	73	-70
7	45	51
9	39	35
10	18	-20
11	20	-24

H,6,5

6	43	-42
4	30	-28
2	43	45
1	73	72
-1	59	-65
-2	37	36
-3	17	-23
-4	31	37
-5	32	-37
-7	38	44
-8	19	-16
-10	71	78
-12	22	27
-13	30	32
-14	114	121

H,6,6

-14	43	50
-13	61	64
-11	24	23
-10	31	-33
-9	66	-73
-7	41	48
-6	66	72
-4	27	-34
-3	35	42
-2	27	31
-1	40	-43
0	89	88
1	72	71
2	37	35

3	28	25
4	30	-28
5	28	-31
6	56	56
8	18	13
9	15	14

H,6,7

9	52	57
8	54	57
6	55	53
5	48	-49
4	33	32
3	51	57
1	18	-19
0	59	62
-1	27	-31
-2	28	30
-3	33	-32
-5	37	43
-6	21	20
-7	25	-31
-8	86	92
-9	24	-23
-10	20	-23
-11	27	-25
-12	53	55
-13	15	-13

H,6,8

-13	16	-14
-12	29	-34
-11	26	29
-8	21	21
-7	45	-46
-5	17	15
-4	56	63
1	53	-55
5	21	-22
6	28	25
7	35	-40
8	62	65

H,6,9

6	32	36
-2	27	-25
-3	34	36
-4	16	-20
-5	42	-42
-6	40	47
-8	64	-69
-9	33	-39
-11	42	46
-12	20	-22

H,6,10

-12	22	21
-8	36	36
-7	18	16
-4	31	-30
-3	29	-31
-2	53	53
-1	20	-18

H,6,11

-1	27	27
-3	19	-22
-4	21	23
-6	65	-65
-7	76	-75
-8	37	-36
-9	32	34
-10	40	-41

H,6,12

-8	71	-73
-7	30	-30
-6	24	-27
-5	32	-32
0	22	22

LISTFC FOR ** Q27SLA **

H,7,9

-7	29	29
-2	20	-21
1	20	24

H,7,8

2	25	25
1	37	43
0	13	-17
-3	23	-24
-4	19	21
-6	18	16

H,7,7

-8	35	37
-7	30	-36
-4	41	-46
-3	20	21
-2	26	-32
-1	28	28
0	16	-19
4	27	27

H,7,6

1	32	30
0	46	43
-5	39	-47
-6	17	-17
-7	31	-35
-8	28	32
-9	34	-41
-10	23	27

H,7,5

-10	24	32
-9	44	-52
-7	45	-50
-6	39	-48
-5	22	-23
3	16	-15
7	25	-26
8	39	-38

H,7,4

8	18	21
6	23	-22
2	28	33
1	22	-25
0	41	-40
-4	24	-24
-6	37	-41
-7	40	-42
-8	20	-21
-9	26	-25
-10	25	27

H,7,3

-9	16	-17
-5	25	-24
-2	18	19
-1	30	29
0	59	60
1	26	-35
3	15	11
4	36	-40
6	21	-20
7	18	18

H,7,2

10	30	35
9	25	29
8	39	-42
7	23	23
3	57	-61
1	47	-46
0	49	53
-1	64	-66
-2	38	-34
-9	26	-28

H,7,1

-7	31	-35
-5	20	-16
-3	23	23
-2	66	69
-1	26	-30
0	16	15
1	18	-19
2	63	-66
4	44	-49
5	25	27
6	22	-18
7	35	39
8	25	24
9	40	45

H,7,0

10	17	20
8	45	45
7	50	54
4	23	-21
1	22	-24
0	41	-43

H,8,0

0	102	114

H,8,1

4	33	38
3	48	58
2	17	23
0	24	34
-1	73	-88
-2	42	50
-3	33	-33
-6	14	15

H,8,2

-2	32	36
-1	24	-24
0	17	23
1	42	-48
2	41	46
3	26	32

H,8,3

1	16	-24
0	32	36

H,8,4

-1	26	-27
1	16	-16
2	31	-30